

TECHNISCHE UNIVERSITÄT MÜNCHEN

In vitro* screening of selected organic nanomaterials with PC12, H4IIE, and *T. thermophila

Rajesh Rathore

Vollständiger Abdruck der von der Fakultät Wissenschaftszentrum Weihenstephan für Ernährung, Landnutzung und Umwelt der Technischen Universität München zur Erlangung des akademischen Grades eines

Doktors der Naturwissenschaften

genehmigten Dissertation.

Vorsitzender: Univ.-Prof. Dr. J. C. Munch

Prüfer der Dissertation:

1. apl. Prof. Dr. Dr. K.-W. Schramm
2. Univ.-Prof. Dr. W. Liebl

Die Dissertation wurde am 05.12.2013 bei der Technischen Universität München eingereicht und durch die Fakultät Wissenschaftszentrum Weihenstephan für Ernährung, Landnutzung und Umwelt am 26.02.2014 angenommen.

Erklärung

Ich erkläre hiermit an Eides statt, dass ich die vorliegende Arbeit ohne unzulässige Hilfe Dritter und ohne Benutzung anderer als der angegebenen Hilfsmittel angefertigt habe. Die aus anderen Quellen direkt oder indirekt übernommenen Daten und Konzepte sind unter Angabe des Literaturzitates gekennzeichnet.

सर्वतीर्थमयी माता सर्वदेवमयः पिता।
मातरं पितरं तस्मात् सर्वयत्नेन पूजयेत्॥

(DE: Ist die Mutter die Verkörperung aller Wege zur Anbetung, so ist der Vater die Verkörperung aller Gottheiten. Beide, Mutter und Vater, sollen deshalb mit allem Bemühen geehrt werden)

EN: Mother is the embodiment of all pilgrimages; father is the embodiment of all deities. Hence, mother and father are to be revered with all the efforts)

Dedicated to my Parents and my wife Gita

Table of Contents

List of tables	iv
List of figures.....	v
Summary.....	ix
Zusammenfassung	x
List of Poster and Podium Presentation.....	xii
List of Training and workshop attended.....	xii
Other Scientific activity.....	xii
List of publications	xiii
Abbreviation and acronyms.....	xiv
Chapter 1: Introduction.....	2
1.1.1 Classification and distribution of Nanomaterials.....	6
1.1.2 Characterization of Nanomaterials for Toxicological Evaluation	7
1.1.3 Regulatory status on Nanomaterials	8
1.1.4 <i>In vitro</i> Models for Nanotoxicities Testing.....	10
1.2 Fullerenes and binary mixtures.....	11
1.3 Catecholamines.....	13
1.3.1 Biosynthesis of Catecholamines	13
1.3.2 Gene expression in PC12 and <i>T. thermophila</i>	16
1.3.2.1 Rat Pheochromocytoma cells (PC12).....	16
1.3.2.2 <i>Tetrahymena thermophila</i>	16
1.4 EROD activity	18
Research objectives	19
Chapter 2: Materials and Methods.....	23
2.1 Experimental model organism and their maintenance.....	23
2.1.1 Rat hepatoma cell line, H4IIE.....	23
2.1.2 Ciliated protozoa, <i>T. thermophila</i>	23
2.1.3 Pheochromocytoma cells of the rat adrenal medulla, PC12	26
2.2 Nanomaterials	27
2.2.1 Preparation of Aqu-nC ₆₀ , hydroxyfullerene and Printex [®] 90.....	27
2.2.2 Characterization of Nanomaterials	28
2.3 Interaction of PCDD/F and C ₆₀ fullerenes	29
2.3.1 Preparation of Aqu-nC ₆₀ and its Blank	29
2.3.2 Preparation of mixture	30

2.3.3 <i>In vitro</i> induction of EROD activity	30
2.3.4 Metabolic Activity Measurement	31
2.4 Interaction of organic nanoparticles with dopaminergic system in PC12 cells	32
2.4.1 Cell culture and nanoparticle treatment	32
2.4.2 Detection of Catecholamine in PC12 by HPLC-ED	32
2.4.3 RNA isolation and cDNA synthesis	34
2.4.4 Cell viability and oxidative stress determination	44
2.5 Interaction of organic nanoparticle with eukaryotic protozoa <i>T. thermophila</i>	44
2.5.1 Population growth rate test	44
2.5.2 Determination of Cell viability	45
2.5.3 ROS generation	45
2.5.4 Determination of Catecholamines	45
2.6 Expression changes of selected genes in <i>T. thermophila</i> by carbon based nanoparticles	49
2.6.1 RNA isolation and Real-time RT-PCR	49
2.6.2 Analysed genes	49
2.6.4 Dichlorofluorescein Assay	50
2.7 Statistical analysis and software used	51
Chapter 3: Results and Discussion	53
3.1 PCDD/F and C ₆₀ fullerenes	53
3.1.1 TCDD and Aqu-nC ₆₀	53
3.1.2 PCB 126 and Aqu-nC ₆₀	54
3.1.3 Discussion	57
3.2 Nanomaterial exposure to PC12 cells	60
Discussion	66
3.3 Interaction of nanoparticles with <i>T. thermophila</i>	71
3.3.1 Stability and size distribution of nano-formulation	72
3.3.2 Growth dynamics of <i>T. thermophila</i> in presence of nanomaterials	74
3.3.4 Oxidative stress by nanomaterial	74
Discussion	75
3.4 Gene expression changes in <i>T. thermophila</i> by nanomaterials	77
Discussion	83
3.5 Microscopic behavior of <i>T. thermophila</i> in nanomaterial environment	86
Discussion	87
Chapter 4: Conclusions	89

4.1 Fullerene and EROD induction.....	89
4.2 Interaction of organic nanomaterial with neural cell line	89
4.3 Phenotypic behavior of <i>T. thermophila</i>	90
4.4 Genotypic behavior of <i>T. thermophila</i>	90
Acknowledgements.....	92
References:	94
Appendix:	104

List of tables

Table 1	Important properties in material characterization for toxicity studies	8
Table 2	Genomic DNA elimination reaction components	40
Table 3	Cycling condition for PCR	41
Table 4	Primer sequences and Tms for the amplification reactions of 11 genes in PC12 cells	43
Table 5	List of primers and genes used in SyberGreen qPCR expression analysis	50
Table 6	Hydrodynamic size distribution in fullerene suspension as a function of concentration. DLS analysis was performed on serial dilutions of a fullerene suspension in Osterhout medium. The average hydrodynamic size is represented as mean diameter (d.) \pm standard deviation (SD) in nm.	73

List of figures

Figure 1	Possible mechanisms by which nanomaterials interact with biological tissue. Examples illustrate the importance of material composition, electronic structure, bonded surface species (e.g., metal-containing), surface coatings (active or passive), and solubility, including the contribution of surface species and coatings and interactions with other environmental factors (e.g., UV activation)	5
Figure 2	Biosynthetic pathway of catecholamine. Tyrosine-3- monooxygenase, L-aromatic amino acid decarboxylase, 3,4-dihydroxyphenylalanine, dopamine β -hydroxylase, phenylethanolamine-N-methyl-transferase, Monoamine oxidase and 3,4-dihydroxyphenylacetic acid are abbreviated to TMO, AAAD, DOPA, DBH, PNMT, MAO and DOPAC respectively.	15
Figure 3	Dose-response curves of EROD. Induction of EROD activity <i>in vitro</i> by TCDD with nanoparticle formulation of C ₆₀ and TCDD with blank matrix of nanoparticle formulation after 24, 48, and 72 h of incubation. Blanks were prepared but without C ₆₀ and amount of TCDD added were similar to that of experimental sample. Regression curves are shown.	55
Figure 4	Adsorption and entrapment of TCDD by fullerene nanoparticles	55
Figure 5	24, 48, 72 h <i>in vitro</i> induction of EROD in H4IIE cells by 0.1, 0.4, 0.8 pmol of PCB 126 per ml in presence of Aqu-nC ₆₀ and corresponding control. Control samples were same as sample containing Aqu-nC ₆₀ but without fullerenes. Data points and error bars represent the mean and standard error of the mean (SEM) of three independent experiments. Statistically significant differences (Ordinary one-way ANOVA followed by Holm-Sidak's multiple comparison test), are indicated with an asterisk (* p<0.05, ** p<0.01, *** p<0.001)	56
Figure 6	EROD activity by 3.021 pmol per ml of PCB126 in presence of 0, 30.6, 122.5, 245, 490 and 980 pmol per ml of C ₆₀ during 24, 48 and 72 h incubation period. Statistically significant differences (Ordinary one-way ANOVA followed by Holm-Sidak's multiple comparison test), are indicated with an asterisk (* p<0.05, ** p<0.01, *** p<0.001). Data points and error bars represent the mean and standard error of the mean (SEM) of at least three independent experiments, in which each treatment was applied four times.	56
Figure 7	The effects of Aqu-nC ₆₀ in H4IIE cells. Cells were exposed to a medium with or without nano-C ₆₀ (980 pmol per ml) for 24, 48, 72 h before the addition of fresh medium containing different concentration of PCB-126. Data points and error bars represent the mean and standard error of the mean (SEM) of four independent experiments. Statistically significant differences (Ordinary one-way ANOVA followed by Holm-Sidak's multiple comparison test), are indicated with an asterisk (***) p<0.001)	57
Figure 8	Fullerenol size distribution in cell RPMI-1640 A) by intensity; B) by volume. The hydrodynamic diameter of particle was 33.57 nm. The first peak (d. nm = 33.57 nm) in size distribution by intensity contributes 92.8 percent while second peak (d. nm = 3598 nm) contributes 7.2 percent.	61
Figure 9	Laser diffraction hydrodynamic size data for fullerene in the RPMI-1640 medium	62

	used for <i>in vitro</i> toxicity experiments (obtained by means of DLS). The size distribution by A) intensity, B) volume in cell culture medium. Intensity-weighted average was used to determine hydrodynamic size, while volume distribution was used to determine relative amounts. The effects of dilution of suspension and time have no significant difference ($p < 0.01$) on the size of nanomaterial section C.	
Figure 10	The amount of catecholamine in PC12 cells after 6 and 24h treatment with Fullerene (C ₆₀), Fulleranol (C ₆₀ (OH) ₂₄) and Printex [®] 90 nanomaterial: a) dopamine; b) noradrenaline	63
Figure 11	Effect of nanoparticles on ROS generation. After exposure with nanoparticles for 24 h and later with DCFH-DA for 45 min. Fluorescence was measured with a microplate reader. The intensity of fluorescence expressed as means \pm SDs of three experiments. Asterisk indicates a statistically significant change compared to control (one-way ANOVA).	64
Figure 12	Gene expression alteration of tyrosin hydroxylase (<i>Th</i>), monoamine oxidase A (<i>MaoA</i>), and catechol-O-methyltransferase (<i>Comt</i>) in PC12 cells after 24 h-treatment with 1, 20 and 50 μ g/ml of Fullerene (C ₆₀), Fulleranol.	64
Figure 13	Gene expression alterations of thioredoxin reductase 1 (<i>Txnrd</i>), glutathione reductase (<i>Gss</i>), and glutathione peroxidase 1 (<i>Gpx</i>) in PC12 cells after 24 h-treatment (b) 1, 20 and 50 μ g/ml of Fullerene (C ₆₀), Fulleranol and Printex [®] 90.	65
Figure 14	Gene expression alterations of G protein-coupled receptor 37 (<i>Gpr37</i>), α -synuclein (<i>Snca</i>), and <i>Parkin</i> in PC12 cells after 24 h-treatment of 1, 20 and 50 μ g/ml of Fullerene (C ₆₀), Fulleranol *** p-value <0.001, ** p-value <0.01, * p-value <0.05 change compared with control.	66
Figure 15	Signaling pathways at synapse between two-nerve endings of PC12 cells.	70
Figure 16	Transmission electron microscopy (TEM) analysis was used to characterize the morphology aqueous-nC ₆₀ . A JEOL 2100 HT (JEOL Ltd., Japan) TEM was used, Stock fullerene suspension (80 μ g/ml) were deposited onto copper grids and morphology.	71
Figure 17	Laser diffraction hydrodynamic size data for fulleranol in the Osterhout medium used for <i>in vitro</i> toxicity experiments (obtained by means of DLS). Shown are the intensity and volume distribution of fulleranol-Osterhout formulation. Intensity-weighted average was used to determine hydrodynamic size, while volume distribution was used to determine relative amounts.	71
Figure 18	Laser diffraction hydrodynamic size data for fulleranol in the Osterhout medium used for <i>in vitro</i> toxicity experiments (obtained by means of DLS). Shown are the intensity and volume distribution of fulleranol-Osterhout formulation. Intensity-weighted average was used to determine hydrodynamic size, while volume distribution was used to determine relative amounts.	73
Figure 19		74

- Growth dynamics of *Tetrahymena (T.) thermophila* cells exposed to different concentration of Fullerenol. The presented cell numbers were the mean of three different experiments, each performed with at least three replicates. Cells were counted in haemocytometer square and data were transformed by taking the square root of the observation.
- Effects of nanoparticle formulation on ROS generation by *Tetrahymena thermophila* after 6 and 24 h exposure period. a) fullerene, b) fullereneol. The data are represented as the mean \pm SEM of at least three independent experiments. Each experiment was performed with eight replicates (n=8). As a standard and positive ROS control for DCF assay, different concentration of H₂O₂ were used (method section)
- Fullerene (C₆₀) dependent potentiation of *glutathione s-transferase (GST)* over 3, 6, 12, 24 h; mRNA expression level are represented as fold change of gene expression. Bars and error bars represent the mean and standard error of the mean (SEM) of three independent experiments. Statistically significant differences (ordinary ANOVA followed by Holm-Sidak Multiple comparison test) with respect to the vehicle control are indicated as: * p < 0.05, ** < 0.01, *** < 0.001.
- Fullerene (C₆₀) dependent potentiation of *Dopamine- β -hydroxylase (DBH)* over 3, 6, 12, 24 h; mRNA expression level are represented as fold change of gene expression. Bars and error bars represent the mean and standard error of the mean (SEM) of three independent experiments. Statistically significant differences (ordinary ANOVA followed by Holm-Sidak Multiple comparison test) with respect to the vehicle control are indicated as: * p < 0.05, ** < 0.01, *** < 0.001.
- Fullerene (C₆₀) dependent potentiation of *Catalase (CAT)* over 3, 6, 12, 24 h; mRNA expression level are represented as fold change of gene expression. Bars and error bars represent the mean and standard error of the mean (SEM) of three independent experiments. Statistically significant differences (ordinary ANOVA followed by Holm-Sidak Multiple comparison test) with respect to the vehicle control are indicated as: * p < 0.05, ** < 0.01, *** < 0.001.
- Fullereneol - C₆₀(OH)₂₄ dependent potentiation of *glutathione s-transferase (GST)* over 3, 6, 12, 24 h; mRNA expression level are represented as fold change of gene expression. Bars and error bars represent the mean and standard error of the mean (SEM) of three independent experiments. Statistically significant differences (ordinary ANOVA followed by Holm-Sidak Multiple comparison test) with respect to the vehicle control are indicated as: * p < 0.05, ** < 0.01, *** < 0.001.
- Fullereneol - C₆₀(OH)₂₄ dependent potentiation of *Dopamine- β -hydroxylase (DBH)* over 3, 6, 12, 24 h; mRNA expression level are represented as fold change of gene expression. Bars and error bars represent the mean and standard error of the mean (SEM) of three independent experiments. Statistically significant differences (ordinary ANOVA followed by Holm-Sidak Multiple comparison test) with respect to the vehicle control are indicated as: * p < 0.05, ** < 0.01, *** < 0.001.
- Fullereneol - C₆₀(OH)₂₄ dependent potentiation of *Catalase (CAT)* over 3, 6, 12, 24 h; mRNA expression level are represented as fold change of gene expression. Bars and error bars represent the mean and standard error of the mean (SEM) of three independent experiments. Statistically significant differences (ordinary

ANOVA followed by Holm-Sidak Multiple comparison test) with respect to the vehicle control are indicated as: * $p < 0.05$, ** < 0.01 , *** < 0.001 .

Figure 27 Optical micrographs the interaction of various concentration of fullerene and *T. thermophila* over 3, 6, 12 and 24 h with a video camera fitted in inverted microscope. Owing to the high mobility of the control cells, images were taken at a lower magnification. **86**

Figure 28 Optical micrographs the interaction of various concentration of fulleranol and *T. thermophila* over 3, 6, 12 and 24 h with a video camera fitted in inverted microscope. Owing to the high mobility of the control cells, images were taken at a lower magnification. The black arrow indicates the formation of fibrous material by cells. **87**

Summary

The increase in commercial production and inevitable release of nanomaterials into the environment accelerates concerns about their potential toxicity. Furthermore, the concomitant release of xenobiotics pose health hazard to human, and might have potential long-term risk to human health. In Fullerene-PCDD/F study, we found that Aqu-nC₆₀ does not show any induction of EROD activity in rat liver H4IIE cells *in vitro*, and furthermore, the simultaneous and sequential exposure of Aqu-nC₆₀ with TCDD induces EROD activity to the same extent as in the absence of fullerenes, in spite of high affinity of C₆₀ for dioxin. However, In PCB126; co-exposure induces elevated EROD activity and sequential exposure increases response up to 2-fold of control. Our *in vitro* observations suggest a potential source of drug-drug type interactions of fullerenes with xenobiotics particularly in a sequential exposure.

To understand the potential neurotoxicity of these three organic nanoparticles: fullerene-C₆₀, fulleranol-C₆₀(OH)₂₄ and Printex[®]90; PC12, a dopaminergic neuronal cell line, was used to investigate toxicity. Both at six and 24 h, fullerene decreased the dopamine in dose-dependent manner while fulleranol and Printex[®]90, at one µg/ml and 6 h time point, increased the dopamine levels (measured by HPLC-ED). These nanomaterials did not affect adrenaline level of PC12 after 24 h exposure. Fullerene shows dose dependent increase in oxidative stress, however, fulleranol shows increased oxidative stress only at 50 µg/ml. The fullerene (1, 20 µg/ml) up-regulated the expression of following gene: *Th*, *Comt* and *Maoa*. Although, fulleranol, one µg/ml, induces *Th* and *Comt* gene up to 2-fold, it did not induce *Maoa* gene at any concentration of exposure. The data suggest that fullerene and fulleranol may alter genes directly related to Parkinson's disease than with the dopamine metabolizing.

Finally, *T. thermophila* exposed to these nanomaterials was investigated by using dichlorofluorescein assay, cytomorphology, growth dynamics, and qRT-PCR assays. The stress response observed after fullerene exposure is more evident after 24 h, with an increase in gene expression while changes in *glutathione-s-transferase (GST)* expression after fulleranol exposure were already visible at an early stage. The levels of *catalase* after fullerene exposure increased over time, at the highest concentration, while an opposite tendency at lower concentrations. After fulleranol exposure, *catalase* undergoes substantial modifications, although without reaching the same fold levels reached by fullerene. After fullerene exposure dopamine β-hydroxylase (DBH) increases at the lowest concentration at an early stage, while at a later stage the increase was observed for the highest concentration.

Zusammenfassung

Die Steigerung der kommerziellen Produktion und die unvermeidliche Freisetzung von Nanomaterialien in die Umwelt bestärkt Bedenken über deren mögliche Toxizität. Darüber hinaus stellt die gleichzeitige Freisetzung von Xenobiotica eine Bedrohung der menschlichen Gesundheit dar und könnte zu deren langfristigen Gefährdung führen. In unserer Fulleren-PCDD/F-Untersuchung fanden wir, dass Aqu-nC₆₀ *in vitro* keinerlei Anregung der EROD-Aktivität in Rattenleberzellen (H4IIE) bewirkte und weiter, dass die gleichzeitige und nacheinander erfolgende Einwirkung von Aqu-nC₆₀ und TCDD die EROD-Aktivität in gleichem Maß wie bei der Abwesenheit der Fullerene anregt, trotz der hohen Affinität von C₆₀ zu Dioxin. Mit PCB126 jedoch, führt die Koexposition zu erhöhter EROD-Aktivität und sequentielle Exposition erhöht die Wirkungsantwort bis zum zweifachen Wert der Kontrolle. Unsere *in vitro* Beobachtungen deuten ursächlich auf mögliche Substanz-Substanz – Typ Wechselwirkungen von Fullerenen mit Xenobiotica besonders bei sequentieller Einwirkung hin.

Um die mögliche Neurotoxizität folgender drei organischer Nanopartikel zu verstehen: Fulleren-C₆₀, Fullerenol-C₆₀(OH)₂₄ und Printex[®]90, wurde die dopaminerge Zelllinie PC12 zu Toxizitätsuntersuchungen verwendet. Sowohl bei 6h, als auch bei 24h erniedrigte Fullerenkonzentrationsabhängig den Dopaminstatus, während Fullerenol und Printex[®]90 bei 1 µg/mL die Dopaminkonzentration nach 6h erhöhten. Diese Nanomaterialien beeinflussten das Adrenalinlevel nach 24h nicht. Fulleren bewirkte eine dosisabhängige Zunahme von oxidativem Stress, Fullerenol dagegen lediglich bei 50 µg/mL. Das Fulleren (1, 20 µg/mL) regelte die Expression von *Th*, *Comt* und *Maoa* hoch. Obwohl Fullerenol (1 µg/mL) bei *Th* und *Comt* bis zu verdoppelte Werte hervorrief, erhöhte es *Maoa* bei keiner Expositionskonzentration. Die Daten deuten darauf hin, dass Fulleren und Fullerenol Gene, die direkt mit der Parkinsonkrankheit verbunden sind, eher beeinflussen können, als die Gene der Dopaminmetabolisierung.

Abschließend wurde *T. thermophila* das diesen Nanomaterialien ausgesetzt wurde unter Anwendung von Dichlorfluoreszein Assay, Zytomorphologie, Wachstumsdynamik and qRT-PCR Assays untersucht. Die beobachtete Stressantwort war deutlicher nach 24h Exposition gegenüber Fulleren bei einer Zunahme der Genexpression, während Veränderungen bei der Expression der Glutathion s-transferase (*GST*) nach Fullerenexposition bereits in einem

frühen Stadium sichtbar wurden. Die Katalasekonzentrationen erhöhten sich zeitabhängig nach der Fullerenexposition mit der höchsten Konzentration während eine gegenläufige Tendenz bei niedrigeren Konzentrationen beobachtet wurde. Die Fullerenexposition bewirkte wesentliche Änderungen bei der Katalase, obwohl diese nicht das bei Fulleren beobachtete Niveau erreichten. Nach Fullerenexposition erhöhte sich das Dopamine β -hydroxylase (DBH)-Niveau bei der niedrigsten Konzentration in einem frühen Stadium, während es bei der höchsten Konzentration in einem späteren Stadium beobachtet wurde.

List of Poster and Podium Presentation

1. **Rathore R.**, Levy-Lopez W., Bernhöft S.; Schramm K.-W. Presence of aqueous fullerene nanoparticles (aqu-nC₆₀) do not alter ethoxyresorufin-o-deethylase (EROD) activity induced by 2, 3, 7, 8-tetrachlorodibenzo-p-dioxin (TCDD). International Symposium on Toxicity Assessment (ISTA15), Hong Kong. 2011 (**Podium** Presentation)
2. Kunze J., Urbanek M., **Rathore R.**, Schramm K.-W. Emission of Mutagenicity and PAH from fossil fuel in comparison to Ethanol blends, ISTA15, Hong_Kong. 2011 (**Poster** Presentation)
3. **Rathore R.**, Schramm K.-W. Interaction of PCDD/F and C₆₀ fullerenes. Dioxin2011, Brussels, Belgium. 2011 (**Podium** Presentation)
4. **Rathore R.**, Schramm K.-W., *In Vitro* Screening of Fullerenes (C₆₀): pure and in combination with xenobiotic organic compounds, ECO Summer School 2011-ECO, Leiden, Netherlands. 19-30SEP2011 (**Podium** Presentation)
5. **Rathore R.**, Schramm K.-W., EROD activity modulation of TCDD and PCB 126 in presence of aqueous suspensions of nano-C₆₀ECO Summer School 2012, Madrid, Spain. (**Poster** Presentation)
6. Zingarelli V., **Rathore R.**, Schramm K.-W., Expression changes of dopaminergic and other stress related genes in *T. thermophila* by carbon based nanoparticles. ECO summer School 2013, Chiemsee, Germany. (**Poster** Presentation)
7. **Rathore R.**, Schramm K.-W. *In Vitro* Screening of Fullerenes: pure and in combination with xenobiotic organic compounds. ECO summer School 2013, Chiemsee, Germany. (**Podium** Presentation)

List of Training and workshop attended

1. Protection and Commercialization of Intellectual Property, DEC 2010, Germany.
2. Research Management Training Workshop, OCT2011, Munich Germany.
3. Project Management in Biotech Industries, DEC2011, Garching, Germany.
4. German Language course for beginner, Neuherberg, Germany.
5. Secondment ECO-itn, 07MARCH-30MAY 2012, INIA, Madrid, Spain.
6. LMU Entrepreneurship Seminar, Germany (OCT 2012)

Other Scientific activity

1. Euroscience Open Forum (ESOF2010), Torino, Italy.
2. Introductory Autumn School-ECO, Munich, Germany.2010
3. Nanoparticles and Nanomaterials in Aquatic Systems, Lake Constance, Germany. 2010
4. 1st Winter School-ECO, Idestein, Germany. 2011
5. 21st SETAC Annual Meeting, Milan, Italy. 2011
6. ECO Summer School 2012, Verona, Italy (JUN2012)
7. CADASTER, Munich, Germany. (OCT 2012)

List of publications

1. **Rathore R.**, Schramm K.-W., EROD activity modulation of 2, 3, 7, 8-Tetrachlorodibenzo-p-dioxin and 3, 3',4,4',5-Pentachlorobiphenyl (PCB 126) in presence of aqueous suspensions of nano-C₆₀ (ATLA 42, 1–10, 2014)
2. **Rathore R.**, Pfister G., Schramm K.-W., Interaction of organic nanoparticles (Fullerene, Fullerenol and Printex®90) with dopaminergic system in PC12 cells (submitted)
3. **Rathore R., Zingarelli V.**, Schramm K.-W., Impact of selected stress-relate-biomarker in *Tetrahymena thermophila* by organic nanoparticles (under preparation)
4. **Rathore R.**, Baba M., Pfister G., Zingarelli V., Schramm K.-W., The change in the level of catecholamine in *T. thermophila* after exposure to organic nanomaterials.

Abbreviation and acronyms

A	Adrenaline
AAAD	L-aromatic amino acid decarboxylase
AhR	Aryl hydrocarbon Receptor
AS	Analytical solution
AS50	Auto sampler 50
cAMP	Cyclic adenosine mono-phosphate
CAs	Catecholamines
COMT	Catechol-o-methyltransferase
DA	Dopamine
DHBA	3,4-dihydroxybenzylamine
D β H	Dopamine beta hydroxylase
DNA	2-Deoxyribonucleic acid
DOPA	3,4-dihydroxyphenyl alanine
DOPAC	3,4-dihydroxyphenyl acetic acid
DPD	Dihydropyrimidine dehydrogenase
EROD	7-Ethoxyresorufin-O-deethylase
ED	Electrochemical detector
ER	Endoplasmic reticulum
GP40	Gradient pump 40
GPCRs	G-protein coupled receptors
hER α	Human estrogen receptor α
HPLC	High performance liquid chromatography
IS	Internal standard
LC	Liquid chromatography
LOD	Limit of detection
LOC	Limit of quantification
LPO	Lipid per-oxidation
MAO	Monoamine oxidase
MW	Molecular weight
NA	Noradrenalin
PAH	Polynuclear aromatic hydrocarbons
PCB	Polychlorinated Biphenyles
PCDD	Polychlorinated Dibenzo-p-dioxins
PCDF	Polychlorinated dibenzofurans
POP	Persistent organic pollutants
TCDD	2,3,7,8-Tetrachlorodibenzo-p-dioxin
TEQ	Toxic equivalent

INTRODUCTION

Chapter 1: Introduction

The realization that the field of nanotechnology has the ability to provide many socioeconomic benefits has instigated the rapid growth of the types and quantities of available nanomaterials. Carbon nanomaterials (CNMs) namely buckminsterfullerene (C_{60}) and its derivatives have shown great promise in many areas of applications ranging from solar cells and drug delivery to water purification. Nanomaterials form molecular systems of well-defined shape, and offer a surface that does not arise from a periodic structure. The various studies have demonstrated that CNMs, including fullerene, can penetrate both cell membranes (Foley et al., 2002) and living tissues (Rouse et al., 2007), and shown to be toxic both *in vitro* and *in vivo* conditions (Tao et al., 2009, Oberdorster et al., 2006). Fullerenes could enter living organisms via several routes- the respiratory, the digestive systems and the skin.

According to Registration, Evaluation, Authorization and Restriction of Chemicals (REACH) regulation of European Chemical agency (ECHA), all substances on the European Market, which are manufactured or imported in a quantity of 1 ton or more per year, will have to be registered by June 1, 2018. Fullerenes and CNTs are produced in large quantities in factories with capacities as high as 1,500 tons/year (Frontier Carbon Corporation, Tokyo, Japan; Fullerene International Corporation, Tucson, AZ, USA). In view of its large production and wide applications, fullerene will inevitably be released into the environment and thus raise environmental and health concerns due to its probable toxicity. Indeed, even without intended production, it is found in particulates emitted from coal-burning power plants.

In the 1985—synthesis of a new form of carbon (Kroto et al., 1985) electrified the scientific world, and since many different applications of C_{60} in industry- biology and medicine- have been studied. Fullerene C_{60} is a molecule 0.7 nm in diameter which consisting of 60

carbon atoms (Wang and Buseck, 1991). Water-soluble fullerene systems are promising candidates for many medical technologies and a crucial components for emerging cosmetics, electronic and mechanical materials (Lens, 2011, Benn et al., 2011, Wang et al., 2004, Smalley and Yakobson, 1998). Fullerene shows strange solubility and is virtually insoluble in water (Heymann, 1996). Instead of completely precipitating, some C₆₀ form suspended and water-stable aggregates up to 100-ppm concentrations (Andrievsky et al., 2002, Grigoriy et al., 1995, Scrivens et al., 1994). The aqueous nano-suspension of C₆₀ (Aque-nC₆₀) consists of a pristine C₆₀ core (of 10–2000 C₆₀ molecules, depending on size of crystal) surrounded by a low derivatized C₆₀ layer that forces the aggregate to be miscible in the aqueous phase (Andrievsky et al., 1995b). New insights in nano-toxicity suggest that the toxicity of CNMs is due not only to their own intrinsic toxicity, but also to the effect of these CNMs on the fate, transport and exposure of toxic substances (Colvin, 2003). So, after discharge, C₆₀ may interact with other xenobiotic compounds as demonstrated by sorption studies with phenanthrene carried out by Yang et al. (Yang et al., 2006) Long et al. reported that carbon nanotubes are superior sorbents for dioxin removal (Long and Yang, 2001). On the other hand, the potential use of C₆₀ and other nanoparticles as drug carriers indicate that compounds associated with nanoparticles are available, as also shown in a study by Zhang et al. (Zhang et al., 2007), who found that bioaccumulation of cadmium in fish was enhanced in the presence of TiO₂-nanoparticles (Zhang et al., 2007). Nevertheless, studies carried out with antibodies against fullerenes suggested that water-soluble fullerenes can readily pass cell membranes and are preferentially located at or near mitochondria (Foley et al., 2002).

As an important future technology, nanotechnology presents an opportunity for positively influencing economic development in the long term through intensive research and the effective translation of the research results into innovative products. Nanotechnology, involves the production of a diverse array of nanomaterials (NMs), which include nano-

objects and nanoparticles (NP). Nanomaterials have, at least, one dimension less than 100 nm; whereas nano-objects have two dimensions less than 100 nm (e.g., carbon nanotubes) and nanoparticles are defined as particles with three dimensions of less than 100 nm. It should, however, also be taken into account that nanoscale particles are not entirely new.

Natural and unintentionally produced particles of this size have long been entering the environment and leading to an exposure of humans and the environment. Historical examples (e.g. ruby glass, fullerene in space) show that nanotechnology has by no means come into use only recently. However, nanomaterial generating a special interest due to improvement in measurement technology and possibilities in new and targeted design at nanometer scale.

It is expected that the importance of nanotechnology will continue to flourish and that workers, consumers and the environment will be increasingly exposed. Due to the rapid expansion of nanotechnology and the increasing range of nanomaterials under production and development, it is essential that the potential impacts on human and environmental health be addressed appropriately. NPs exhibit, due to their small size, greater relative surface area than the corresponding conventional forms. Additionally, small size often results in higher reactivity and altered surface properties, which can be exploited in a variety of consumer products, such as cosmetics, drug delivery, paints, medicines, food and suntan lotions. In some products, NPs released directly into the environment such as remediation of polluted environments (Aitken et al., 2006). Any potential deleterious effects, therefore, need to be assessed in order to understand environmental impacts and potential effects on human health. Such work will require the linking of physicochemical characteristics of NP to their biological behavior.

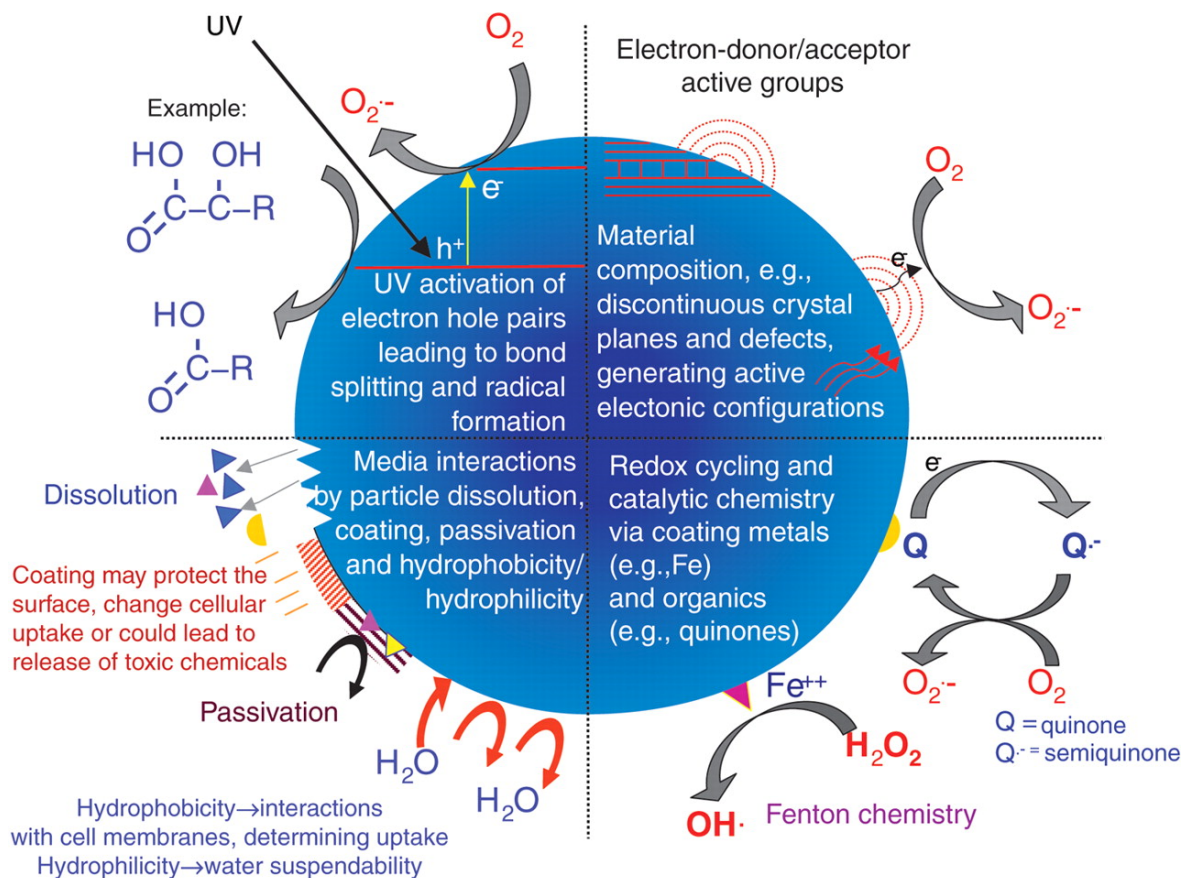


Figure 1: Possible mechanisms by which nanomaterials interact with surrounding system. The figure exemplify the importance of material composition, electronic structure, bonded surface species (e.g., metal-containing), surface coatings (active or passive), and solubility, including the contribution of surface species and coatings and interactions with other environmental factors (e.g., UV activation) Adopted from: Nel and co-author (Nel et al., 2006). Copyright 2006 by the American Association for the Advancement of Science.

The chemical composition, surface structure, solubility, shape, and aggregation: These parameters can modify cellular uptake, protein binding, translocation from portal of entry to the target site, and the possibility of causing tissue injury. At the target site, NM may trigger tissue injury by one or more mechanisms. Potential routes of NM exposure include gastrointestinal tract (GIT), skin, lung, and systemic administration for diagnostic and therapeutic purposes. NM interactions with cells, body fluids, and proteins play a role in their biological effects and ability to distribute throughout the body. NM binding to proteins

may alter mobility and accessibility to different tissues. Accelerated protein denaturation or degradation on the nanoparticle surface may lead to functional and structural changes, including interference in enzyme function (Vertegel et al., 2004). This damage could result from splitting of intramolecular or intermolecular bonds by catalytic chemistry on the material surface (Nel et al., 2012, Nel et al., 2006). Throughout their uptake and transport through the body, NM will encounter a number of defenses that can eliminate, sequester, or dissolve nanoparticles. In addition, cells and tissues have effective antioxidant defenses that deal with ROS generation.

1.1.1 Classification and distribution of Nanomaterials

There are many types of nanomaterial have manufactured and a variety of others are going to appear in near future. For this thesis, most current nanomaterials are classified in to three types: 1. Carbon based material; 2. Metal based materials; 3. Dendrimers. Carbon based material—these nanomaterials are composed mostly of carbon, most commonly taking the form of a hollow spheres, ellipsoids, or tubes; spherical and ellipsoidal carbon nanomaterials are referred to as fullerenes, while cylindrical ones are called nanotubes. Metal based materials—these nanomaterials include quantum dots, nanogold, nanosilver and metal oxides, such as titanium dioxide; quantum dot is a closely packed semiconductor crystal comprised of hundreds or thousands of atoms, and whose size is on the order of a few nanometers to a few hundred nanometers. Changing the size of quantum dots changes their optical properties. Dendrimers—these nanomaterials are nanosized polymers built from branched units. The surface of a dendrimer has numerous chain ends, which can be tailored to perform specific chemical functions.

1.1.2 Characterization of Nanomaterials for Toxicological Evaluation

In order to understand the modes of action of nanomaterials-to corroborate the processes of their environmental fate and behavior, to be able to extrapolate results between nanomaterials-it is essential to characterize the materials used in the different studies as far as possible and necessary. There is also no current general agreement on the “minimum information” on characterization that should be provided in an ecotoxicology study, although base-sets of data have been suggested as a starting point for regulatory tests (Stone et al., 2010). The OECD has created a list that takes into account those materials which are already in production (or close to commercial use), their production volume, and the likely availability of materials for testing (OECD, 2008). The OECD list comprises fullerenes (e.g., C₆₀), single- and multi-walled carbon nanotubes (SWCNTs and MWCNTs, respectively), carbon black, polystyrene, dendrimers, nanoclays, and nanoparticles of Ag, Fe, TiO₂, Al₂O₃, CeO₂, ZnO, and SiO₂ (OECD, 2008).

Table 1: Important properties in material characterization for toxicity studies (Sahu and Cascaciano, 2009).

Property	Importance for toxicity testing	Comments
Particle size distribution	Essential	
Degree/state of agglomeration	Important	
Particle shape/shape distribution	Important	
Chemical composition/purity	Essential	
Solubility	Essential (where applicable)	
Surface properties		
Specific surface area/porosity	Essential	Surface roughness may be important
Surface chemistry/reactivity	Essential	
Surface Adsorbed species	Important	In some cases may be the mechanism of toxicity (e.g. complement)
Surface charge/Zeta potential	Important (essential under aqueous condition)	Especially in aqueous biological environments, may change according to the environment)
Physical properties	Important	
Density	If applicable	
Crystallinity	If applicable	
Microstructure	If applicable	
Optical and electronic properties	If applicable	
Bulk powder properties	If applicable	May be important for dosimetry/exposure
Concentration	Essential	Can be measure by mass, surface area, or number concentration

1.1.3 Regulatory status on Nanomaterials

The coverage of nanotechnology by the legal documents is discussed by various authors (Franco et al., 2007, Frater et al., 2006, Davies, 2006). A number of legal instruments have the task of protecting workers, consumers and the environment without specifically dealing with nanotechnology. e.g.: Regulation (EC) No 1907/2006 of the European parliament and of the council of 18 December 2006 concerning the Registration, Evaluation, Authorisation and Restriction of Chemicals (REACH); Regulation (EC) No. 1907/2006 (some of the following rules and regulations have been repealed by the REACH Regulation)

- Waste-management directives (Directive 2006/12/EC on wastes; Directive 91/689/EEC on hazardous wastes; Directive 2000/53/EC on used vehicles)
- Waste Incineration Directive 2007/76/EC
- Water Framework Directive 2000/60/EC
- Directive on integrated pollution prevention and control (IPPC-RL); Directive 96/61/EC
- Federal soil protection ordinance
- Federal Emission Control Ordinance
- Sewage-sludge ordinance.
- Laws, regulations and administrative provisions of the Member States relating to restrictions on the marketing and use of certain dangerous substances and preparations, Directive 76/769/EEC
- Biocide Directive; Directive 98/8/EC
- Directive concerning the placing of plant protection products on the market, 91/414/EEC
- Occupational safety directives; 89/391/EEC, 98/24/EC
- Existing Substances Regulation; Regulation (EEC) No. 793/93
- Assessment of risks to humans and the environment of existing substances (EC) No. 1488/94
- Classification, packaging and labelling of dangerous substances, Directive 67/548/EEC
- Preparations Directive; Directive 1999/45/EC
- Directive on the safety of toys; Directive 88/378/EEC
- Directive on general product safety; Directive 2001/95/EC
- Cosmetics Directive; Directive 76/768/EEC
- Directive on the restriction of the use of certain hazardous substances in electrical and electronic equipment; Directive 2002/95/EC
- Consumer goods; Regulation 2004/1935/EC
- Foodstuffs legislation; inter alia, Regulation 2002/178/EC

Special rules and regulations relating to nanomaterials are not currently available. There has been no substance-specific statutory duty to perform studies especially for nanomaterials. Fullerenes represent an exception here since they are not an EINECS substance, on reaching a tonnage threshold, and are subject to a duty of more extensive testing. Under REACH, substances in nano-form that are in EINECS (e.g., titanium dioxide) shall be regarded as existing substances; substances in nano-form that are not in EINECS (e.g. carbon allotropes–fullerenes–other than those listed in EINECS) shall be regarded as new substances. The extent to which nanomaterials are to be assessed on their own within the

framework of the new chemicals legislation (REACH) is not entirely clear. Suitable aids for the assessment of insoluble or nanoscale materials are not currently available. REACH enables the assessment of new uses but the extent to which this option is applicable to nanomaterials must be examined. In addition, with regard to the areas like foodstuffs, consumer goods and cosmetic products, there is currently no special regulation of nanomaterials. For example, no particle sizes are laid down in the purity criteria for the 12 authorized food additives silicon dioxide (E 551) and titanium dioxide (E 171). Nanomaterials may be added to products and articles in order to achieve a biocidal effect (e.g. silver).

1.1.4 *In vitro* Models for Nanotoxicities Testing

In addition to saving time and money, the aim here is animal welfare. The methods investigate, inter alia, the local damage to the skin and eye, the skin permeation and the genotoxicity. Various *in vitro* methods have discussed specifically in connection with their application to nanomaterials. Cell-free *in vitro* studies provide information on the interactions with proteins, the activation of the complement system and the induction of oxidative stress. The cellular systems produce, inter alia, data on the translocation of the nanomaterials, on genotoxicity, and on the biological effect mechanism in cells at the portal of entry and the systemic target organs. For example, the Comet Assay is for the determination of a genotoxic effect. The oxidative stress, which is discussed as the cause of damage and activation of cells (Oberdörster et al. 2005b), is—in opinion of various authors—detected by means of: measurement of dichlorofluorescein, oxidized glutathione, and nitrosated proteins (Hess et al. 2005, Janssen et al. 1993, Quinlan et al. 1995).

In vitro methods are currently not suited for assessing, with sufficient certainty, the effects of nanomaterials since the sensitivity and specificity required to predict the effects resulting from nanomaterials in humans are questioned (Sayes et al. 2007, Maynard 2006e).

Furthermore, *in vitro* methods currently have a further methodological disadvantage since they were, as a rule, developed for dissolved substances. It is difficult to turn various nanomaterials into a finely dispersed suspension. They sediment or remain on the surface of the medium.

Different types of cells (immortalized mouse microglia-BV2, rat dopaminergic neurons-N27, primary culture of embryonic rat striatum) are reported for testing the potential toxic effect of nanomaterial *in vitro* (Matesanz et al., 2013, Pisanic et al., 2007, Long et al., 2007, Hussain et al., 2006). The most widely used cell model for NPs neurotoxicity study is PC12 cells which is a cultured neuronal phenotype and was used as a paradigm for neurobiological and neurochemical studies (Grau and Greene, 2012, Teng et al., 2006, Banker and Goslin, 1998, Greene and Tischler, 1976). Several reports that assess the nanomaterial toxicity in PC12 are available in scientific domain (Zhao et al., 2012, Xue et al., 2012, Soenen et al., 2012, Kim et al., 2011, Yuan et al., 2010, Przybytkowski et al., 2009, Khatchadourian and Maysinger, 2009).

1.2 Fullerenes and binary mixtures

Fullerenes (C_x) were discovered in 1985 in soot resulting from ablation of graphite with a laser (Kroto et al., 1985). They are entirely composed of carbon atoms, which form hollow spheres like a football/soccer ball. The C_{60} fullerene is a remarkable stable compound consisting of a polygon with 60 vertices and 32 faces, 12 of which are pentagonal and 20 hexagonal. The diameter is about 0.7 nm, which is roughly the size of many small pharmaceutical molecules (Lee et al., 2007). Each carbon atom is placed at a vertex and each atom has the valences satisfied by two single bonds and one double bond. Thus, both the inner and outer surface is covered with π electrons constituting an aromatic structure that resembles the structure of the layers in graphite (Kroto et al., 1991, Kroto et al., 1985). The molecular weight is about 720 (Kroto et al., 1991). The C_{60} fullerene is also known as

buckminsterfullerene or buckyball (Dugan et al., 1996, Kroto et al., 1991). Numerous fullerenes with other carbon numbers also exist. Furthermore, a metal atom can be trapped inside the cage of fullerenes (Wang et al., 2006). The polyhydroxy fullerenes are termed fullerlenols or fullerols (Djordjević et al., 2006, Roger and David, 1993). The solubility of the pristine C_{60} is 3000, 39, 11, 1.4, 0.04 and 0.027 mg/l in toluene, distilled octanol, tetrahydrofuran, ethanol, acrylonitrile and methanol, respectively (Kulkarni and Jafvert, 2008). It is practically insoluble in water; the solubility is less than 0.1 ng/l (Bedrov et al., 2008). However, C_{60} can form stable dispersed clusters in solution. Thus, it clusters on adding C_{60} dissolved in an organic solvent to water, followed by removal of the solvent, which may not be complete. Clusters can also be prepared by vigorous extended mixing in water (Andrievsky et al., 1995a, Dhawan et al., 2006, Kulkarni and Jafvert, 2008). Opposite to aromatics, the pristine fullerenes have no hydrogen bond atoms or other groups attached to their cage. Therefore, they are unable to participate in substitution reactions. As they consist entirely of sp^2 -hybridized carbons, they have a strong electron-attracting ability and, therefore, they are oxidizing agents (Nielsen et al., 2008). Due to the electron-withdrawing effect, it is possible to add chemical groups that can donate a pair of electrons (nucleophiles), therefore, numerous compounds can be added to the fullerene cages. For example, formation of epoxides occurs by addition of oxygen to the C = C double bonds (Roger and David, 1993). In addition, the C_{60} cage can easily add free radicals as it has 30 carbon double bonds to which free radicals can be added (Krusic et al., 1991, Roger and David, 1993). Therefore, it is described as a ‘radical sponge’. Thus, the fullerol $C_{60}(OH)_{22}$ is a potent hydroxyl radical scavenger for radicals generated by the Fenton reaction (Bogdanović et al., 2004). The heating in oxygen at 200 °C causes formation of C-O adducts and at 400–500 °C substantial decomposition occurs. Due to the generation by combustion processes, fullerenes are present in city air aggregates and kitchen gas stove burner emission aggregates (Murr et al., 2006).

Moreover, despite its insoluble nature, fullerene can form stable aqueous suspensions containing high concentrations of C₆₀ aggregates (Aqu-nC₆₀) by some environmentally relevant processes, including the extended mixing of fullerene with water (Cheng et al., 2004) and interaction with natural organic matter (NOM) (Terashima and Nagao, 2007, Espinasse et al., 2007). These aqueous suspensions of nC₆₀, suggesting potential migration in surface and groundwater systems, allow them to reach receptor organisms such as fish. Additionally, just as the artificial and natural organic matter, nC₆₀ may also enhance the diffusive mass transfer of the HOCs through the aqueous boundary layer at the organisms (Mayer et al., 2007), which is often considered the rate-limiting step for diffusive uptake (Sijm and van der Linde, 1995). Accordingly, the mobility and bioavailability of the nC₆₀ - associated pollutants may be enhanced. Nevertheless, C₆₀ have soil sorption values approaching those associated with DDT and PCBs and other highly retained materials. Generally, the sorption of organic materials such as C₆₀ to soil renders them unavailable for interaction with the soil micro-flora but using ¹⁴C-C₆₀, it has been shown that C₆₀ will accumulate in earthworms and this suggests that retention in soil may not limit trophic transfer (Li et al., 2010).

1.3 Catecholamines

1.3.1 Biosynthesis of Catecholamines

Catecholamine is a monoamine-an organic compound originated from amino acid tyrosine containing catechol (benzene with two hydroxyl side groups) and amine groups. Some of them are biogenic monoamines. In human body, the most abundant catecholamines are adrenaline (epinephrine), noradrenaline (norepinephrine) and dopamine. They are produced via phenylalanine and tyrosine. Tyrosine is created from phenylalanine by hydroxylation by the enzyme phenylalanine hydroxylase. Then, tyrosine reached to catecholamine-secreting neurons. Here, tyrosine is oxidized by tyrosine-3-monooxygenase in the presence of BH₄

(6-[®]-L-erythro-tetrahydrobiopterin) to add another oxygen to form 3,4-dihydroxyphenylalanine (L-DOPA). Dopamine is the first catecholamine to be synthesized by the decarboxylation of L-DOPA. Noradrenaline and adrenaline derived, in turn, from further modifications of dopamine. The Fig. 2 illustrates the biosynthetic pathway of catecholamine.

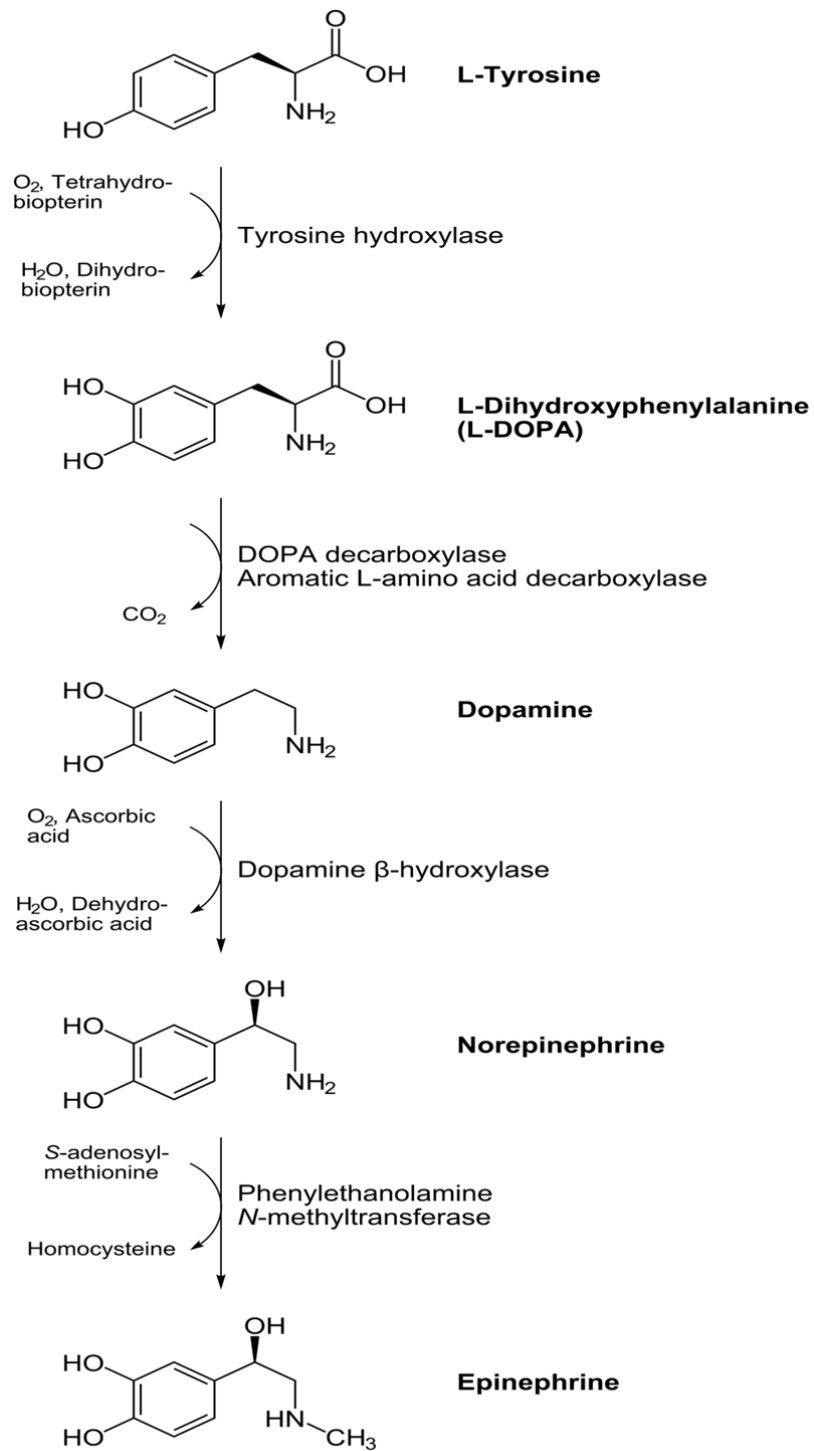


Figure 2: Biosynthetic pathway of catecholamine. *tyrosine-3-monoxygenase*, *L-aromatic amino acid decarboxylase*, *3,4-dihydroxyphenylalanine*, *dopamine β -hydroxylase*, *phenylethanolamine-N-methyl-transferase*, *monoamine oxidase*, and *3,4-dihydroxyphenylacetic acid*.

1.3.2 Gene expression in PC12 and *T. thermophila*

1.3.2.1 Rat Pheochromocytoma cells (PC12)

The PC12 cell line derives from the rat pheochromocytoma and it is often used as an in vitro model to understand the physiology of central dopamine (DA) neurons (Roda et al., 1980, Tischler, 2002). A number of factors contribute to the wide use of PC12 cells: inexpensive, easy to handle, and mimic many features of central DA neurons. In fact, PC12 cells produce catecholamines (Markey et al., 1980, Roda et al., 1980, Vaccaro et al., 1980). In particular, they have DA (Greene and Rein, 1978) as the key catecholamine and bear DA receptors on their outer membrane (Sampath et al., 1994). In light of the presence of DA and DA receptors, as well as DA uptake mechanisms, PC12 cell lines are considered to be closer to DA terminals compared with their ancestors (i.e. chromaffin cells of the adrenal medulla) (Fornai et al., 2007). PC12 cells represent a model to predict the neurotoxicity of a variety of compounds acting on central DA neurons with significant implications for the treatment of neurological disorders. The potential toxicity of the most effective therapeutic agent in Parkinson's disease (e.g. L-3,4-dihydroxy-phenylalanine, L-DOPA), which once it was found to be toxic for PC12 cells, generated serious concerns about the gold standard therapy (Basma et al., 1995, Walkinshaw and Waters, 1995). However, comparative studies carried out in vivo often led to different, sometime opposite conclusions: showing the absence of toxicity or even a neurotrophic effect of L-DOPA (Fornai et al., 2000).

1.3.2.2 *Tetrahymena thermophila*

A prominent experimental ciliate species is the fresh water ciliate *Tetrahymena thermophila*, which was first used as a model organism in the 1950s. The *Tetrahymena* genus is typified by an ovoid body shape and *T. thermophila* are usually about 50×20 µm in size. *Tetrahymena thermophila* has been and remains a useful model organism; it has a completely sequenced macronuclear genome (MAC) (Eisen et al., 2006), and it has contributed understanding of telomeres (Blackburn and Gall, 1978), telomerase and their

protective role in genetics (Greider and Blackburn, 1985). The sequencing of the macronuclear genome of *Tetrahymena thermophila* in 2006 and the creation of a genomic database (www.ciliate.org) (Stover et al., 2006) have also advanced its use for ecotoxicogenomics studies. Genomics, among other techniques, is increasing its role in the ecotoxicological field for the relevance of the effects of chemicals on the gene expression patterns and consequently for the finding of new molecular markers. This will act as early warning signals for environmental stressor (Gerhardt et al., 2010).

Additionally *Tetrahymena thermophila* is an excellent model organism for nanotoxicology studies for its ability to internalize nanoscale (100 nm or less) and microscale (100-100,000 nm) particles. As particle ingesting organisms *Tetrahymena spp.* have in fact already been used in a series of nanotoxicology studies testing different types of nanoparticles (eg. nano ZnO, nano CuO (Mortimer et al., 2010); CdSe QD (Werlin et al., 2011); TiO₂ nanotube layers (Feschet-Chassot et al., 2011), included carbon based materials (Ghafari et al., 2008); MWCNTs (Guo et al., 2008), 2008) at different end points (eg. cell viability, growth rate, enzymatic activity, morphological alterations).

The MAC genome of *Tetrahymena thermophila* has been shotgun sequenced (Eisen et al., 2006); it is highly A-T rich, with only 24% G-C content (Asai and Forney, 1999). The *Tetrahymena* genome encodes a relatively large number of genes with nearly 27,500 predicted protein-coding genes in the MAC. This is a high number compared to many other single celled eukaryotes, such as yeasts, which often contain fewer than 7000 predicted genes. Even small multicellular organisms such as *C. elegans* only possess ~20,000 genes (Finlay et al., 1998). The *Tetrahymena* gene number is comparable to that found in humans who have ~23,000 genes (Collins et al., 2004, Venter et al., 2001), although alternative splicing of genes could further expand the human protein profile by as much as 60 % (Gustafsson et al., 2004). *Tetrahymena's* large number of genes is not due to a whole genome duplication event or even segmental duplications, similar to those seen in humans

and other vertebrates, multiple plants and a myriad of other species (Van de Peer, 2004), but instead arose through duplication events. The most common duplication events result in genes that are located adjacent to one another. Thus some genes have been expanded into families, and various families have been expanded, whereas others remain as unique genes (Eisen et al., 2006). *Tetrahymena* utilize all 64 codons to encode different amino acids. The traditional stop codons, UAA and UAG, encode for glutamine. The single remaining stop codon, UGA is the only stop codon in *Tetrahymena*. However, it can also code for selenocystine (Eisen et al., 2006).

1.4 EROD activity

Aromatic hydrocarbons such as 2, 3, 7, 8-Tetrachlorodibenzo-*p*-dioxin (TCDD) are able to pass through biological membranes and specifically binding to the aryl hydrocarbon receptor (AhR). This is known to participate in multiple mechanisms of the normal physiology in vertebrates being able to generate biological and toxicological effects. The AhR mediates the induction of specific enzymes, in particular, the cytochrome P450 1A1 (CYP 1A1). By means of this bioassay, the induction of CYP 1A1 can be determined as the sum of the whole compounds able to elicit a response in a determined environmental sample. The EROD bioassay measures the catalytic activity of cytochrome P4501A (CYP1A), a mixed function oxidase (MFO) enzyme, as 7-ethoxyresorufin-*O*-deethylase (EROD) activity in cultured rat liver cells exposed to environmental extracts. EROD is induced by the presence of certain polycyclic aromatic hydrocarbons (PAH) and related compounds (e.g., nitrogen heterocyclics and sulfur-, oxygen-, nitro-, amino-, and alkyl-substituted PAH) and polyhalogenated hydrocarbons (PHH) in environmental samples. The PHHs include the highly toxic and persistent polychlorinated dioxins (PCDDs), dibenzofurans (PCDFs), biphenyls (PCBs), and naphthalenes, as well as the brominated analogs of these compounds. These classes of compounds induce CYP1A and hence EROD activity in cells by binding to the cytosolic aryl hydrocarbon receptor (AhR). This AhR-

mediated mechanism of EROD induction is believed to involve in many of the toxic effects associated with PHHs and PAHs.

The H4IIE bioassay has advantages over traditional analytical chemistry techniques in that it reveals the cumulative biological activity of numerous structurally similar contaminants, each with differing potencies. This assay can also reveal the potential interactions that can occur between contaminants when they are present in environmental samples as complex mixtures. This H4IIE bioassay has a high degree of sensitivity (detection limit < 10 femtomoles 2, 3, 7, 8- tetrachlorodibenzo-*p*-dioxin [TCDD]) and can be rapidly performed.

Research objectives

The research objectives of this study were as follows

1. TCDD and PCB 126 are an important class of environmental pollutants because of their notable amounts in the environment, their toxicological risks, and their strong persistence in soils and sediments. The transport, partitioning, and bioavailability of these contaminants in groundwater and surface waters are known to be highly dependent on the interactions of these compounds with existing colloids. As reported by Fröhlich et al. (Frohlich et al., 2010) that nonmetallic carboxyl polystyrene particles (20–60 nm) inhibited the enzymatic activity of several P450 enzymes, suggesting that particles in the nano-size range can produce unexpected effects on liver cell function. Therefore, Co-exposure and sequential exposure of nanoparticle with xenobiotic may cause over or under activity of xenobiotic. To determine the effects of C₆₀ on the toxicity of existing pollutants TCDD and PCB 126, we asked the following questions: I, Do the nanoparticles and TCDD/PCB 126 interact synergistically and/or; II, Do they trap TCDD/PCB126 and inhibit its action and/or; III, Does a nanoparticle itself act as an AhR agonist?

2. The effect of manganese, silver and copper nanoparticles on PC12 gene expression have been reported in the literature (Wang et al., 2009). We investigate following genes,

mentioned by Wang and co-author (Wang et al., 2009): for dopamine metabolism—the tyrosine hydroxylase gene (*Th*), monoamine oxidase A gene (*Maoa*), and catechol-O-methyltransferase gene (*Comt*); for redox mechanism—glutathione peroxidase 1 gene (*Gpx*), glutathione synthetase gene (*Gss*), and thioredoxin reductase 1 gene (*Txnrd*); and pathogenesis of neurodegeneration in Parkinson's disease (PD)— α -synuclein gene (*Snc α*), Gprotein-coupled receptor 37 gene (*Gpr37*), and parkin gene (*Park2*). From best of our knowledge, this is the first study on organic-nanoparticle induced dopaminergic neurotoxicity in PC12 cell. The purposes of this study were to describe the effect-with increased window of observation-of fullerene, fullerenol and Printex®90 on the dopaminergic system of PC12 cell, and to explore the potential molecular mechanisms.

3. To determine if carbon nanomaterial-fullerene and fullerenol- have/not have *in vitro* toxic effects on eukaryotic cells. We investigate by means of cellular population growth dynamics, cytomorphology, and fluorescent assay; and to correlate at deeper and generally more sensitive gene expression level. In this study, we examined the effect on key physiological biomarkers: *glutathione-S-transferase*, *catalase*, *Dopamine- β -hydroxylase* and *calcium translocating P-type ATPase*. We relate the results from three different kinds of *in vitro* assays: cellular level based DCF-assays, cytomorphology and growth dynamics (by means of inverted optical microscopy), and gene expression (by means of RT-PCR), and proposed biomarkers for detecting stress caused by nanomaterial that might be detected at a level nontoxic at other assays.

Materials and Methods

Chapter 2: Materials and Methods

2.1 Experimental model organism and their maintenance

2.1.1 Rat hepatoma cell line, H4IIE

The H4IIE cells were derived from the Reuber hepatoma H-35 by Pitot and co-workers (Pitot et al., 1964). It is a continuous cell line and was characterized with regard to aryl hydrocarbon hydroxylase (AHH) activity. Besides excellent growth characteristics and low basal cytochrome P450IA1 activity, the H4IIE cells to have inducible AHH enzyme activities. To characterize the AHH induction response of the H4IIE cells to 2, 3, 7, 8-tetrachlorodibenzo-p-dioxin (TCDD), the prototypic PHH, the H4IIE rat hepatoma cell culture bioassay is useful in detecting TCDD. And found that the H4IIE cells are very good in their response to TCDD with a detection limit of 10 fmol (Tillitt et al., 1991).

2.1.2 Ciliated protozoa, *T. thermophila*

The ciliated protozoan *Tetrahymena thermophila* has been extensively used in the last decades, as model organism in basic research, for its high degree of functional homology with human and mammalian genomes. The other peculiar characteristics are: small dimension-easy handling; ease of culture-less sophistication requirement; fast generation time-testing through several generation; high abundance in aquatic environments-on the spot testing, because of which it becomes very popular in ecotoxicological studies. Interestingly, the peculiar biological features above mentioned, added to other favorable characteristics, such as low maintenance costs, large cell size, well defined life cycle, have made this organism a very appealing alternative laboratory model for animal research- in accordance with the 3Rs principle (replacement, refinement and reduction) (Lukacinova et al., 2007).

PPY- medium

Culture medium based on proteose peptone and yeast extract with the addition of glucose and trace elements (Plesner et al., 1964). To avoid pH shifts during the culture growth or due to the addition of test chemicals the PPY-medium is pH stabilized by a biological buffer. The medium was used for the cultivation of experimental stock, for pre-culturing of organisms and as nutrient supply for the growth test.

Composition:

1. Organic contents:
 - a. 3.5 g/L proteose peptone
 - b. 0.7 g/L Yeast extract
 - c. 3.5 g/L Glucose

2. Salt/trace elements added separately to the culture medium:

Salt solution 1 (added as 100x concentrated):

- 50 mg/L $\text{CaCl}_2 \cdot 2\text{H}_2\text{O}$
- 5 mg/L $\text{CuCl}_2 \cdot 2\text{H}_2\text{O}$
- 1.25 mg/L $\text{FeCl}_3 \cdot 6\text{H}_2\text{O}$

Salt solution 2 (added as 100x concentrated):

- 100 mg/L $\text{MgSO}_4 \cdot 7\text{H}_2\text{O}$
- 25 mg/L $\text{Fe}(\text{NH}_4)_2(\text{SO}_4)_2 \cdot 6\text{H}_2\text{O}$
- 0.5 mg/L $\text{MnCl}_2 \cdot 4\text{H}_2\text{O}$
- 0.05 mg/L ZnCl_2

3. Biological pH Buffer:

2.093 g/L Mops-[3-n(N-Morpholino) Propanesulfonic acid buffer], adjust pH to 7.2 by NaOH

Preparation of 10 mL (100x concentrated) salt solution 1 and 2:

Salt solution 1:

- a. Weight out 50 mg $\text{CaCl}_2 \cdot 2\text{H}_2\text{O}$ and dissolve in 8.75mL MilliQ water (solution a)
- b. Weight out 50 mg $\text{CuCl}_2 \cdot 2\text{H}_2\text{O}$ and dissolve in 10mL MilliQ water (solution b)
- c. Weight out 50 mg $\text{FeCl}_3 \cdot 6\text{H}_2\text{O}$ and dissolve in 10mL MilliQ water (solution c)

Add 1 mL of solution (b) and 0.25 mL of solution (c) to solution (a)

Salt solution 2:

- d. Weight out 100 mg $\text{MgSO}_4 \cdot 7\text{H}_2\text{O}$ and 25 mg $\text{Fe}(\text{NH}_4)_2(\text{SO}_4)_2 \cdot 6\text{H}_2\text{O}$ and dissolve in 9.725 mL MilliQ water (solution d)
 - e. Weight out 20 mg $\text{MnCl}_2 \cdot 4\text{H}_2\text{O}$ and dissolve in 10 mL MilliQ water (solution e)
 - f. Weight out 20 mg ZnCl_2 and dissolve in 10 mL MilliQ water (solution f)
- Add 0.25 mL of solution (e) and 0.025 mL of solution (f) to solution (d)

Steps:

1. Weight out the corresponding amount of the organic constituents of the PPY-medium
2. Fill a graduated beaker with mq H_2O up to about $9/10^{\text{th}}$ of the final volume (e.g. 900 mL H_2O to prepare 1000 mL PPY medium)
3. Dissolve the organic constituents in the prefilled beaker under magnetic stirring
4. Add the salt solution 1 and 2 (both the solutions are 100x concentrated, take $1/100^{\text{th}}$ of the final volume each)
5. Add biological pH buffer (Mops)
6. Adjust pH with NaOH (3.2%) to a volume of 7.2 mL (approx 5mL for 1000 mL medium)
7. Remove the magnetic bar
8. Fill up with MilliQ water the desired final volume
9. Allocate the medium to conical flask containing 40 mL each
10. Autoclave the medium for 20 min and store it at 4C in the dark

Osterhout-medium (Käkinen et al., 2011)

In one liter of MilliQ water containing

1. 104 mg NaCl
2. 8.5 mg MgCl_2
3. 4 mg MgSO_4
4. 2.3 mg KCl
5. 1 mg CaCl_2

Autoclave at 121 °C for 15', store at RT

Long-term culture of the cells was managed in amber borosilicate glass crimp cap vials with rubber stopper and an aluminum cap is placed on the top and crimped. Single chick-pea and 10 mL Millipore water were taken together into glass stock vials and kept overnight at 4°C. Afterwards, the vials were sterilized for 20 min and stored one day at room temperature. 100 µL exponential growing cell cultures were added into the glass vial at sterile condition and preserved for several months.

The experimental stock culture was prepared for every week from long-term stock culture. This culture was reared in PPY-medium and serve as starter culture for the preparation of logarithmically growing pre-culture. 200-300 μL cell aliquot was transferred from the vial by piercing of septum with a sterile syringe and added into 40 mL PPY medium in a 300 mL Erlenmeyer flask with fine porous silicon gum head. The porous cap of the flask allows an adequate oxygen supply. Temperature of the culture flask was maintained to 28 °C as it for chemical toxicity studies, too. For routine purposes, it was prepared on Friday and incubated over weekend to have experimental stock throughout the following week.

Cells of *Tetrahymena thermophila*, strain *SB210*, purchased from the Stock Centre of the Cornell University (USA), were grown axenically at 28°C in PPY medium, as described previously (Wang et al., 2010). Once the logarithmic phase of growth (2×10^5 cells/ml) was reached, the cells were incubated at 28 °C in PPY medium for another 24 hours. The cells were then centrifuged for 5 min at 300 g and washed twice in Osterhout medium (Käkinen et al., 2011). Cell number was determined microscopically by mean of hemocytometer

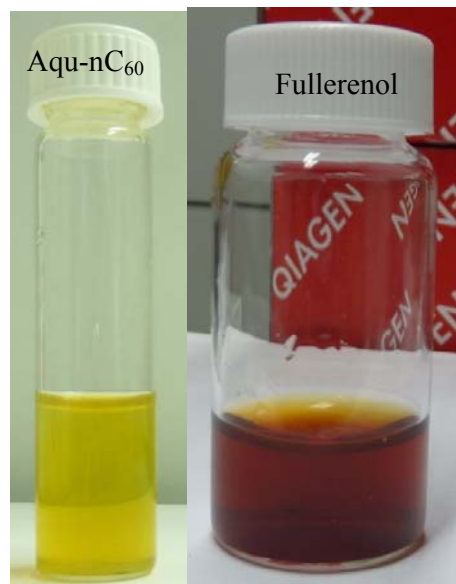
2.1.3 Pheochromocytoma cells of the rat adrenal medulla, PC12

The PC12 cell line (CRL-1721; LOT: 58650893) was obtained from American Type Culture Collection (Collection, 2011). Cells were cultured in 75 cm² flasks in RPMI-1640 medium supplemented with 10% horse serum, 5% fetal bovine serum (both heat inactivated), penicillin (50 units/ml) and streptomycin (50 mg/ml), in a humidified atmosphere with 5% CO₂ at 37 °C. At about 80% confluence of passage lower than fifteen, PC12 cells were transferred to 6-well plates at seeding density 10⁶ cells/ml, cultured for an additional 24 h, and then treated with one of the three types of nanoparticles. After 6 and 24 h of treatment, cells were collected for RNA isolation and dopamine analysis.

2.2 Nanomaterials

2.2.1 Preparation of Aqu-nC₆₀, hydroxyfullerene and Printex®90

Aqu-nC₆₀ stock nanoparticle formulation was prepared by solvent exchange method and the concentration was determined by UV-visible spectrophotometric method as described by Andrievsky et al. (Andrievsky et al., 1995b). Specifically, C₆₀ fullerene powders (40 mg) were dissolved completely into 40 ml of toluene using a magnetic stirrer. This solution referred as the C₆₀-toluene stock solution. The purple C₆₀-toluene stock solution was transferred to a beaker containing 100 ml MilliQ water and 3 ml ethanol.



The mixture was then sonicated using a dip probe sonicator (Bandline SONOPULS GM 70) operated until the toluene phase disappeared. The resulting yellowish/ brown suspension was filtered through a 0.7 μm glass fiber filter (Life Sciences, Pall Corporation, Michigan, USA). Nitrogen was purged for four hours. Several batches of these were prepared and mixed to prepare uniform stock solution and stored in bottle covered with aluminum foil. A 50, 20 and 1 $\mu\text{g/ml}$ fullerenol in RPMI-1640 were prepared from the 1000 $\mu\text{g/ml}$ fullerenol stock solution prepared by dissolving weighed fullerenol in the MilliQ. Intensity-weighted average was used to determine hydrodynamic size, while volume distribution data was used to determine relative amounts. A 50, 20 and 1 $\mu\text{g/ml}$ Printex®90 in RPMI-1640 were prepared from the 1000 $\mu\text{g/ml}$ Printex®90 stock solution in MilliQ prepared by means of bath sonication.

2.2.2 Characterization of Nanomaterials

2.2.2.1 UV-V spectrophotometric determination

The concentration of Aqu-nC₆₀ nanoparticle formulation was determined by the UV-visible spectrophotometric method. The C₆₀ concentration in the stock suspension was determined with UV-visible spectroscopy modified from literature (Dhawan et al., 2006). Standard dilution series of C₆₀ (0–40 mg/L) were prepared in toluene, and their absorbance at 335 nm was recorded on a UV/Vis spectrophotometer (Ultraspec 3300 pro, Aersham Biosciences) with pure toluene as a baseline to prepare the calibration curve. For measurements during the experiments, a 5-ml nC₆₀ sample was placed into a 20-ml beaker and kept in an oven at 95 °C until completely dry. The dry deposit was dissolved in toluene and transferred into a 50-ml flask for subsequent UV-Vis absorbance measurements, and concentrations of C₆₀ were calculated with previously recorded calibration curves. The particle size of Aqu-nC₆₀ was measured by a Field Flow Fractionation (FFF) separation system (CF2000, Centrifugal FFF) with light scattering detector (PN3070). A UV detector at a wavelength of 254 nm was used as a concentration detector to determine relative amounts of the eluted particles.

2.2.2.2 Particle morphology by TEM

Transmission electron microscopy (TEM) was performed to morphologically characterize the particle suspensions. Both pristine particles as well as particles incubated in culture media for 24 h at 30 °C or 28 °C were analyzed. The samples were prepared by dropping aliquots of the particle suspensions onto carbon-coated copper grids and leaving the solvent to evaporate. Subsequently the samples were analyzed using a JEOL 2100 HT (JEOL Ltd., Japan) operated at an accelerating voltage of 200 kV with integrated Energy Dispersive X-ray (EDX) spectroscopy (Oxford Inca). The size of the particles (ferret diameter) in the TEM micrographs was measured using the image processing and analysis software ImageJ (National Institutes of Health, USA).

2.2.2.3 Particle size distribution by Zeta Sizer

The average hydrodynamic particle size (Z-average) of fullerene and fullerenol was determined by means of dynamic light scattering (DLS) using Zetasizer Nano ZS Plus apparatus (Malvern Instrument Ltd., Malvern, UK; Zetasizer Ver. 6.01 and Serial Nr. MAL1016038). RPMI-1640 medium was used as a background control. For each concentration time point, at least four measurements were taken. The auto-mode for was used for determining number of run per measurement, the attenuator and the number of runs per measurement.

2.2.2.4 Measurement of suspension stability

Zeta potential (ζ -Potential) measurements were performed using disposable capillary cuvettes and the Zetasizer Nan-ZS Plus apparatus. The zeta potential of fullerene and fullerenol in MilliQ are reported.

2.3 Interaction of PCDD/F and C₆₀ fullerenes

2.3.1 Preparation of Aqu-nC₆₀ and its Blank

Aqu-nC₆₀ stock nanoparticle formulation was prepared by the solvent exchange method and the concentration was determined by the UV-visible spectrophotometric method as described by Andrievsky et al. (Andrievsky et al., 1995b). Specifically, C₆₀ fullerene powders (20 mg) were allowed to dissolve completely into 20 ml of toluene using a magnetic stirrer. This solution was referred to as the C₆₀-toluene stock solution. The purple C₆₀-toluene stock solution was transferred to a beaker containing 50 ml ultrapure water and 1.5 ml ethanol. The mixture then was sonicated using a dip probe sonicator (Bandline SONOPULS GM 70) operated until the toluene phase disappeared. The resulting yellowish/brown suspension was filtered through a 0.7- μ m glass fiber filter (Life Sciences, Pall Corporation, Michigan, USA). Several batches of these were prepared and mixed to prepare

a uniform stock solution and stored in a bottle covered by aluminum foil. Blank Aqu-nC₆₀ (treated water) was prepared as mentioned above except for the addition of fullerene (C₆₀).

2.3.2 Preparation of mixture

2.3.2.1 TCDD and Aqu-nC₆₀

The TCDD stock solution was prepared by dissolving in dimethylsulfoxide/ isopropanol (4/1 v/v). Two hundred µl of 50 ng/ml TCDD stock solution (was spiked separately in 20 ml scintillation vials with aluminium sealing of the cap) containing 10 ml of Aqu-nC₆₀ and its blank were taken. After spiking TCDD, samples were covered with aluminum foil to prevent possible photodegradation and were intermittently shaken at room temperature for 4 days. Afterwards, the samples were left undisturbed for more than 3 days to ensure sorption equilibrium. From Aqu-nC₆₀-TCDD and Blank-TCDD solutions, different dilutions were prepared.

2.3.2.2 PCB126 and Aqu-nC₆₀

PCB126 standard solution was prepared by adding 3.7 mg PCB126 in 10 ml of DMSO: IPA (4:1) and shaking until there were no visible particles. From this standard solution, two different sets of solutions were prepared. Set I; 2500, 10000, 20000 pg per ml of PCB126 in Aqu-nC₆₀ was prepared, Set II; 200 µl of PCB126 standard solution was added to 100%, 50%, 25%, 12.5%, 7.5% of Aqu-nC₆₀. After this procedure the samples were aged for seven days to ensure sorption equilibrium.

2.3.3 *In vitro* induction of EROD activity

In vitro EROD assays with the *H4IIE* rat hepatoma cell line were conducted according to the method described by Hofmaier et al (Hofmaier et al., 1999) and Schwirzer et al (Schwirzer et al., 1998) with slight modification. In brief, cells were plated at a density of ~10,000 cells/well in 96-well plates and cultured for 24 h prior to exposure. Culture media were then substituted with 100 µl media containing TCDD or test compounds. The

concentration of organic solvents in media was 0.5% in the final assay mixture. Various concentrations of compounds were added and the plates were incubated for 24, 48, and 72 h. At the end of the incubation time, exposure medium was substituted by 100 μ l of new DMEM containing 7-Ethoxyresorufin (8 μ M) and dicumarol (10 μ M). After 30 minutes incubation at 37 °C without plate cover, the 100 μ l reagent solutions were transferred to a second 96 well plate which already contained 200 μ l ethanol per well. After this, the fluorescence was measured at 535 nm excitation and 590 nm emission. Protein content was measured by employing the BCA-Protein Assay procedure.

In case of sequential exposure, cells were first exposed to Aqu-nC₆₀ for 24, 48 and 72 h then exposed to TCDD/PCB 126 for 24 h and the remaining procedure was similar as described above (co-exposure of Aqu-nC₆₀ and TCDD/PCB126). Cytotoxicity was determined by the resazurine assay. Experiments were repeated on several batches of cells. Data were stored in a spreadsheet with Microsoft Excel 2010 software.

2.3.4 Metabolic Activity Measurement

This test was carried out directly after the EROD-assay. After performing the EROD-assay, the cells are fixed with 50 μ l 1.2 % Glutaraldehyde solution per well. After 5-10 minutes this solution is taken away and wells are washed with 200 μ l of PBS twice. Then, a mixture of Resazurin solution/DMEM culture medium 1 % (i.e. 200 μ l of Resazurin in 19.8 ml DMEM) was done and 200 μ l of this solution were given per well with a multi-channel pipette. The plates were covered with a lid. After 90 min incubation at 37 °C, fluorescence was measured at 535/590 nm excitation/emission (Tecan Fluorostar). The fluorescence of wells incubated with extracts were compared in percentage to the amount of fluorescence achieved in a control sample (in quadruplicate) incubated only with a mixture of medium with 0.5 % DMSO/Isopropanol 4:1.

The dye binds intra-cellular to carboxyl- and phosphate groups of lysosomic membranes of intact cells. The amount of resazurin uptake in the cells correlates directly with the amount

of undamaged cells. Percentages above 85 % of intact cells mean low toxicity values. In this case, the EROD test was considered successful and adequate to TE-equivalent quantification.

The cells were washed with 300 µl PBS twice, and then the plates are tapped gently in clean paper tissue to dry them. Plates were stored at -20 °C until performing the Protein test.

Note: Resazurin is light sensitive! The resazurin stock solution was done dissolving 100 mg Resazurin in 10 ml PBS.

2.4 Interaction of organic nanoparticles with dopaminergic system in PC12 cells

2.4.1 Cell culture and nanoparticle treatment

The PC12 cell line (CRL-1721; LOT: 58650893) was obtained from American Type Culture Collection (Collection, 2011). Cells were cultured in 75 cm² flasks in RPMI-1640 medium supplemented with 10% horse serum, 5% fetal bovine serum (both heat inactivated), penicillin (50 units/ml) and streptomycin (50 mg/ml), in a humidified atmosphere with 5% CO₂ at 37 °C. At about 80% confluence of passage lower than fifteen, PC12 cells were transferred to 6-well plates at seeding density 10⁶ cells/ml, cultured for an additional 24 h, and then treated with one of the three types of nanoparticles. After 6 and 24 h of treatment, cells were collected for RNA isolation and dopamine analysis.

2.4.2 Detection of Catecholamine in PC12 by HPLC-ED

Instrumentation and reagents:

The quantitative estimation of noradrenaline and dopamine from PC12 cell and biological control materials were performed employing high-performance liquid chromatography (HPLC)-electrochemical detection (ED).

The HPLC system consisted of a GP40 gradient pump, an ED40 electrochemical detector, AS50 autosampler (all items were purchased from Dionex Corporation, 1228 Titan Way, Sunnyvale, CA 94085, USA). AS50 auto-sampler was equipped with a 100 μ l loop. An analytical column “Clin Rep® Catecholamines in Plasma” was filled with reversed-phase C18 material (Recipe, Munich, Germany) is kept in a column oven, which maintains constantly 25°C temperature. A PEEK pre-column filter with a 3 μ m Peek/PTFE frit (Recipe, Munich, Germany) is placed between the sample injection valve and the HPLC column to protect the column from particles originating from the sample and pump/valve seal-wear. The ED40 amperometric detector (Dionex) was used to control detector voltage and record the current. A glassy carbon electrode (Dionex) served as the working electrode, and is used together with an Ag/AgCl reference electrode and a stainless steel auxiliary block as the counter electrode (all from Dionex, Germany). That working electrode is manually set at a potential of +700 mV versus Ag/AgCl reference electrode. The total run time of analysis is fixed for 15 min (with re-equilibration of the column) at a flow rate of 0.5 ml/min. Current flow is maintained below 10 nA by polishing the working electrode to achieve a more sensitive detection of catecholamines.

The mobile phase was purchased from the Clin Rep® commercial HPLC kit which is used in a completely isocratic mode for the determination of catecholamines. The sample preparation columns including elution vials containing aluminium oxide suspensions for the adsorption of catecholamines and other necessary solutions (buffers for adsorbing, washing etc.) were purchased from the ‘Clin Rep® Catecholamines in Plasma kit’. The internal standard solution (3, 4 dihydroxybenzylamine, DHBA) and standard solution for external calibration containing noradrenaline, adrenaline, DHBA and dopamine were also collected from the Clin Rep® commercial HPLC kit.

2.4.3 RNA isolation and cDNA synthesis

Total RNA isolation

In this procedure, total RNA is isolated from the PC12 cells and purified. All RNA molecules longer than 200 nucleotides are purified, providing an enrichment for mRNA since rRNA and tRNA are size selectively excluded (<200 nucleotides). First, the PC12 cells are lysed and homogenised. The purification is then achieved by total RNA binding to a column whereas impurities are washed away. After this, the purified RNA is eluted with water.

Approximately 10^6 cells were collected for each sample. Total RNA was extracted from viable cells using QuatiTect® Reverse Transcription Kit (Qiagen, Germany) following the manufacturer's protocol. RNA quantity was measured using a NanoDrop1 ND-1000 UV-Vis Spectrophotometer (NanoDrop Technologies, Wilmington, DE).

Procedure

All steps of the procedure are performed quickly at room temperature to avoid RNA degradation. Amount of starting material: Each well contains at the end of the bioassay incubation approximately 1×10^5 cells. According to kit estimations, 10^5 animal cells yield to 1-3.5 μg of total RNA. As the purified RNA is collected in 40 μL of water, the concentration of total RNA in elute should be, at least, 25 $\text{ng}/\mu\text{L}$. The purified RNA amount is determined with a NanoDrop spectrophotometer. These amounts are clear below the maximum binding capacity of the column (100 μg) and below the maximal amount of starting material (1×10^7 cells).

1.-Wash the cells on the plate

Remove the medium and rinse the wells once with 200 μ L of sterile, RNase free PBS, tap the plates on clean paper tissue.

2.-Disrupt the cells by adding Buffer RLT

Add 200 μ L of buffer RLT. Using 300 μ L aerosol resistant tips, lyse the cells by pipetting up and down the RLT buffer of each well 10 times (avoid contact of the foam with the tip filter).

Note 1: Ensure that no cell clumps are visible before proceeding to step 3.

Note 2: Buffer RLT may form a precipitate upon storage. If necessary, re-dissolve by warming, and then place at room temperature (15-25°C).

3.-Create binding conditions by adding ethanol 70 %

Dispense the lysate into an RNase free Eppendorf tube. In case of non-homogeneity, vortex the mix (incomplete homogenization can cause clogging in the column). Then, add 200 μ L of 70% ethanol to generate appropriate binding conditions to the column. Mix thoroughly to assure homogeneity.

4. Transfer completely the sample (and any precipitate that may have formed) to an RNeasy spin column placed in a 2 mL collection tube.

Close the lid gently and centrifuge for 15 s at ≥ 10000 rpm. Discard the flow-through.

Reuse the collection tube in step 5.

5.-Add 700 μ L of buffer RW1 to the RNeasy column.

Close the lid gently and centrifuge for 15 s at ≥ 10000 rpm. Discard the flow-through.

Reuse the collection tube in step 6.

6.-Check that ethanol has been added to the RPE buffer before use (addition of 4 volumes of ethanol 96-100 % to the working solution). Add 500 μ L of buffer RPE to the RNeasy column to wash the membrane.

Close the lid gently and centrifuge for 15 s at ≥ 10000 rpm. Discard the flow-through.

7.-Add 500 μ L of buffer RPE to the RNeasy column to wash the membrane for a second time.

Close the lid gently and centrifuge for 2 min at ≥ 10000 rpm. Discard the flow-through.

Empty the collection tube and centrifuge for an additional minute.

Note: The long centrifugation dries the spin column membrane, ensuring that no ethanol is carried over during RNA elution. Residual ethanol may interfere with downstream reactions. After centrifugation, carefully remove the RNeasy spin column from the collection tube so that the column does not contact the flow-through. Otherwise, carryover of ethanol will occur.

8.-Place the RNeasy spin column in a new 2 ml collection tube and discard the old one.

Close the lid gently and centrifuge at full speed for 1 minute.

9.-Elution: place the RNeasy spin column in a fresh 1.5 ml tube; add 40 μ L of RNase-free water directly to the membrane.

Close the lid gently and centrifuge for 1 min at ≥ 10000 rpm to elute the RNA. Keep at 80°C until use.

Measurement of the isolated RNA

The NanoDrop ND-1000 Spectrophotometer with the software ND-1000 v3 1.2 (password: Adamski) is used (Building 34, Room 0318 BIO I). Select “*Nucleid acid*” mode. Under “*Sample type*” Select “*RNA-40*” measurement mode. Place 1.5 μ L HCl 5 % in the dropper to clean the device. After initialization, dry the surface delicately with a paper tissue. Clean with 1.5 μ L bi-distilled water and dry again. This step is to avoid HCl remains in the system that could damage the RNA sample. Place 1.5 μ L bi-distilled water and press “*Blank*”. This

is the blank reference. After drying the surface with a paper tissue, place 1.5 μL of sample and press “*Measure*”. In the screen will be displayed the RNA concentration and the absorbance spectrum. Clean the NanoDrop measurement surface with HCl 5 % and water before leaving. Working principle: The UV absorbance at 260 nm is used to determine the RNA concentration whereas the RNA purity with respect to protein contamination is analysed calculating the 260 nm/280 nm ratio. Lower ratios ($< 1.6/1.8$) indicate RNA contamination by protein and above 2.1/2.2 mean nucleic acids degradation. A ratio of 2 means 100 % RNA purity. Lower 260 nm/230 nm ratios (< 1.0) indicate the presence of impurities in the RNA sample. Typical contaminants absorbing at 230 nm are guanidine, thiocyanate, and phenol. Insufficient resuspension of RNA can also mean lower 260 nm/230 nm ratios.

cDNA synthesis: Reverse Transcription

Introduction

Following the RNA isolation, the cDNA is synthesized from RNA template by reverse transcription. In this step the QuantiTect Reverse Transcription Kit (QIAGEN, Hilden, Germany) is used. This procedure consists of two parts: elimination of genomic DNA followed by the reverse transcription itself. The purpose of the mRNA to cDNA conversion is to obtain cDNA to be used as a template for quantitative real-time PCR. In addition, cDNA is more stable than RNA and can be stored for longer periods.

Procedure

Reagents and buffers are stored at -20°C . The reactions are carried out in a total volume of 20 μL with 14 μl of isolated total RNA that are approximately 300 ng (the protocol is optimized to work with a RNA range from 10 pg to 1 μg). Work on ice to minimize the risk of RNA degradation and try to avoid contamination of the RNA with RNases.

Thaw template RNA on ice. Thaw gDNA Wipeout Buffer, Quantiscript Reverse Transcriptase, Quantiscript RT Buffer, RT Primer Mix, and RNase-free water at room temperature (15-25 °C).

Mix each solution by flicking the tubes. Centrifuge briefly to collect residual liquid from the sides of the tubes and then store on ice.

Dissolve any precipitates in gDNA Wipeout Buffer by vortexing. If necessary, briefly incubate the buffer at 37 °C until the precipitates dissolve.

2. Genomic DNA elimination reaction (on ice)

Mix 2 µl of gDNA Wipeout Buffer, seven x with 12 µl of each template RNA. Keep the tubes on ice.

3. Incubate for 2 min at 42°C. Then place immediately on ice.

Note: Do not incubate at 42 °C for longer than 10 min.

Table 2: Genomic DNA elimination reaction components

Component	Volume/reaction
gDNA Wipeout Buffer, 7x	2 µl
Template RNA (diluted with RNase free water)	12 µl
Total reaction volum	14 µl

Prepare the reverse-transcription master mix on ice

The reverse-transcription master mix contains all components required for first-strand cDNA synthesis except template RNA. For convenience, pre-mix RT Primer Mix and 5 x Quantiscript RT Buffer in 1:4 ratio if RT Primer Mix will be used routinely for reverse transcription. This pre-mix is stable when stored at -20 °C. Mix and store on ice. Pipet 6 µl of the reverse-transcription master mix in each tube. Store on ice.

5. Add template RNA from step 3 (14 µl) to each tube containing reverse-transcription master mix.

Add the total volume of the Genomic DNA elimination reaction (14 µl). The total volume is 20 µl. Note: This process can be done with a total volume of 10 µl instead of 20 µl.

6. Incubate for 15 min at 42 °C.

7. Incubate for 3 min at 95 °C to inactivate Quantiscript Reverse Transcriptase

Store reverse-transcription reactions on ice and proceed directly with real-time PCR, or for long-term storage, store reverse-transcription reactions at -20 °C.

Note: The heating steps 3, 6, and 7 are carried out in a Robocycler PCR ((Building 34, Room 0339 BIO I)

Instructions for the Robocycler:

- a) Turn on the machine (rear switch). The screen will turn on.
- b) Turn on the control panel (frontal red switch).
- c) Place your 50 µL PCR tubes on the plate and close the lid being sure it is really hermetically closed (click sound).
- d) In the screen will be displayed the first window (window 1). There are in total 4 windows (4 steps) and each window allows setting the temperature (set temp) and time of each step. As we are not performing PCR be sure that the repetition cycles of the windows are set on 0.
- e) In window 1, set the desired temperature (42 °C) using the pink arrows and numbers. Set the heating time.
- f) Press Next window button. It will appear window 2. In windows 2 set the cycles and heating periods in 0. Repeat the procedure for windows 3 and 4.
- g) Press enter to accept the heating data.
- h) Press run to start the procedure. Press exit after finishing.

i) To heat 15 minutes at 42°C and then 3 minutes at 95°C (Cycle 1, windows 1), program the windows 1 and 3 such as indicated in e) but ignore windows 2. Set the number of cycles in one.

Real-time RT-PCR

SYBR Green method

Real time PCR allows the quantification of the starting amount of the cDNA synthesised from the extracted RNA template. The real-time PCR principle is based on the detection of a fluorescent reporter that increases with each cycle of amplification in the PCR. There are two methods to achieve this, with sequence specific probes (i.e. TaqMan Probes) or with a dye that binds double-stranded DNA (i.e. SYBR Green). In this stage of the work, the SYBR green dye was chosen to perform the real time PCR. It is not so accurate as sequence specific probes (it binds to any generated double stranded DNA product) but cheaper and allows assessing if the selected primers, general methodology, and operational steps are correctly working in this research.

Introduction

The QuantiFast SYBR Green PCR Kit is optimized for use in a two-step cycling protocol, with a denaturation step at 95 °C and a combined annealing/extension step at 60 °C. The PCR starts with an initial incubation step of 5 minutes at 95 °C to activate HotStarTaq Plus DNA Polymerase.

Procedure

1. Thaw the reagents (2 x QuantiFast SYBR Green PCR Master Mix, template cDNA, primers, and RNase-free water and mix the individual solutions).

Prepare 5 μ M solutions of the primers. Prepare a concentrated solution (100 pmol / μ l = 100 μ M) by diluting the primers in RNase free water, as indicated by the manufacturer for each primer.

Then take 10 μ l and dilute it to 200 μ L in RNase free water to obtain a 5 μ M solution.

Store the 5 μ M solution in ice during use.

2. Prepare a reaction mix

For 384-well block cyclers, the final reaction volume should be 10 μ l.

Due to the hot start, it is not necessary to keep samples on ice during reaction setup or while programming the real-time cycler.

3. Mix the reaction mix thoroughly and dispense 9 μ l into the PCR plate (384-well block).

5. Program your real-time cycler according to the program outlined in Table 3.

Data acquisition should be performed during the combined annealing/extension step.

The number of cycles is set on 40.

Table 3: Cycling condition for PCR

Step	Time	Temperature (°C)
PCR initial heat activation	5 min	95
2-step cycling	10 s	95
Combined annealing/extension	30 s	60
Number of Cycles	40	

6. Place the PCR plates in the real-time cycler and start the cycling program.

7. Only the first time the primers are used it is necessary to perform melting curve analysis of the PCR product(s) to verify their specificity and identity.

See the instructions below to perform a melting curve analysis with the real-time cycler 7900 HT.

Instructions for the real-time 7900HT Instrument (Applied Biosystems):

- Turn on the computer and the instrument.
- Click on the SDS 2.2 software icon. (No password is necessary, press OK)
- Go to File, select New, and New Document.
- In New document, select the type of assay (absolute quantification), type of plate (384 wells), and template (blank template). Click OK and it will appear a new plate document.

- e) Click the Instrument tab of the new open plate document.
- f) Click the Real-time or Plate-read tab.
- g) Click Connect. Note: This has to be done ½ hour before starting the measurement because the green detector needs a pre-heating to work properly.
- h) From the Tools menu, select Detector Manager.
- i) Choose the detector you need (SYBR) or click File, select New and the Add detector dialog box will appear. Passive reference: ROX (fluorescent signals are normalized).
- j) Copy the detector selected to the plate document. Configure in the plate the samples (standard, unknown) to be measured with the detector chosen. Absolute quantification “unknown” is all wells containing PCR reagents and test samples for quantification.
- k) Create a plate document and save it.
- l) In the Instrument tab, click the sample volume (µl) and type the volume of reactions to be run (10 µl).
- m) Configure the temperatures and times of each PCR step. In the Instrument tab, click Thermal Profile and give the times and temperatures. If performing an absolute quantification run with a dissociation curve (first time you use a primer), add a temperature ramp to generate dissociation curve data. From the Instrument tab, click Thermal Profile tab and click Add dissociation stage. The software inserts a T ramp at the end of the thermal profile.

Table 4: Primer sequences and T_ms for the amplification reactions of 11 genes in PC12 cells

Gene name	Primer sequence (5'-3')	T_m (°C)
<i>Comt</i>	CCTGACTTCCTGGCGTATG TTCTCCAAGCCGTCTACAAC	54.5
<i>Dat</i>	TGGACTTCTACCGACTCTG GGAGGTGGTGATGATTGC	52
<i>Gapdh</i>	AACCTGCCAAGTATGATG GGAGTTGCTGTTGAAGTC	48.2
<i>Gpr37</i>	CTCCAGGGTTCCCATTAC GTCGGTTAGTGCTATTCC	50
<i>Gpx1</i>	CATTGTTTGAGAAGTGCGAGGTG ACTGGGTGCTGGCAAGGC	58.3
<i>Gss</i>	CCAGCGTGCCATAGAGAAC CCCTTTCAGAGACATCTCAAATC	55
<i>Maoa</i>	CAGACACACCAGACAACAC TACGGACATAGGCACTGAG	52.7
<i>Park2</i>	CGGATGAGTGGAGAGTGC TGGCGGTGGTTACATTGG	53.6
<i>Snca</i>	ACTATGAGCCTGAAGCCTAAG CGTTGGAAGTGAAGCACTTG	53.7
<i>Th</i>	CTGTTCTCAACCTGCTCTTC TGGCTTCAAATGTCTCAAATAC	52.5
<i>Txnrd1</i>	TGGAAGAGCATGGTATCAAG CACGGTCTCTAAGCCAATAG	51.8
<i>Vmat2</i>	AGCATCTTCTTACTATAACAAC AAACAGCAGCCCAACTTG	52

Catechol-O-methyltransferase gene (*Comt*), dopamine transporter gene (*Dat*), glyceraldehyde-3-phosphate dehydrogenase gene (*Gapdh*), G protein-coupled receptor 37 gene (*Gpr37*), glutathione peroxidase 1 gene (*Gpx1*), glutathione synthetase gene (*Gss*), monoamine oxidase A gene (*Maoa*), parkin gene (*Park2*), α -synuclein gene (*Snca*), tyrosine hydroxylase gene (*Th*), thioredoxin reductase 1 gene (*Txnrd1*), and vesicular monoamine transporter-2 gene (*Vmat2*).

2.4.4 Cell viability and oxidative stress determination

The cells were fixed with 50 µl 1.2 % Glutaraldehyde solution per well. After 5-10 min, this solution was removed taken away and wells are washed with 200 µl of PBS twice. Then, a mixture of Resazurin solution/RPMI-1640 Culture medium 1 % (i.e. 200 µl of Resazurin in 19.8 ml RPMI1640) were prepared and 200 µl of this solution are added per well. The plates were covered with a lid. After 90 min incubation at 37 °C, fluorescence was measured at 535/590 nm excitation/emission (Tecan Fluorostar). The fluorescence of wells, incubated with extracts, was compared in percentage to the amount of fluorescence achieved in a control sample (in quadruplicate).

2.5 Interaction of organic nanoparticle with eukaryotic protozoa *T.*

thermophila

2.5.1 Population growth rate test

The ciliated protozoa *T. thermophila*, strain *SB210* from Stock Centre, Cornell University, USA was cultured at 28°C in 40 ml of proteose peptone yeast medium (PPY) as described in Schultz (1997). To prepare the culture for toxicity testing, 500 µl from stock culture was transferred into 40 ml of sterile PPY and grown for 2 days over the weekend. Then, 5 ml of culture was transferred to 40 ml of sterile PPY in Erlenmeyer flasks and grown for 24 h. During the exponential growth phase (10^5 cells/ml) the cells were harvested by centrifugation at 300 x g for 5 min and washed twice with Osterhout's medium (Osterhout, 1906). For monitoring cell count, cells were immobilized with 10% formalin and counted using a haemocytometer under a low power (10 x) objective. Cells were adjusted to a cell density of 10^4 cells/ml. After exposure, 15 µl of cell suspension were mixed with 15 µl of 4% formaldehyde and then 30 µl of Trypan Blue solution was added. The cells were counted by means of haemocytometer at least two times and for three repeated experiments.

2.5.2 Determination of Cell viability

2.5.3 ROS generation

Generation of intracellular ROS in *Tetrahymena* cells was measured using ROS fluorescent probe 2', 7'- Dichlorofluorescein (DCDHF) diacetate (DA). Non-fluorescent probe DCFH-DA readily cross the cell membrane and then is hydrolysed by intracellular esterases to nonfluorescent 2',7'-Dihlorodihydrofluorescein (Bass et al., 1983). In the presence of ROS 2', 7'-Dihlorodihydrofluorescein rapidly converts to the fluorescent product 2, 7-dichlorofluorescein (DCF). The cells (1.4×10^5 cells/ml) were first incubated in microcentrifuge tubes (Costar, Cambridge, MA, USA, 2-ml capacity) with different nanomaterials (nC_{60} , $C_{60}(OH)_{24}$) for 6 and 24 h. After removing the suspension, cells were loaded with 120 μ M DCFH-DA in Osterhout's medium for 45 min and incubated at 28°C in the dark. Because of the fluorescent probe, which could remain in cell suspension, dye was removed by centrifugation (300xg for 5 min). The cells were washed twice with Osterhout medium and transferred to 96-well plates for measurement. As a positive control for ROS assay, we first tested H_2O_2 with concentration range of 10-2000 μ M at different time point (up to 2 h). The fluorescence of dichlorofluorescein (DCF) was quantified using Tecan microplate reader (Tecan Spectra Fluor Plus, Crailsheim, Germany) at the excitation and emission wavelengths of 485 and 535 nm, respectively.

2.5.4 Determination of Catecholamines

CAs can be determined by the usage of different methods. One option is the radio enzymatic analytical method. The disadvantage is the performance of an additional thin layer chromatography step to differentiate A, NA and DA (Koch and Polzin, 1987). Another method is the detection using gas chromatography combined to mass spectrometry (GC/MS) after derivatisation of catecholamines. This method is expensive, time consuming

and not suitable for routine catecholamine analysis (Kumar et al., 1991). For sensitive, specific and rapid detection and quantification of CAs in plasma the most popular technique is still high performance liquid chromatography connected to an electrochemical detector (HPLC/ECD) (Durstewitz et al., 1999, Tormey et al., 1999, Valet and Saulnier-Blache, 1999). The presence of the 1,2-benzenediol structure in CAs leads to electrochemical activity (oxidative conversion to the o-benzoquinone form) and thus measurability by EC detection. For this detection method, no chemical transformation is needed and it is possible to detect Catechol related substances. Some studies used HPLC connected to an ultra violet (UVD) or fluorometric detector (FD). The disadvantage of this method is the unspecific UV and F detector, which are not sensitive enough to detect CAs through the background noise. The quantification of substances in biological samples is generally difficult because a large number of biogenic substances can disturb the analysis. The used EC detector can detect CAs selective and specific caused by the fact that only compounds can be detected which oxidize on the surface of the working electrode under the used voltage conditions. The resulting rising current is proportional to the concentration of the oxidized compound and CAs can easily, sensitively and specifically identified.

The quantitative estimation of noradrenaline, adrenaline and dopamine from PC12 or *Tetrahymena thermophila* cell and biological control materials was performed employing high-performance liquid chromatography (HPLC)-electrochemical detection (ED).

The HPLC system consisted of a GP40 gradient pump, an ED40 electrochemical detector, AS50 autosampler (all were purchased from Dionex Corporation, 1228 Titan Way, Sunnyvale, CA 94085, USA). AS50 auto-sampler was equipped with a 100- μ l loop. An analytical column "Clin Rep® Catecholamines in Plasma" was filled with reversed-phase C18 material (Recipe, Munich, Germany) is kept in a column oven that maintains constantly 25°C temperature. A PEEK pre-column filter with a 3- μ m Peek/PTFE frit (Recipe, Munich, Germany) is placed between the sample injection valve and the HPLC

column to protect the column from particles originating from the sample and pump/valve seal-wear. The ED40 amperometric detector (Dionex) was used to control detector voltage and record the current. A glassy carbon electrode (Dionex) was served as the working electrode, and is used together with an Ag/AgCl reference electrode and a stainless steel auxiliary block as the counter electrode (all from Dionex, Germany). That working electrode is manually set at a potential of +700 mV versus Ag/AgCl reference electrode. The total run time of analysis is fixed for 15 min (with re-equilibration of the column) at a flow rate of 0.5 ml/min. Current flow is maintained below 10 nA by polishing the working electrode to have a more sensitive detection of catecholamine.

The mobile phase was purchased from the Clin Rep® commercial HPLC kit which is used in a completely isocratic mode for the determination of catecholamine. The sample preparation columns including elution vials containing aluminium oxide suspensions for the adsorption of catecholamine and other necessary solutions (buffers for adsorbing, washing and etc.) were purchased from the 'Clin Rep® Catecholamines in Plasma kit'. The internal standard solution (3,4 dihydroxybenzylamine, DHBA) and standard solution for external calibration containing noradrenaline, adrenaline, DHBA and dopamine were also collected from the Clin Rep® commercial HPLC kit.

Blood plasma samples (biological control materials, level I+II, Recipe, Munich, Germany) are pipetted together with 200 µl (=2000 pg) internal standard DHBA into the sample preparation columns and extracted according to the instruction manual of the manufacturer (Thomas, 1998). Samples of PC12 were also extracted and measured under identical conditions as described for blood plasma samples.

The analytical precision, accuracy and the lower limits of determination were determined from biological control materials. The recovery rates for the catecholamine in the control

samples and PC12 samples are above 80%. The detection limit for all catecholamine in HPLC-ED is below 5 ng/L.

Prior to the detection step, each sample was extracted. The sample preparation column contains a defined amount of activated aluminum oxide (22 mg), which was suspended in a 2M Tris-HCl buffer solution. The pH value of this buffer is adjusted to enable a maximal and selective adsorption of the catecholamine (received without pH information). Desired volume of cell culture and TRIS-buffer (1000 µL) is spiked with an internal standard (200 µL). These were placed into the sample preparation column. The columns are vortexed for 15 min. Therefore, the catecholamines were adsorbed at the aluminum oxide. The cell culture is now free of catecholamine and removed by vacuum station. Three consecutive washing steps removed interfering substances, being co-adsorbed at the aluminum oxide. Afterwards 160 µl catecholamine were eluted on stabilizing conditions from the sample preparation column. Finally 40 µl of elute was injected into the HPLC system.

The standard chromatogram of a catecholamine mixture was compared with the chromatogram of analyte present in the test sample. Each chromatogram has been compared with that of the standard. The peaks of analyte in the standard mixture were checked whether they represented and correlated to the analyte in the sample with respect to the retention time. Concentration of catecholamines was calculated by the recovery of internal standard (IS) is as follows formulas:

$$REC = \frac{Area_{IS, Sample} \times 10 \times 160}{Area_{IS, Standard} \times 3 \times 2000}$$

Where, Sample amount = 3; Amount of IS in 200 µL = 2000 pg; Elution volume of sample = 160 µL Concentration of IS = 10 pg/µL

2.6 Expression changes of selected genes in *T. thermophila* by carbon based nanoparticles

2.6.1 RNA isolation and Real-time RT-PCR

Approximately 10^6 cells were collected from each sample. Total RNA was extracted from viable cells using QuatiTect® Reverse Transcription Kit (Qiagen, Germany) following the manufacturer's protocol. RNA quantity was measured using a NanoDrop1 ND-1000 UV-Vis Spectrophotometer (NanoDrop Technologies, Wilmington, DE).

After the RNA isolation, cDNA synthesis was performed using QuantiTect Rev. Transcription Kit 205310 (Qiagen GmbH, Germany). Real-time quantitative PCR was performed as per the protocol mentioned in QuantiFast SYBR Green PCR Kit 204054 (Qiagen GmbH, Germany) using AB7900HT (Applied Biosystems, USA). Each PCR reaction was conducted in a total volume of 10 μ l: 1 μ l of cDNA was mixed with 9 μ l of QuantiFast SYBR Green master mix. The PCR reactions were performed in 384-well plates (ABgene®PCR Plates, ThermoScientific) with MicroAmp Optical Adhesive Film (Applied Biosystem, USA). The cycling parameters: a 5 min PCR initial heat activation at 95 °C; followed by 40 cycles of 2-step cycling: denaturation at 95 °C for 10 s and combined annealing/extension at 60 °C for 30 s; gradual ascending temperature ladders for generating melting curves. Each reaction was run at least in duplicate and the mean value was used for calculation.

2.6.2 Analysed genes

Gene expression analysis was carried out on the following genes: *β -actin*, *Dopamine β hydroxylase*, *Glutathione S-transferase*, *Catalase*, and *Calcium translocating P-type ATPase*. Primers for the genes, whose function is described in the Tetrahymena Genomic Database (TGD: <http://ciliate.org/index.php/home/welcome>), were designed using Primer 3

software (<http://frodo.wi.mit.edu/>) and specificity of primer sequences was confirmed using NCBI Primer BLAST software (<http://www.ncbi.nlm.nih.gov/tools/primer-blast/>). The primers used in the study are listed in table 5.

Table 5: List of primers and genes used in SYBRGreen qPCR expression analysis.

Gene	Forward Primer	Reverse Primer	Amplicon Size	Accession no.
β – actin	CGTTGACTCTGGTGATGGTG	TCGGCAGTGAAGAGAAGTT	159 bp	THERM_00190950
Dopamine β hydroxylase 2*	CAGCATCTATTGCTGGGTC	GGCAACATCCAAAAGAGGAG	239 bp	THERM_00158280
Catalase (CAT1)*	AAGTTCTGCAAGGCCAAGGT	TAGCGCACTTGAGGTTGGTT	262 bp	THERM_01146030
Glutathione Peroxidase	TGGTTCATACATGCATCCTCTC	GAAGCGGCGTAAAATGAAAC	150 bp	THERM_00661720
Glyoxalase	AAAGAGGTGCCAAGTGTGCT	AAGGGGGTCCTTAAGGGGT	173 bp	THERM_00678260
Calcium-translocating P-type ATPase*	TGGCACAAAAAGTAAGATGACCAAA	ACCAAAGATAGCATGTAAAGTAAGG	213 bp	THERM_00780510
Glutathione S transferase*	GGAGTTGGCAAGGGTCCTAATGATG	GGGAGAAGGAAGGTGTTTTACCTTG	194 bp	THERM_00077550

2.6.4 Dichlorofluorescein Assay

Generation of intracellular ROS in *Tetrahymena* cells was measured using ROS fluorescent probe 2', 7'-Dichlorofluorescein (DCFH) diacetate (DA). Non-fluorescent probe DCFH-DA readily cross the cell membrane and then is hydrolyzed by intracellular esterases to nonfluorescent 2',7'- Dichlorodihydrofluorescein (Bass et al.,1983). In the presence of ROS 2', 7'-Dichlorodihydrofluorescein rapidly convert to the fluorescent product 2, 7-dichlorofluorescein (DCF). The cells (1.4×10^5 cells/ml) were first incubated in microcentrifuge tubes (Costar, Cambridge, MA, USA, 2-ml capacity) with different nanomaterials (nC_{60} , $C_{60}(OH)_{24}$) for 6 and 24 h. After removing the suspension, cells were loaded with 120 μ M DCFH-DA in Osterhout's medium for 45 min and incubated at 28°C in

the dark. Because of the fluorescent probe, which could remain in cell suspension, dye was removed by centrifugation (300xg for 5 min). The cells were washed twice with Osterhout medium and transferred to 96-well plates for measurement. As a positive control for ROS assay, we first tested H₂O₂ with concentration range of 10-2000 μ M at different time point (up to 2 h). The fluorescence of dichlorofluorescein (DCF) was quantified using Tecan microplate reader (Tecan Spectra Fluor Plus, Crailsheim, Germany) at the excitation and emission wavelengths of 485 and 535 nm, respectively.

2.7 Statistical analysis and software used

GraphPad Prism® (version 6.02 for Windows; Graph Pad Software, San Diego, CA) was used for statistical analysis with the Significant differences among treatments were determined by ordinary one-way analysis of variance. Statistically significant differences (Ordinary one-way ANOVA followed by Holm-Sidak's multiple comparison test), are indicated with an asterisk (* $p < 0.05$, ** $p < 0.01$, *** $p < 0.001$). For the relative quantitation of mRNA transcripts of the target genes, a $2^{-\Delta\Delta C_t}$ method was used (Schmittgen and Livak, 2008). Results are presented as fold changes compared to untreated controls.

Results and Discussion

Chapter 3: Results and Discussion

3.1 PCDD/F and C₆₀ fullerenes

The measured C₆₀ content in the stock suspension was 54 ± 0.8 mg/L (n = 3). The average radius of gyration of samples were 37 nm (n-average), 62 nm (w-average) and 121 nm (Z-average) as measured by CF2000, and therefore an aggregated nanoparticle consist of approximately 120 molecules of C₆₀, and considering the weighted-average particle size and spherical distribution, 5×10^{15} nanoparticles are present per ml. The average Zeta potential was -34.8 mV.

3.1.1 TCDD and Aqu-nC₆₀

Induction of EROD activity was measured after 24, 48, and 72 h as summarized in Fig. 3, which depicts induction of EROD activity by TCDD as standard, co-exposed with fullerene C₆₀, and in the presence of a matrix without C₆₀. The results show that there is no visible difference in induction activity during different co-exposure experiments. Also, there was no concentration of any test compound that was cytotoxic as determined by the resazurine assay (data not reported). The enzyme induction after 24 h of TCDD application was higher than after 72 h. Moreover, in a sequential exposure experiment, there was no significant difference between measurement of EROD activity in wells pre-exposed to Aqu-nC₆₀ for 24, 48, 72 h and that of control, after 24 h. The ability of nanoparticles to pass the cell membrane and, adsorption of dioxin to the fullerenes (because of high surface to volume ratio of nanoparticles) suggest that the coexistence of C₆₀ nanoparticles and TCDD might change the fate and behaviour of the latter. However, contrary to the hypothesis, we found that C₆₀ nanoparticles did not alter the induction of EROD activity by TCDD significantly.

3.1.2 PCB 126 and Aqu-nC₆₀

a. With increasing PCB 126 concentration

0.1, 0.4, 0.8 pmol per ml of PCB 126 was added to each well of a set (n=7) containing approximately 98 pmol of C₆₀ in each well. The significant ($p < 0.05$ %), very ($p < 0.01$ %) and highly significant ($p < 0.001$ %) increases in induction at 0.8 pmol per ml of 48 h, 0.1 and 0.4 pmol per ml of 72 h, respectively. as shown in Figure 5. To assure the typical response, TCDD standards were also measured in the plate.

b. With constant PCB126 concentration

Figure 6 shows the EROD induction response for 24, 48, 72 h incubation when each well of the 96-well plate contains an equal amount of PCB126, and varying amounts of C₆₀. All the readings with fullerenes are higher compared to the fullerenes. 72 h inductions of EROD activity in wells with Aqu-nC₆₀ were always 11-38 % higher than the inductions of the corresponding wells with no fullerenes. At higher concentrations *i.e.* at 24.5, 49 and 98 pmol per well 3.021 pmol per ml of PCB126 shows a very significant response ($p < 0.001$ %) for the 72 h incubation period. During the sample measurement, TCDD standards were also measured in the same plate.

c. With sequential exposure of Aqu-nC₆₀ and PCB-126

Figure 7 shows the percent change of induction of EROD activity when H4IIE cells were pre-exposed to 98 pmol of C₆₀ for 24, 48, 72 h, and then exposed to PCB 126 (7.56, 15.11 and 30.22 pmol) for 24 h. The results show that the induction of EROD activity by PCB126 is influenced by pre-exposure of C₆₀ and resulted into ~100 percent increase in the response. This increase was almost 2-fold of a 15.11 pmol/ml concentration of PCB 126 after an incubation time of 48 h.

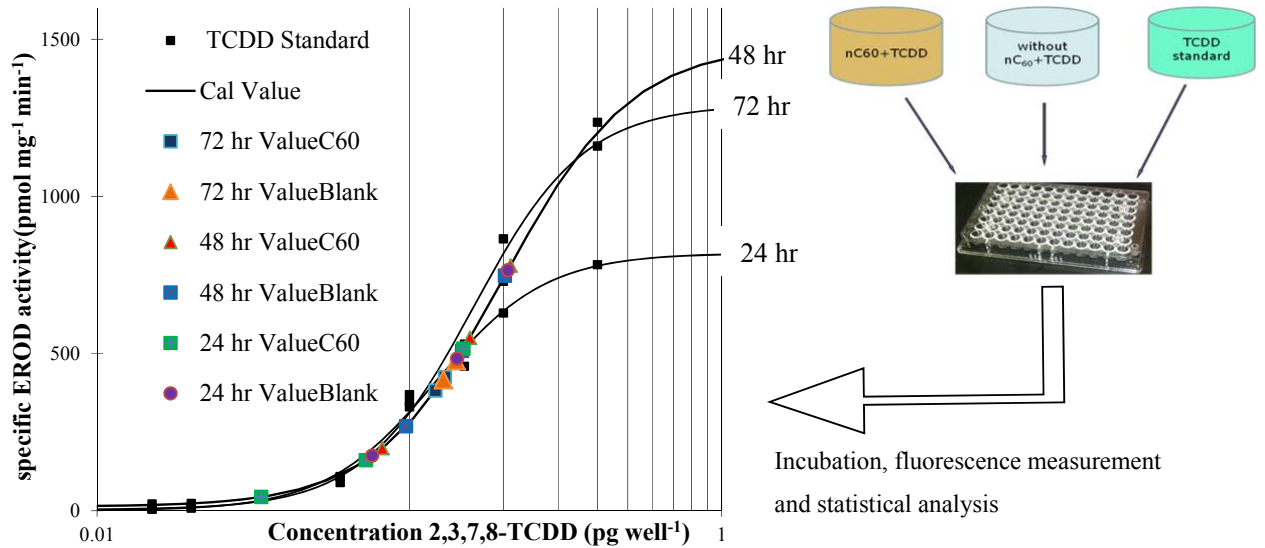


Figure 3: Induction of EROD activity *in vitro* by TCDD with nanoparticle formulation of C₆₀ and TCDD combined or TCDD (X hr ValueC60) with blank matrix without C₆₀ (X hr ValueBlank) after 24, 48, and 72 h of incubation. Blanks were prepared but without C₆₀ and amount of TCDD added were similar to that of experimental sample. The regression curves show concentration-response of TCDD (TCDD Standard) after 24, 48, and 72 h exposure (Cal Value). As it can be seen that there is no difference between EROD activity with and without C₆₀.

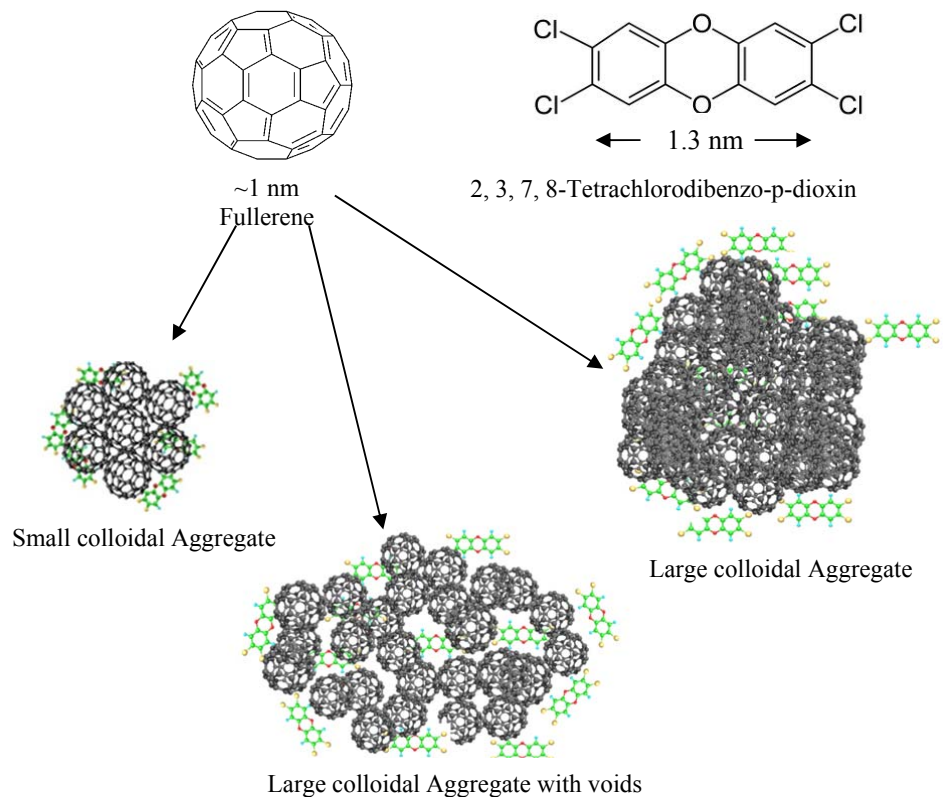


Figure 4: Adsorption and entrapment of TCDD by fullerene nanoparticles

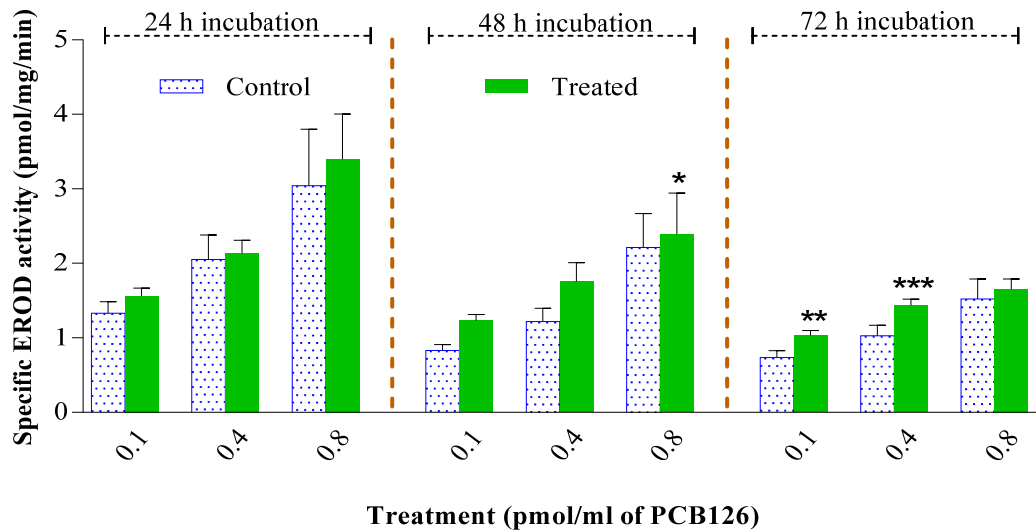


Figure 5: 24, 48, 72 h *in vitro* induction of EROD in H4IIE cells by 0.1, 0.4, and 0.8 pmol of PCB 126 per ml in presence of Aqu-nC₆₀ and corresponding control. Control samples were same as sample containing Aqu-nC₆₀ but without fullerenes. Data points and error bars represent the mean and standard error of the mean (SEM) of three independent experiments. Statistically significant differences (Ordinary one-way ANOVA followed by Holm-Sidak's multiple comparison test), are indicated with an asterisk (* p<0.05, ** p<0.01, *** p<0.001)

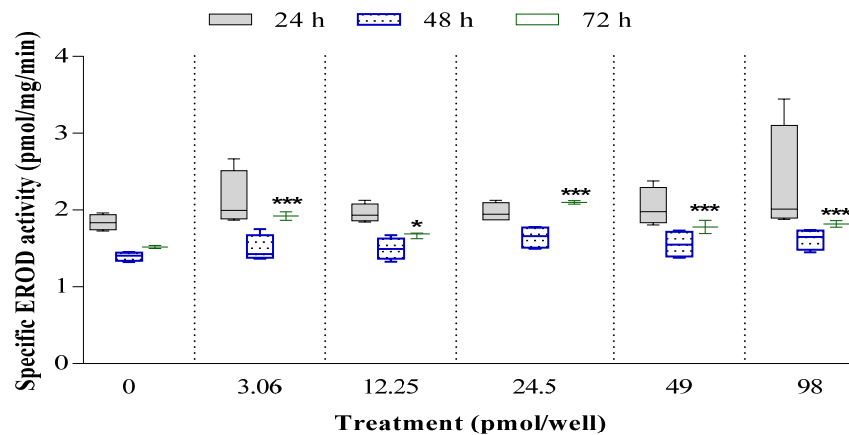


Figure 6: EROD activity by 3.021 pmol per ml of PCB126 in presence of 0, 30.6, 122.5, 245, 490 and 980 pmol per ml of C₆₀ during 24, 48 and 72 h incubation period. Statistically significant differences (Ordinary one-way ANOVA followed by Holm-Sidak's multiple comparison test), are indicated with an asterisk (* p<0.05, ** p<0.01, *** p<0.001). Data points and error bars represent the mean and standard error of the mean (SEM) of at least three independent experiments, in which each treatment was applied four times.

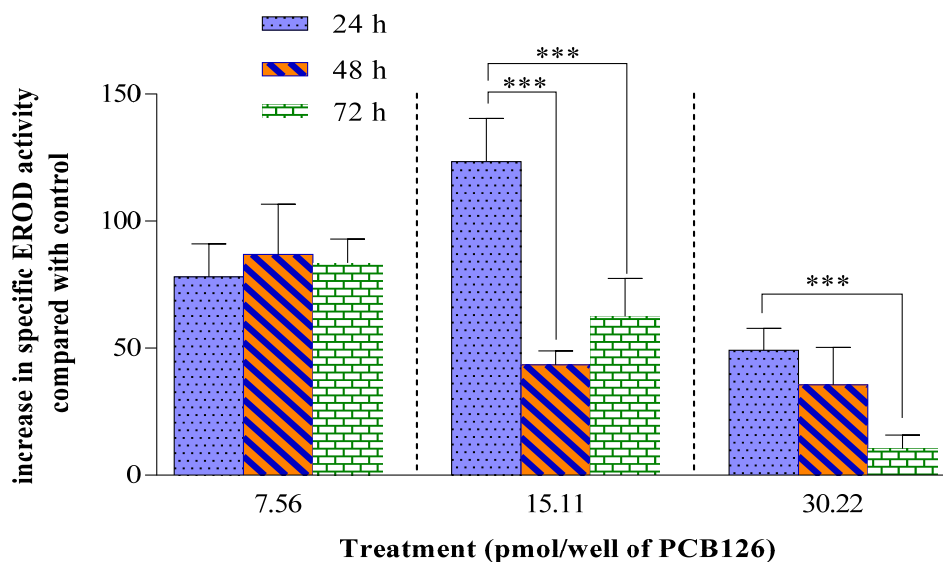


Figure 7: The effects of Aqu-nC₆₀ in H4IIE cells. Cells were exposed to a medium with or without nano-C₆₀ (980 pmol per ml) for 24, 48, 72 h before the addition of fresh medium containing different concentration of PCB-126. Data points and error bars represent the mean and standard error of the mean (SEM) of four independent experiments. Statistically significant differences (Ordinary one-way ANOVA followed by Holm-Sidak's multiple comparison test), are indicated with an asterisk (***) p<0.001)

3.1.3 Discussion

The aqueous suspension of nC₆₀ used in this study for exposure of TCDD/PCB 126 likely consists of aggregates of heterogenous size (in the range of several hundred nanometer) as has been reported in other studies of nC₆₀ (Chang and Vikesland, 2009, Park et al., 2010). The aggregated nC₆₀ likely had a large surface area and in turn, has more adsorption sites such as surface, groove area, and interstitial pores where chemicals can associate (Pan et al., 2008). Free energy calculations indicate that, although dissolving a fullerene aggregate in water presents a high energetic cost, the energy gain of transferring fullerene inside a lipid bilayer is higher, so the balance of the overall process is thermodynamically favorable (Oberdörster, 2004a). It has been reported (Long and Yang, 2001) that there is adsorption of dioxin on fullerenes which indicates that coexistence and concomitant complex formation

of C₆₀ nanoparticles and TCDD is most likely and one of the mechanisms for fullerene nanoparticles in changing the fate and behaviour of the latter. On the contrary, we found that the presence of C₆₀ nanoparticles did not alter the induction of EROD activity by TCDD significantly. This might be due to the essentially planar and rigid stereochemistry of TCDD.

As the absence of unsaturated bonds at the surface of C₆₀, a different interaction with adsorbates can be expected. For example, it has been reported that cellular uptake of gold nanoparticles is mediated by nonspecific adsorption of serum proteins onto the gold surface (Deguchi et al., 2007). The gold nanoparticles enter into the cells via the receptor-mediated endocytosis pathway, in which the protein on the surface binds to a receptor on the cell's surface, and the particles then enter the cell where they might release the adsorbed TCDD. We also measured the affinity of C₆₀ nanoparticles to the AhR by comparing to the potency of these ligands to induce EROD activity. Moreover, it was found that there was no induction of EROD activity when only nC₆₀ was present (data not reported).

The “Trojan horse” concept implies a facilitated entry of toxic molecules adsorbed to nanoparticles into the cells (Limbach et al., 2007). Although the concept of Trojan horse in many studies is implicitly used in nano drug delivery, it can also apply in fate and behavior of xenobiotics. Figure 4 shows the possible scheme of adsorption of TCDD for fullerene. Two possible types of adsorption sites have been proposed for carbonaceous (geo-) sorbents (Haitzer et al., 1998): (i) adsorption on external surface, and (ii) adsorption in nanopores inside the sorbents. The adsorbate molecules might be entrapped in closed interstitial spaces between small aggregates- and would not be bioavailable for the induction activity. However, it cannot be ruled out to consider that this interaction would not only facilitate the entry of xenobiotics in the presence of C₆₀ but also the release from the nanoparticle once inside the cell.

As shown in Figure 5, readings in all three sets: 0.1, 0.4, 0.8 pmol per ml of PCB126 in presence and in absence of 980 pmol per ml of C₆₀ and, also with different time of incubation, for 48, 72 h incubation time; the concentration 0.1 and 0.4 pmol/ml of PCB 126 exhibits 34-51 percent higher EROD activity response (than the corresponding control without nC₆₀). Unlike the dissolved organic matter-associated highly condensed polycyclic aromatic hydrocarbons (PAHs) that are believed to be non-bioavailable (Haitzer et al., 1998), the Fullerene-associated TCDD/PCB126 might be bioavailable because fullerenes can pass through cell membranes and accumulate in living tissues as reported by Oberdöster which suggests that, despite their large size, fullerenes aggregates can penetrate cells and cross the blood-brain barrier (Wong-Ekkabut et al., 2008).

Figure 6 shows the EROD response in samples with increasing amounts of fullerenes and the control with no fullerenes. In case of sequential exposure, Figure 7, when nC₆₀ are pre-exposed, the effect of PCB 126 on EROD activity was found always higher than in the control. It seems that the prior presence of nC₆₀, attenuates the induction activity of PCB-126. This increase in EROD activity could be because of suppression of P450-dependent monooxygenases activities by nC₆₀ as demonstrated by Ueng et al (Ueng et al., 1997, Scown et al., 2010a) with hydrophilic fullerene derivatives both *in vivo* and *in vitro*. Nevertheless, there are reports in literature on P450 induction and inhibition by nanoparticles (Sereemasapun et al., 2008, Scown et al., 2010b, Balasubramanian et al., 2010) particularly by Fröhlich (Frohlich et al., 2010) where they reported that nonmetallic carboxyl polystyrene particles (20–60 nm) inhibited the enzymatic activity of several P450 enzymes (CYP3A4, CYP2D6, and CYP2C9) in both insect cell membrane preparations and liver microsomes, suggesting that nanoparticles can produce unexpected effects on liver cell functions.

3.2 Nanomaterial exposure to PC12 cells

The mean intensity and volume size distribution of fulleranol (Fig 8) and fullerene (Fig 9) samples in RPMI-1640 were determined by Dynamic Light Scattering (DLS) by means of Zetasizer. The theoretical hydrodynamic size of fulleranol is approximately two nm. In this study, fulleranol-RPMI samples exhibited mostly a bi-modal size distribution by intensity, with a small peak at around 35 nm accounting for substantial part of the total particle volume, Fig 8B. This 35 nm peak is indicative of fulleranol aggregates that were formed during sample preparation. Although fullerenols were readily soluble in aqueous based system - MilliQ water, these particles loosely aggregated and gradually precipitated out of solution, and the same could have occurred during the course of DLS sample preparation and measurement. The fulleranol-RPMI intensity peak at 3598 nm was primarily due to larger aggregates - corresponds to a minor (7.2 %) portion of the total particle volume visible as hump in intensity graph. The aggregation behavior, perhaps, owing to high salt-serum contents of RPMI-1640. Colloidal stability of suspension was determined by measuring zeta potential distribution. The mean zeta potential distribution of fulleranol-MilliQ was -29.9 mV (SD 0.45).

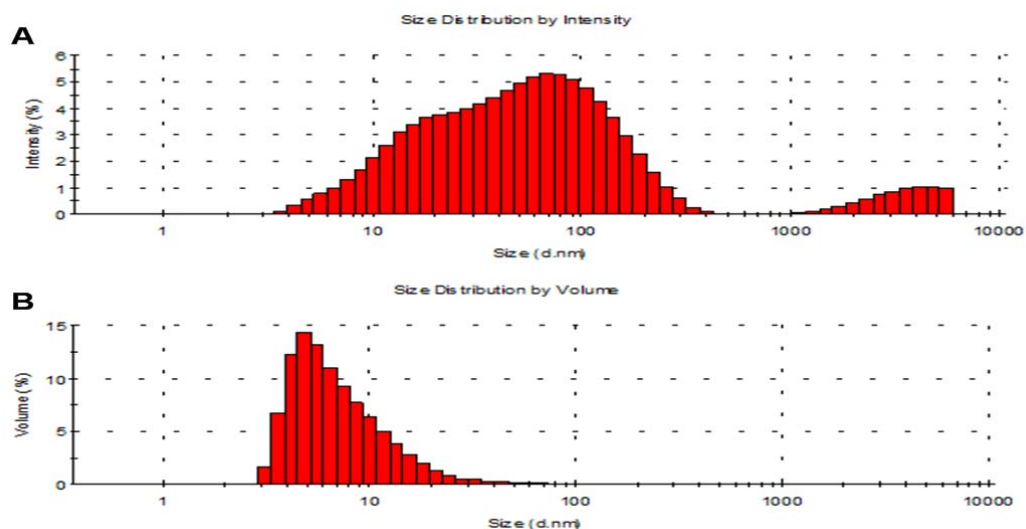


Figure 8: Fullerenol size distribution in cell RPMI-1640 A) by intensity, B) by volume. The hydrodynamic diameter of particle was 33.57 nm. The first peak (d. nm = 33.57 nm) in size distribution by intensity contributes 92.8 percent while second peak (d. nm = 3598 nm) contributes 7.2 percent.

Figure 10 shows the effect of different concentration of fullerene, fullerenol and Printex®90 on the dopamine (Fig. 10 a) and noradrenaline (Fig. 10 b) content in PC12 cells. Data indicate the dose dependent decrease of the dopamine content in PC12 cells; indeed, dopamine content of PC12 cells, after 6 and 24 h time point, decreases significant ($p < 0.001$) at higher concentration (50 $\mu\text{g/ml}$). However, One microgram per ml of nanomaterial, after 6 and 24 h, does not affect the noradrenaline content of PC12 cells. Moreover, no nanomaterial, at defined concentration, affects the noradrenaline content of PC12 cells at 24 h time point.

The reactive oxygen species (ROS) level, a cause of oxidative stress, increased with increase in fullerene concentration in a well of 96-well plate (Fig.11); however, fullerenol did not increase ROS level, except at 50 $\mu\text{g/ml}$ where it showed a ~ 4 -fold increase in ROS compare to control. The nanomaterial treatment did not induce a significant change in metabolic activity of cell (SI Fig. 1).

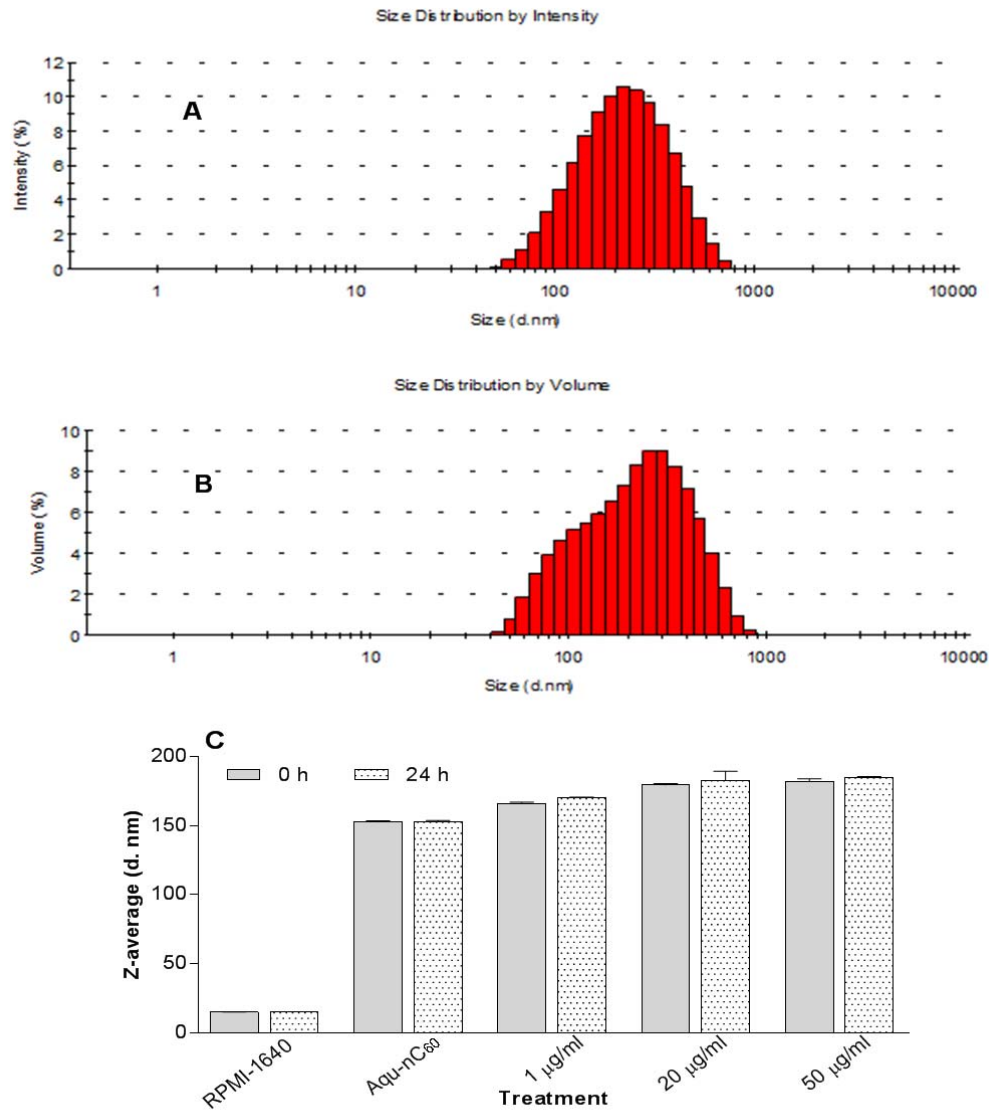


Figure 9: Laser diffraction hydrodynamic size data for fullerene in the RPMI-1640 medium used for *in vitro* toxicity experiments (obtained by means of DLS). The size distribution by A) intensity, B) volume in cell culture medium. Intensity-weighted average was used to determine hydrodynamic size, while volume distribution was used to determine relative amounts. The effect of dilution of suspension and time have no significant difference ($p < 0.01$) on the size of nanomaterial, section C.

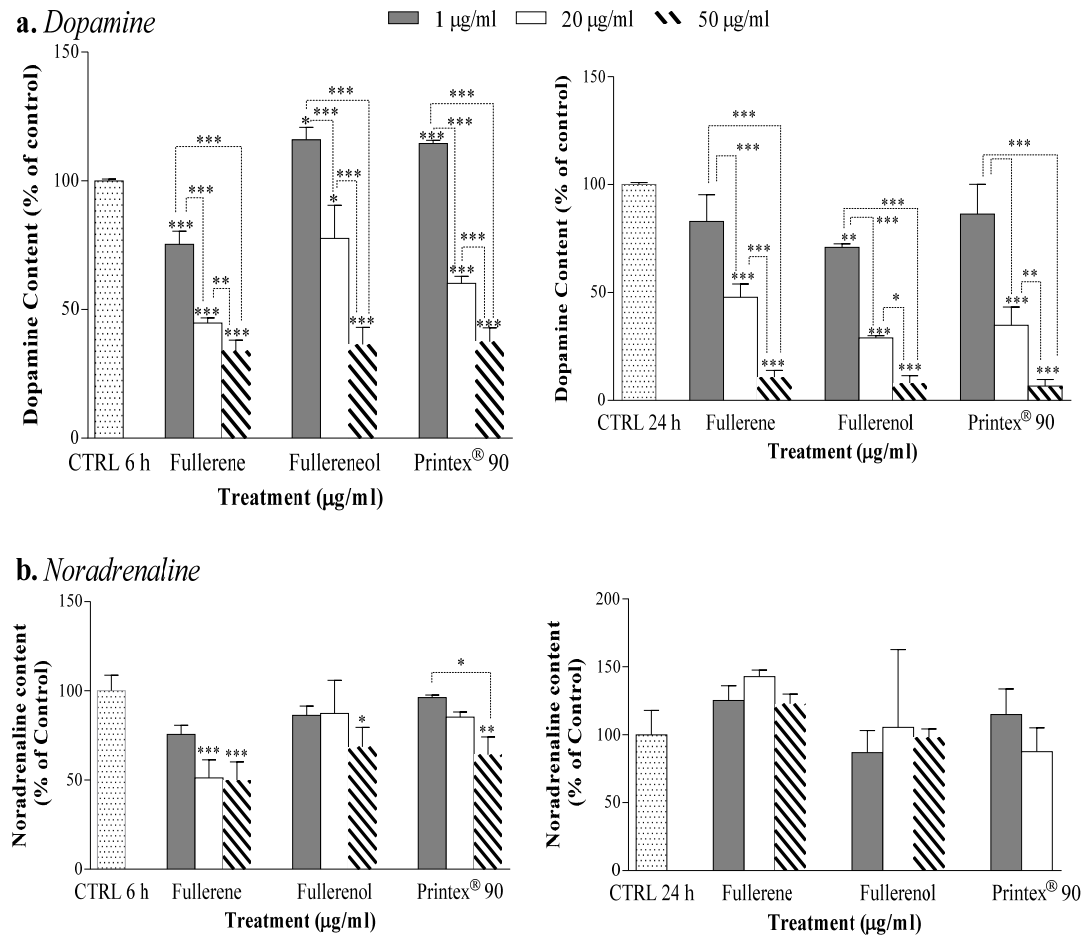


Figure 10: The amount of catecholamine in PC12 cells after 6 and 24h treatment with Fullerene (C₆₀), Fullerol (C₆₀(OH)₂₄) and Printex®90 nanomaterial: a) dopamine, b) noradrenaline.

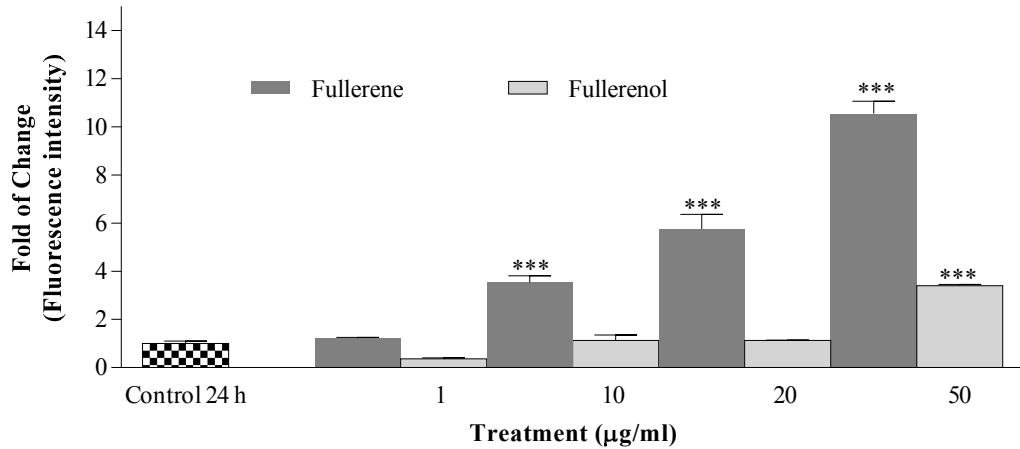


Figure 11: Effect of nanoparticles on ROS generation. After exposure with nanoparticles for 24 h and later with DCFH-DA for 45 min., Fluorescence was measured with a microplate reader. The intensity of fluorescence expressed as means \pm SDs of three experiments. Asterisk indicates a statistically significant change compared to control (one-way ANOVA).

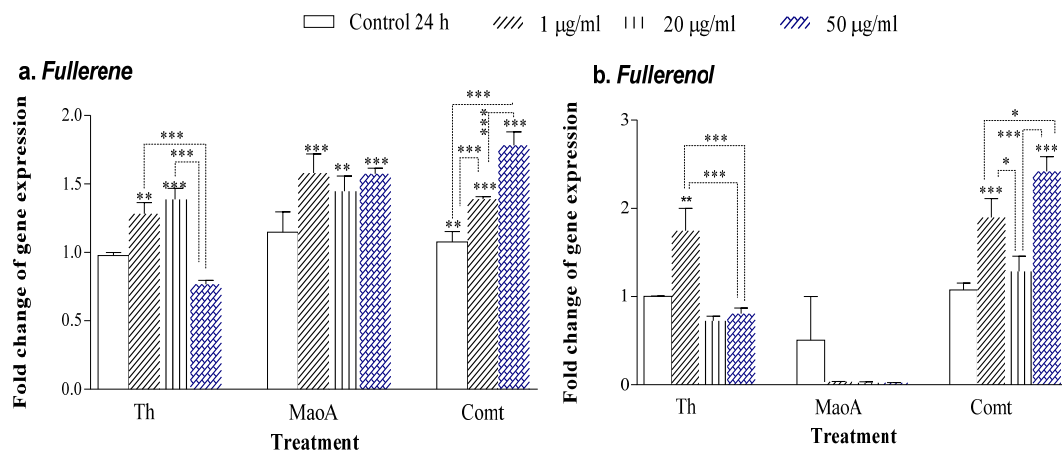
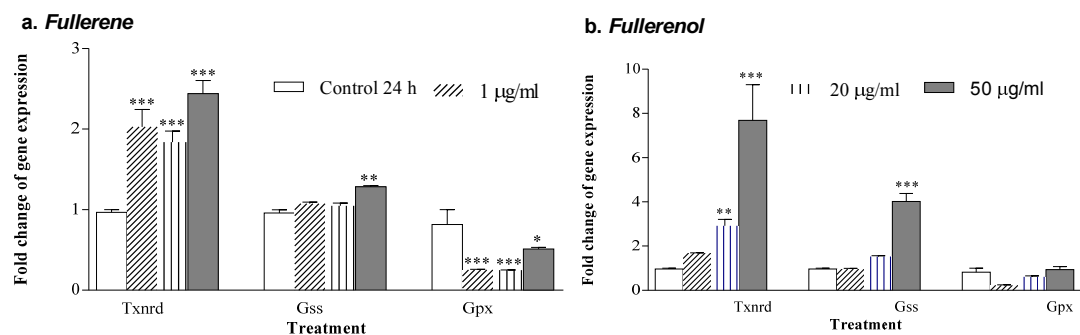


Figure 12: Gene expression alteration of tyrosin hydroxylase (*Th*), monoamine oxidase A (*MaoA*), and catechol-O-methyltransferase (*Comt*) in PC12 cells after 24 h-treatment with 1, 20 and 50 μ g/ml of Fullerene (C_{60}), Fullerenol.

The *Th* gene encodes for the tyrosine hydroxylase enzyme, a rate-limiting enzyme in catechol synthesis. Fullerene and fulleranol, at one $\mu\text{g/ml}$, increases the transcription level of *Th* (Fig. 12), but not at 50 $\mu\text{g/ml}$. Overall transcription level of catechol-O-methyltransferase (*Comt*) gene in PC12, *Comt*—degrade catecholamines such as dopamine, epinephrine, and norepinephrine, increased by presence of nanomaterial. Moreover, Fullerene increased the transcription level of *Maoa* gene, but not by fulleranol, Fig. 12.

After 24 h of exposure, fullerene (at all exposed concentration) up-regulate the expression of *Txnrd* gene while down regulate the *Gpx* gene; however, only 50 $\mu\text{g/ml}$ of fullerene induces *Gss* gene. Fulleranol, a free radical sponge, induces transcription level of *Txnrd* by ~3-fold, ~7-fold at 20 and 50 $\mu\text{g/ml}$, respectively. Fulleranol, at 50 $\mu\text{g/ml}$, up regulated the gene transcript of *Gss*—the rate-limiting enzyme in catecholamine, but response varies between treatments while it does not induce *Gpx*, significantly (Fig. 13).

After 24 h of treatment, fulleranol had no significant effects on the *Gpr37* and *Snca*, However, it shows up-regulation of *Parkin* (at one and 50 $\mu\text{g/ml}$) (Fig. 14).



~

Figure 13: Gene expression alterations of thioredoxin reductase 1 (*Txnrd*), glutathione reductase (*Gss*), and glutathione peroxidase 1 (*Gpx*) in PC12 cells after 24 h treatment (b) 1, 20 and 50 $\mu\text{g/ml}$ of Fullerene (C_{60}), Fulleranol and Printex[®]90.

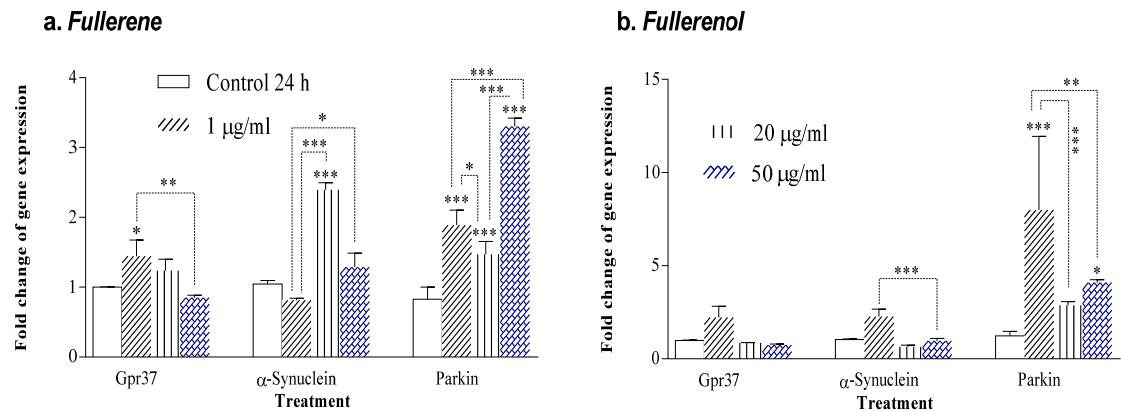


Figure 14: Gene expression alterations of G protein-coupled receptor 37 (*Gpr37*), α -synuclein (*Snc*), and *Parkin* in PC12 cells after 24 h-treatment of 1, 20 and 50 μ g/ml of Fullerene (C₆₀), Fullerol *** p-value <0.001, ** p-value <0.01, * p-value <0.05 change compared with control.

Discussion

Fullerene and fullerol nanoparticle caused significant alterations in genes associated with the dopaminergic system in neuronal pheochromocytoma cells–PC12. As genes may have “expression windows” for transcription alterations, and 24 h time point might not belong to this exclusively—we extended observation to 6 h. Fullerene depletes dopamine in a dose-dependent manner; noradrenaline only after 6 h. Fullerol and Printex®90 decrease the dopamine in both a time- and dose- dependent manner. The organic nanoparticles exhibit no significant change in noradrenaline contents of the cells after 24 h. For a given mass, nanoparticles have highest surface to volume ratio and the adsorption of various chemicals onto the surface of nanoparticles is well documented (Korpany et al., 2012, Ling et al., 2005, Ballesteros et al., 2000, Reinhard et al., 1986). Additionally, the capability of nanomaterial to penetrate the cells and internalize is documented (Rothen-Rutishauser et al., 2006, Nel et al., 2006, Lynch et al., 2006, Oberdörster et al., 2005). Moreover, many enzymes work as functional groups that have numerous subtypes or isoforms of enzymes, and their transcription alterations may be different. Therefore, findings could be “false negative” to functional biochemical changes, and these promote performance *in vivo* or in single cell eukaryotic organisms such as *T. thermophila*. In this study, we examined the

alterations of dopaminergic system-related genes expressed after exposure to organic nanoparticle.

For developing an *in-vitro* in-*vivo* correlation (IVIVC) characterization of NM at *in vitro* level is important model to health risk assessment, physical characterization of the test nanoparticles is essential and critical for *in vitro* toxicity studies (Sahu and Cascaciano, 2009). As reported in literature (Murdock et al., 2008, Andrievsky et al., 2002), sonication of nanoparticles in solution supports particle dispersion and achieves the homogeneity without significant effects on the particle surface charge.

The doses of nanoparticles selected for this study were based on a preliminary trial with PC12 cells (data not shown), which were in agreement with the literature prevailing at that time (Jacobsen et al., 2008) in which Jacobson *et. al.* reported that doses between zero and 200 µg/ml do not induce cell death within 24 h or during long-term subculture exposure (576 h) at 100 µg/ml in FE-1MutaTM Mouse lung epithelial cell line. The doses used in the present study are most likely much higher than would occur at current environmental exposures. However, unintentional generation of aggregates in aqueous environments is a possibility of exposure, particularly if C₆₀ finds widespread use in consumer products ranging from coatings and cosmetics to fuel cells. Besides that available up to now, there are no reports, which describe the effect of such nanoparticles at the lowest dose and cause toxic level gene expression both *in vitro* and *in vivo*.

The PC12 cell line was derived from a pheochromocytoma of the rat adrenal medulla and it mimics many features of the central dopaminergic neuron (Banker and Goslin, 1998) such as the expression of genes for catecholamine such as dopamine and norepinephrine (Collection, 2011), and production of dopamine (Roda et al., 1980). Three key genes are also active which are involved in production and metabolism of dopamine: *Th*, *Maoa* and *Comt*, which encoded for tyrosine hydroxylase, monoamine oxidase A, and carboxy-o-methyl transferase (*Comt*), respectively. Interestingly our results show that fullerene induces

the *Th*, *Maoa* and *Comt* in increasing amplitude and consequently causes a decrease in dopamine both at dose and time dependent manner. The decrease in the dopamine content at 6 and 12 h falls in the similar pattern as reported by Wang et al. (Wang et al., 2009) and Hassan et al. (Hussain et al., 2006), which indicates possible formation of dopamine-quinone and thus toxic effects. Christie *et al.* (Christie et al., 2004) reported an aqueous suspension of C₆₀ (Aque-nC₆₀) of fullerene generates more free radicals than other species under cell-free condition. The Aque-nC₆₀ disrupts normal cellular function through lipid peroxidation and thus ROS are responsible for the membrane damage. They further reported that DNA concentration and mitochondrial activity were not affected by the Aque-nC₆₀ (Sayes et al., 2005). Our data indicated that besides the depletion of dopamine, oxidative stress and enzymatic alterations play an important role in the potential neurotoxicity induced by fullerene. Fullerenol shows inconsistent results for the genes indicating metabolism as it affects both the transcription of the *Th* (at one µg/ml) and *Comt* (at 1 µg/ml and 50 µg/ml) significantly.

Three genes were selected to indicate the redox status and response to nanoparticle treatment, namely *Txnrd*, *Gss* and *Gpx*, which encode thioredoxin reductase 1, glutathione synthetase, and glutathione peroxidase 1, respectively. The redox environment within neural cells is dependent on a series of redox system couplings. The glutathione disulfide/glutathione pair (GSSG/GSH) and the thioredoxin reductase/thioredoxin system are two major components of cell for maintaining a favorable cellular redox environment (Maher, 2006, Patenaude et al., 2005). Here, our results demonstrate that fullerene up regulated the *Txnrd* while down regulating the *Gpx*. However, Fujita and co-worker (Fujita et al., 2010) attempted to characterize time-dependent changes in the gene expression profiles after intratracheal installation in rats with C₆₀ fullerenes at different dosages and reported that *Txnrd* (functions as a peroxidase, reducing hydrogen peroxide and organic hydroperoxides including lipid hydroperoxides) was scarcely altered. The down-regulation

of expression of genes encoding anti-oxidant enzymes explained the increase in oxidative stress measured through the dichlorofluorescein assay. In addition, a previous study has shown that H₂O₂ treatment induced increasing transcription of *thioredoxin reductase* gene in a dopaminergic nigral cell line, SN4741 (Yoo et al., 2003). Fullerenol up-regulate the *Txnrd* and *Gss* by about eight and four-fold change at the dose 50 µg/ml, respectively; and does not show any alteration in transcription of *Gpx*. The fullerenol effect on *Gpx* could be understood by the fact that fullerenol itself is highly reactive with oxygen free radicals (a free radical sponge) (Dugan et al., 1996, Lotharius et al., 1999). This is in align with the reported results that intranigral infusion (anesthetized rats) of exclusive carboxyfullerene did not increase lipid peroxidation in substantia nigra or deplete dopamine content in striatum (Lin et al., 1999).

The *Parkin*, *Snca* and *Gpr37* expression levels are the indicator of neuro-degeneration in PD and Lewy Bodies - *Snca* and *Gpr37* are attributed to pathological neuro-degeneration in PD. In our study, we found that (Fig. 15) fullerene (20 µg/ml) increases the transcription by~ 2.5-fold while fullerenol did not. This could be the MPTP (1-methyl-4-phenyl-1, 2, 3, 6-tetrahydropyridine) treatment like situation where an increase in α -synuclein expression causes symptoms such as Parkinson in humans and animals (Westerink and Ewing, 2008, Przedborski et al., 2001, Vila et al., 2000). The fullerene (1µg/ml) also increases *Gpr37* level significantly but not substantially. *Parkin* is protein acting similar to ligase and mediating the degradation of mis-folded protein such as α -synuclein and *Gpr37*. *Parkin* (E3 ubiquitin ligase) is encoded by the *Parkin* gene in humans and mutation in this gene is known to cause an autosomal recessive juvenile PD (AR-JP) (Kitada et al., 1998), which is the most common cause of early-onset Parkinson disease (Poorkaj et al., 2004). Our data show that both fullerene and fullerenol increase the expression of *Parkin* at 24 h significantly (fullerene- 1.8 to 4-folds; fullerenol- 3 to 7-folds). Fullerenol (20 µg/ml) at 6 h exposure increases *Parkin* transcription level significantly but only mildly.

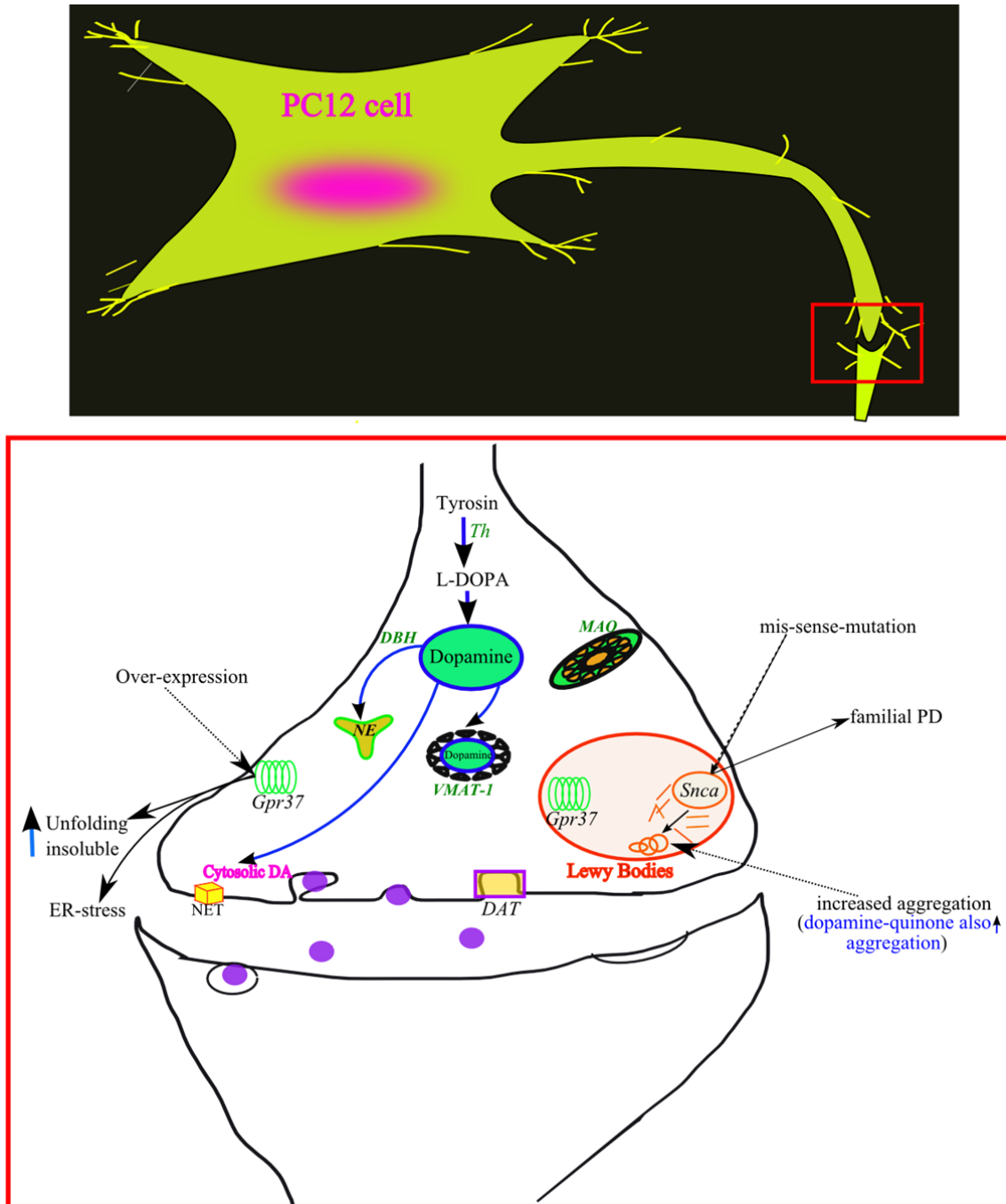


Figure 15: Signaling pathways at synapse between two-nerve endings of PC12 cells. The α -synuclein (*Snca*) and G-protein coupled receptor 37 (*Gpr37*) are involved in pathogenesis of Parkinson disease (PD). The Lewy bodies are consisting of *Gpr37* and *Snca* and considered as pathological hallmarks of PD. Monoamine oxidase (*MAO*), Tyrosine hydroxylase (*Th*), Dopamine (DA), L-3, 4-dihydroxy-phenylalanine (L-DOPA), Vesicular monoamine transporter type-1 (*VMAT-1*), Dopamine transporter (*DAT*), Norepinephrine transporter (NET), Norepinephrine (NE), Dopamine beta-hydroxylase (*DBH*), and Endoplasmic reticulum stress (ER-stress).

3.3 Interaction of nanoparticles with *T. thermophila*

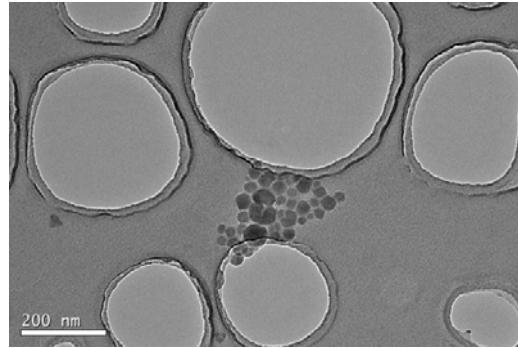


Figure 16: Transmission electron microscopy (TEM) analysis was used to characterize the morphology of aqueous- nC_{60} . A JEOL 2100 HT (JEOL Ltd., Japan) TEM was used, stock fullerene suspension ($80 \mu\text{g/ml}$) were deposited onto copper grids for observing morphology.

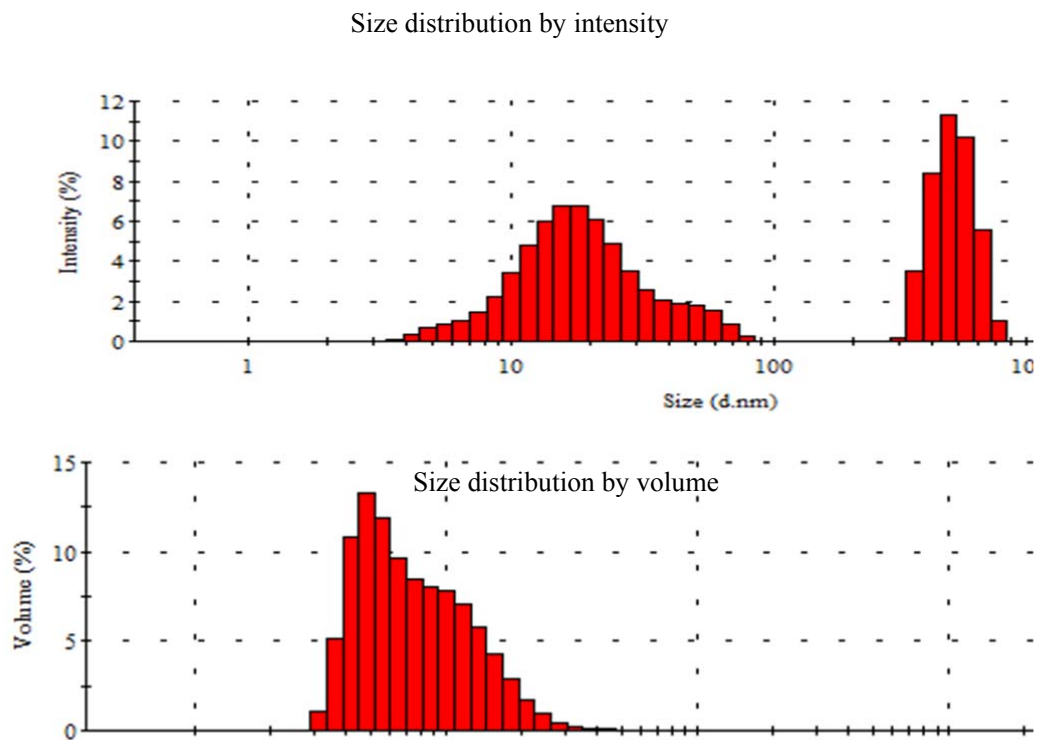


Figure 17: Laser diffraction hydrodynamic size data for fullerol in the Osterhout medium used for *in vitro* toxicity experiments (obtained by means of DLS). Graphs shown are the intensity and volume distribution of fullerol-osterhout formulation. Intensity-weighted average was used to determine hydrodynamic size, while volume distribution was used to determine relative amounts.

3.3.1 Stability and size distribution of nano-formulation

The morphology of nanoparticle (fullerene ad fullerenol) was observed by means of Transmission Electron Microscope (TEM) as shown in Fig. 16. The mean intensity and volume size distributions of fullerene, Fig. 18, and fullerenol samples in Osterhout medium (OSH) were determined by Dynamic Light Scattering (DLS) by means of Zetasizer. The theoretical hydrodynamic size of fullerenol is approximately two nm. In this study, fullerenol-OSH samples exhibited mostly a bi-modal size distribution by intensity, with a small peak at around 21 nm accounting for substantial part of the total particle volume, Fig17. This 20 nm peak is indicative of fullerenol aggregates that were formed during sample preparation. Although fullerenols were highly soluble in aqueous based system tried like MilliQ water, these particles were loosely aggregated and gradually precipitated out of solution, and the same could occurred during course of DLS sample preparation and measurement. The fullerenol-OSH intensity peak at 481 nm was primarily due to larger aggregates and only corresponds to a negligible portion of the total particle volume (not visible in Figure). This aggregation behavior may be attributed to high salt contents of Osterhout media. Colloidal stability of suspension was determined by measuring zeta potential distribution. The mean zeta potential distribution of fullerenol-OSH was -30.4 mV(SD 0.52).

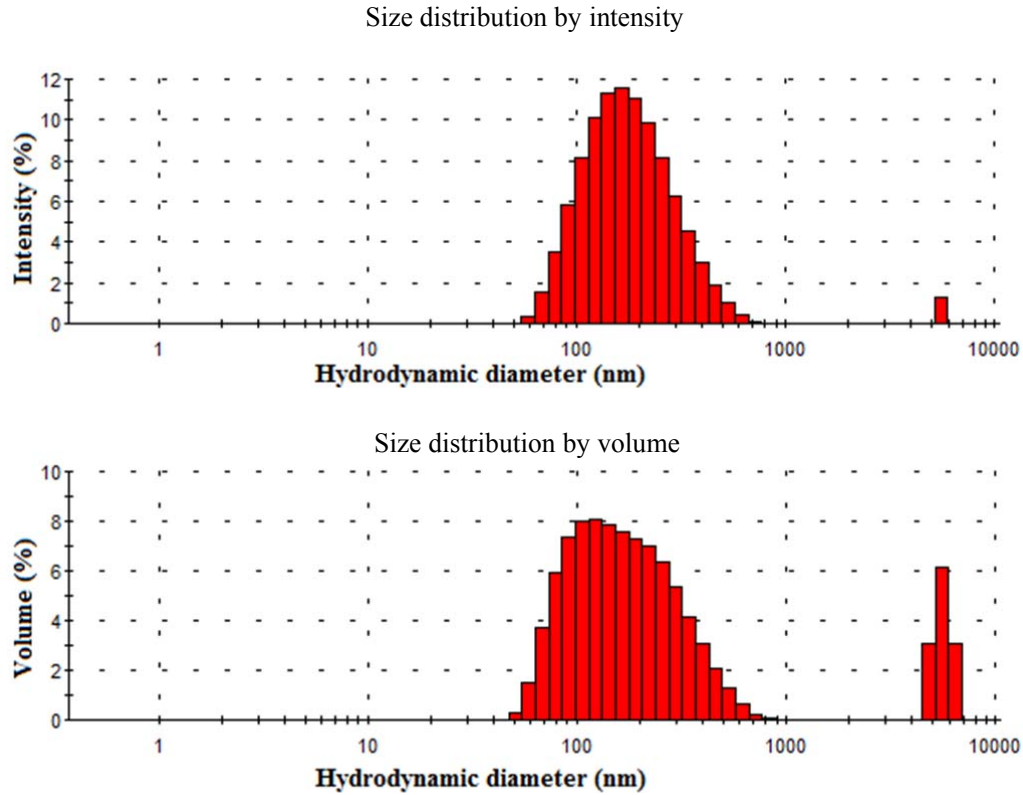


Figure 18: Hydrodynamic size analysis by DLS. Fullerene in the Osterhout medium used for *in vitro* toxicity experiments. Graph shown are the intensity and volume distribution of fullerene-Osterhout formulation. Intensity-weighted average was used to determine hydrodynamic size, while volume distribution was used to determine relative amounts.

Table 6: Hydrodynamic size distribution in fullerene suspension as a function of concentration. DLS analysis was performed on serial dilutions of a fullerene suspension in Osterhout medium. The average hydrodynamic size is represented as mean diameter (d.) \pm standard deviation (SD) in nm.

Concentration ($\mu\text{g/ml}$) in OSH media	Average hydrodynamic diameter		PDI (mean, n=3)	Zeta potential (mean, n=3)
	Peak 1 (SD, relative intensity %)	Peak 2 (SD, relative intensity %)		
1	194.88 (2.6, 98.05)	4316.33 (97.4, 1.95)	0.32	-30.33
20	192.95 (10.8, 98)	5406 (133.7, 2)	0.34	-32.27
80	191.58 (10.7, 98.87)	5366 (79, 2.13)	0.37	-32.27

3.3.2 Growth dynamics of *T. thermophila* in presence of nanomaterials

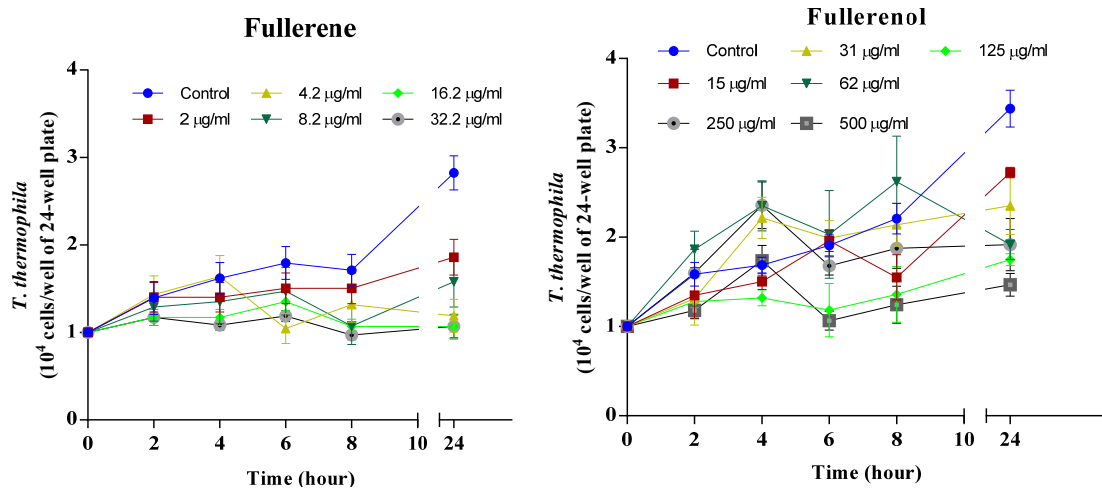


Figure 19: Growth dynamics of *Tetrahymena* (*T.*) *thermophila* cells exposed to different concentration of Fullerenol. The presented cell numbers were the mean of three different experiments, each performed with at least three replicates. Cells were counted in haemocytometer square and data were transformed by taking the square root of the observation.

Time courses of the cell concentration (cells/well of 24-well plate) are shown in Fig. 19.

The presence of fullerene in the culture medium has a considerable inhibition effect on cell growth inhibition; furthermore, inhibition by a concentration was more pronounced at higher time point at a given nanomaterial concentration. In contrast with fullerene, fullerenol at lower concentration (15 µg/ml) promotes the cell growth during first 6 h of exposure, whereas further increase in fullerenol resulted in greater inhibition of cell growth. At 24 h incubation time point, different test culture of *T. thermophila* shows noticeable differences in their viable count.

3.3.4 Oxidative stress by nanomaterial

The fullerene nanoparticle only shows significant difference ($p < 0.05$) at higher concentration (80 µg/ml) at both 6 and 24 h exposure period, Fig 20. However, fullerenol

shows anti-oxidant behavior with approximately 40 percent decrease compared to control at 24 h measurement point.

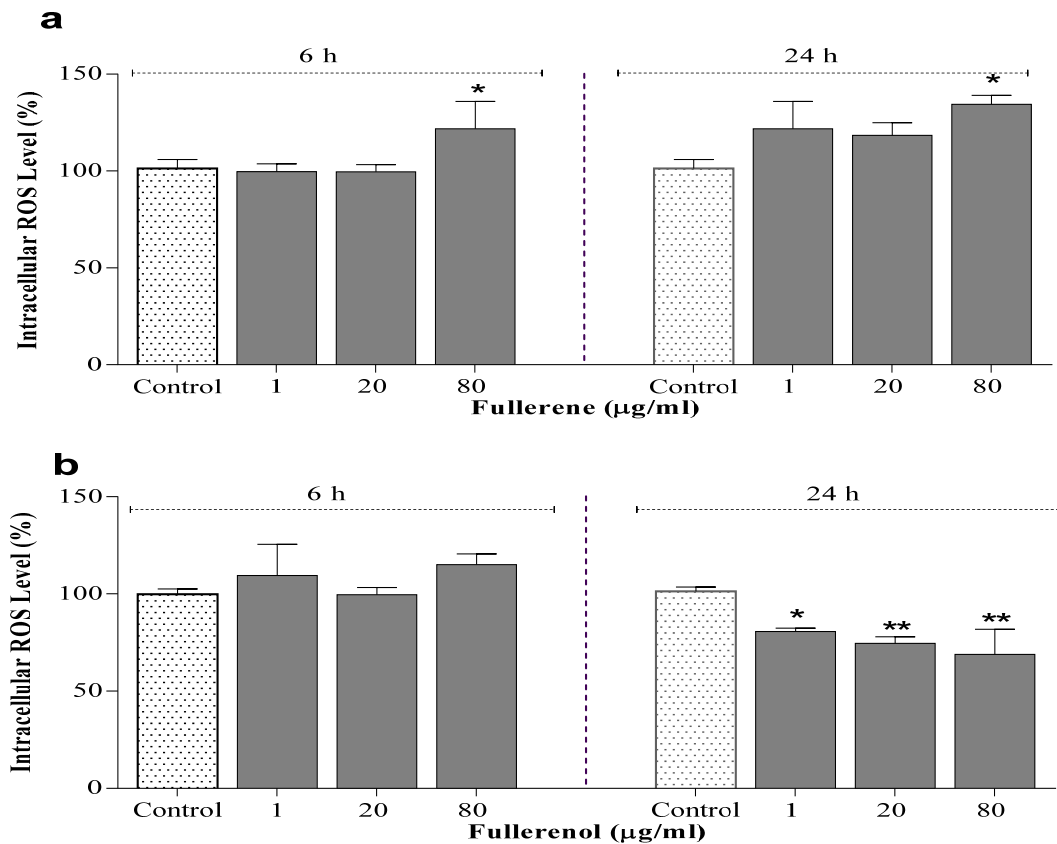


Figure 20: Effects of nanoparticle formulation on ROS generation in *Tetrahymena thermophila* after 6 and 24 h exposure period. a) fullerene, b) fulleranol. The data are represented as the mean \pm SEM of at least three independent experiments. Each experiment was performed with eight

Discussion

The physicochemical properties of C₆₀, contrary to its aromatics the pristine fullerenes have no hydrogen bond atoms or other groups attached to their cage. Therefore, they are unable to participate in substitution reactions. As they consist entirely of sp²-hybridized carbons, they have a strong electron-attracting ability and, therefore, they are oxidizing agents. This reversibly reduced fullerene, can take up to six electrons, may transfer electrons to other species available to its surroundings like DNA and thus cause formation of ROS (Jensen et

al., 1996). Also, Fullerenes can absorb ultraviolet and low visible range light - then generate excited singlet oxygen (Jensen et al., 1996, Oberdörster, 2004b, Usenko et al., 2008). In the presence of C₆₀, both visible and ultraviolet light can generate ROS, particularly as singlet oxygen and superoxide (Pickering and Wiesner, 2005). These by-products can induce oxidative stress leading to a variety of detrimental downstream effects such as lipid peroxidation, change in particular gene expression (Dhawan et al., 2006, Kamat et al., 2000).

Moreover, in a cell-free aqueous solution of the colloidal (nano) C₆₀ (~60 nm aggregates), a profound formation of superoxide anions was observed from electron uptake that was followed by reaction with oxygen and water (Christie et al., 2004). Singlet oxygen may react with amino acids, nucleic acids and the C = C double bonds of membrane phospholipids. Due to formation of ROS, the colloidal C₆₀ caused lipid peroxidation of cell membranes and increased permeability in cell cultures (Christie et al., 2004, Sayes et al., 2005). Thus, these nanomaterials accumulate in the cell, interact with the biological system (including cell membrane), and generate ROS, and cause the cell damage and death.

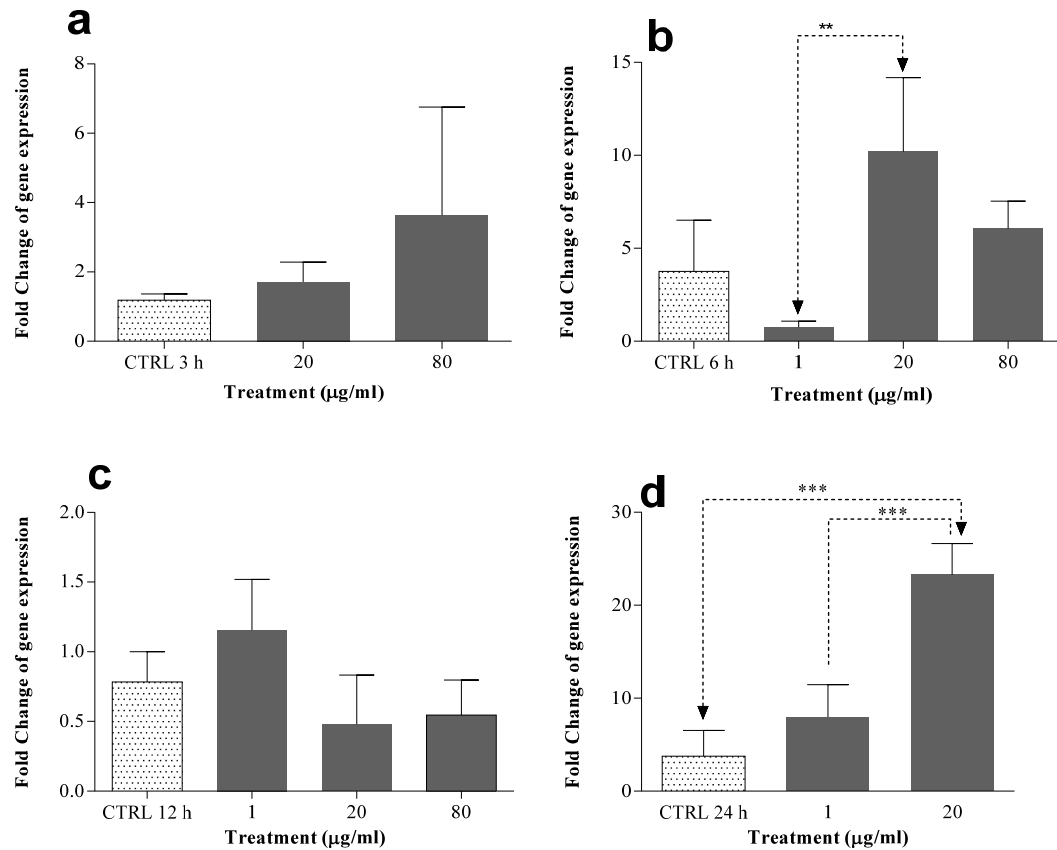
3.4 Gene expression changes in *T. thermophila* by nanomaterials

Figure 21: Fullerene (C_{60}) dependent potentiation of *glutathione s-transferase (GST)* gene expression over 3, 6, 12, and 24 h; mRNA expression level are represented as fold change of gene expression. Bars and error bars represent the mean and standard error of the mean (SEM) of three independent experiments. Statistically significant differences (ordinary ANOVA followed by Holm-Sidak Multiple comparison test) with respect to the vehicle control are indicated as: * $p < 0.05$, ** < 0.01 , *** < 0.001 .

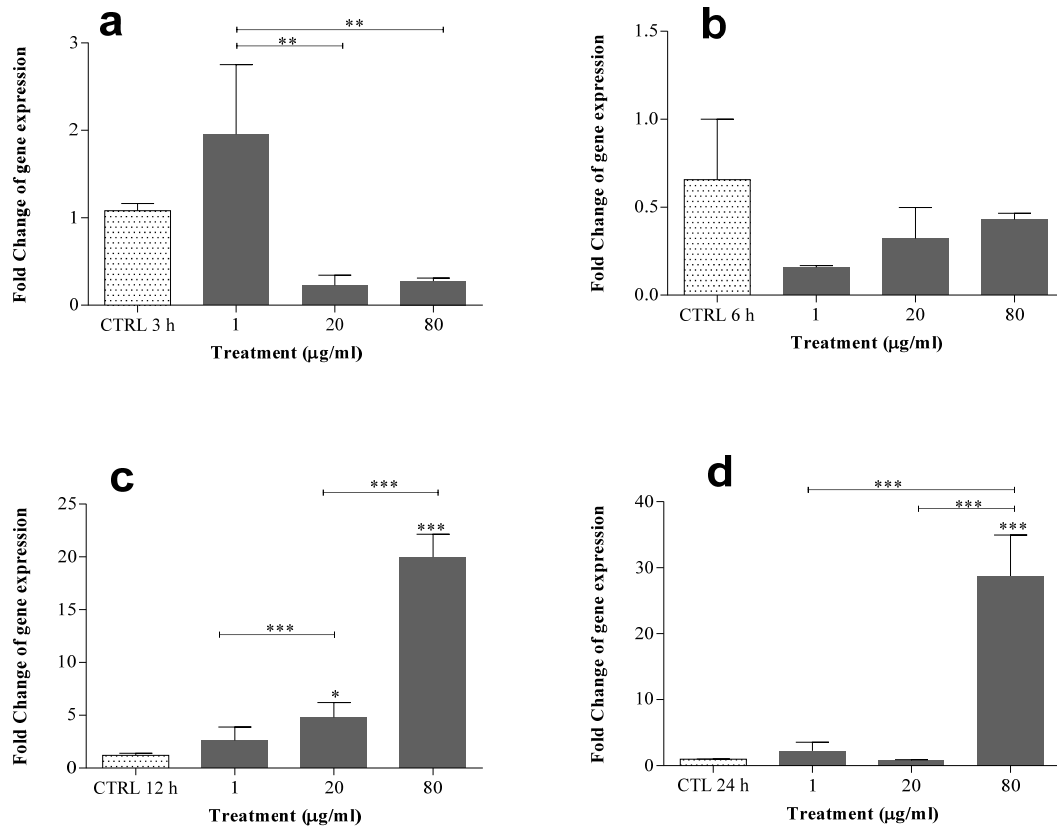


Figure 22: Fullerene (C_{60}) dependent potentiation of *Dopamine- β -hydroxylase (DBH)* gene expression over 3, 6, 12, and 24 h; mRNA expression level are represented as fold change of gene expression. Bars and error bars represent the mean and standard error of the mean (SEM) of three independent experiments. Statistically significant differences (ordinary ANOVA followed by Holm-Sidak Multiple comparison test) with respect to the vehicle control are indicated as: * $p < 0.05$, ** < 0.01 , *** < 0.001 .

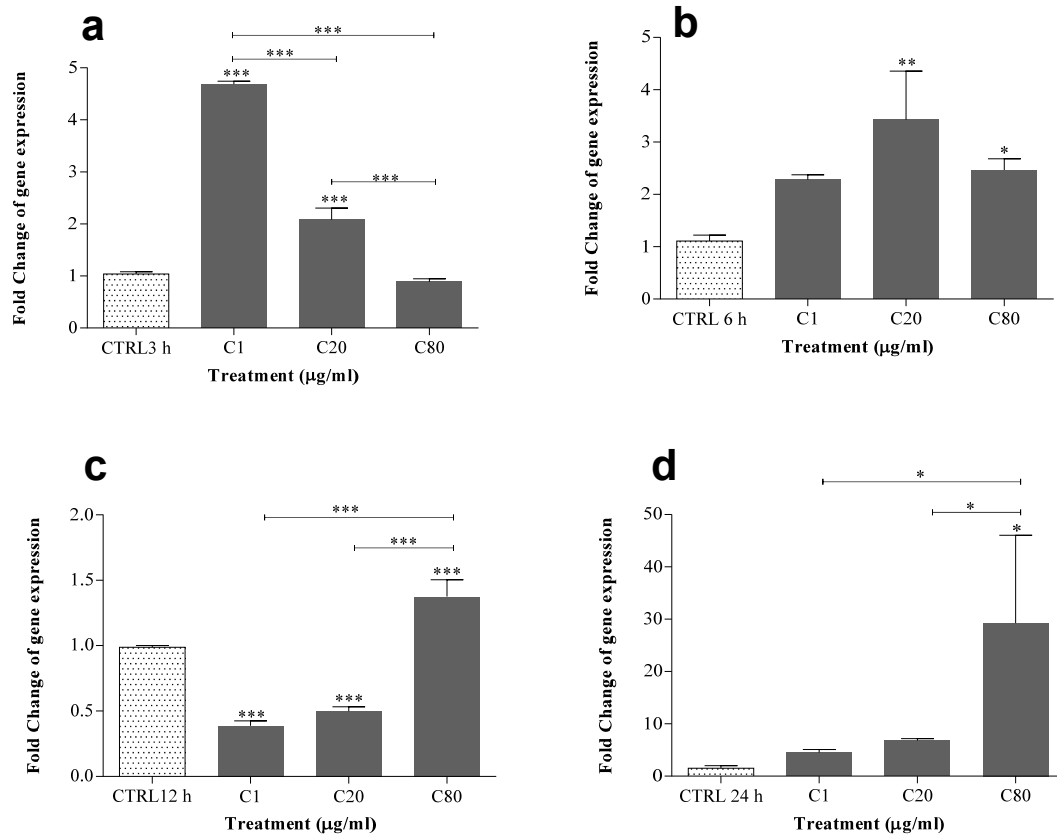


Figure 23: Fullerene (C_{60}) dependent potentiation of *Catalase (CAT)* gene expression over 3, 6, 12, and 24 h; mRNA expression level are represented as fold change of gene expression. Bars and error bars represent the mean and standard error of the mean (SEM) of three independent experiments. Statistically significant differences (ordinary ANOVA followed by Holm-Sidak Multiple comparison test) with respect to the vehicle control are indicated as: * $p < 0.05$, ** $p < 0.01$, *** $p < 0.001$.

Effect of Fullerene

There was discontinuous pattern in induction of *GST* (Fig. 21); Fullerene at 20 ppm was higher ($p < 0.01$) than 1ppm of the same 6 h time point, while there was no significant difference at 24 h time point, and finally there was significant difference ($p < 0.01$) between control and 20 ppm treatment and among the treatment. Because of big difference in the mean of experiments at the data point for 1 and 80 µg per ml of 3 and 24 h time, respectively, did not presented in the graph.

Dopamine- β -hydroxylase (*DBH*) acts as an oxidoreductase on molecule containing phenylethylamine skeleton. Fullerene increases transcription level of *DBH* gene: at 12 h –

~4-folds increase by 20 µg per ml, 20-fold increase by 80 µg per ml; at 24 h – 24-folds increase by 80 µg per ml, Fig. 22.

In *catalase* mRNA expression (Fig. 23), After 3 hours exposure to fullerene, there is a decrease in the expression profile related to the increase in concentration which is extremely significant for each group ($p < 0.001$), despite the concentrations are significantly higher than the control sample ($p < 0.001$). After 6 hours, all the concentrations of fullerene used are able to induce an increase in transcription level of catalase gene, with a very significant increase after 20 ppm exposure and extremely significant increase after exposure to 80 ppm of fullerene. After 12 hours exposure there is an extremely significant decrease in the expression of catalase gene compared to the control, after 1 and 20 ppm exposure, while an extremely significant increase compared to the control is observed for the highest concentration of fullerene (80 ppm). Among the groups the difference are deemed as extremely significant ($p < 0.001$). Finally after 24 hours exposure to fullerene there is an increase with an increase in concentration, but the only significant difference is at the 80 ppm concentration ($p < 0.05$).

Effect of Fullerenol

GST gene encodes the *glutathione s-transferase (GST)*; *GST* is a phase II metabolizing enzyme, which catalyzes the binding of glutathione to xenobiotic. Fullerenol was able to elicit a decrease in transcription level of *GST* gene compared to the control after 3 hours of exposure, while 20 µg per ml being very significant ($p < 0.01$), Fig. 24.

Fullerenol increases transcription level of *DBH* gene: at 80 µg per ml – ~1.5, ~5, ~4.5, and ~1.8-fold increase when incubated in fullerene for 3, 6, 12, and 24 h, respectively; at 20 µg per ml – nearly 2-fold increase at 3, 6 and 24 h time point, Fig. 25.

After 6 hours, catalase gene expression at one μg per ml exposure was extremely significantly higher ($p < 0.01$) than the control. After 12 hours, at 80 μg per ml there is an increase in gene expression which is highly significant ($p < 0.001$), while the decrease at 20 μg per ml was still highly significant ($p < 0.001$). Finally, after 24 hours, there was a significant decrease ($p < 0.001$) at one μg per ml and a significant increase ($p < 0.001$) at 20 μg per ml exposure compared to control samples, Fig. 26.

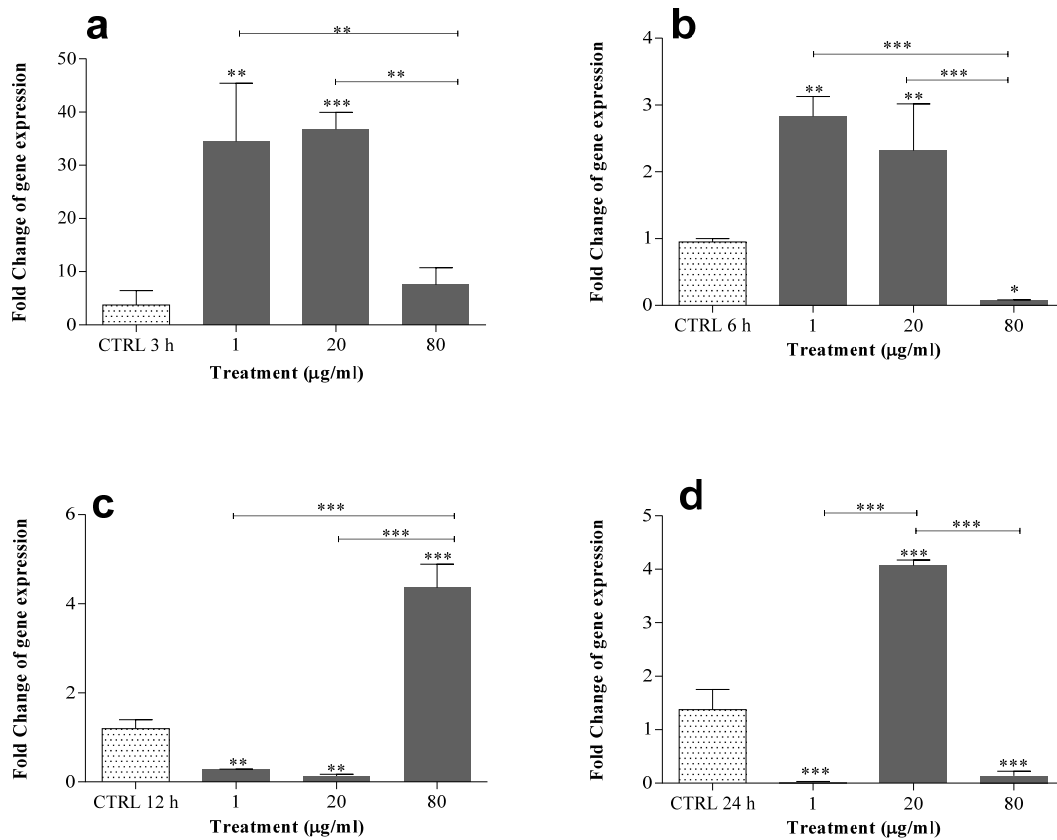


Figure 24: Fulleranol - $\text{C}_{60}(\text{OH})_{24}$ dependent potentiation of *glutathione s-transferase (GST)* gene expression over 3, 6, 12, and 24 h; mRNA expression level are represented as fold change of gene expression. Bars and error bars represent the mean and standard error of the mean (SEM) of three independent experiments. Statistically significant differences (ordinary ANOVA followed by Holm-Sidak Multiple comparison test) with respect to the vehicle control are indicated as: * $p < 0.05$, ** $p < 0.01$, *** $p < 0.001$.

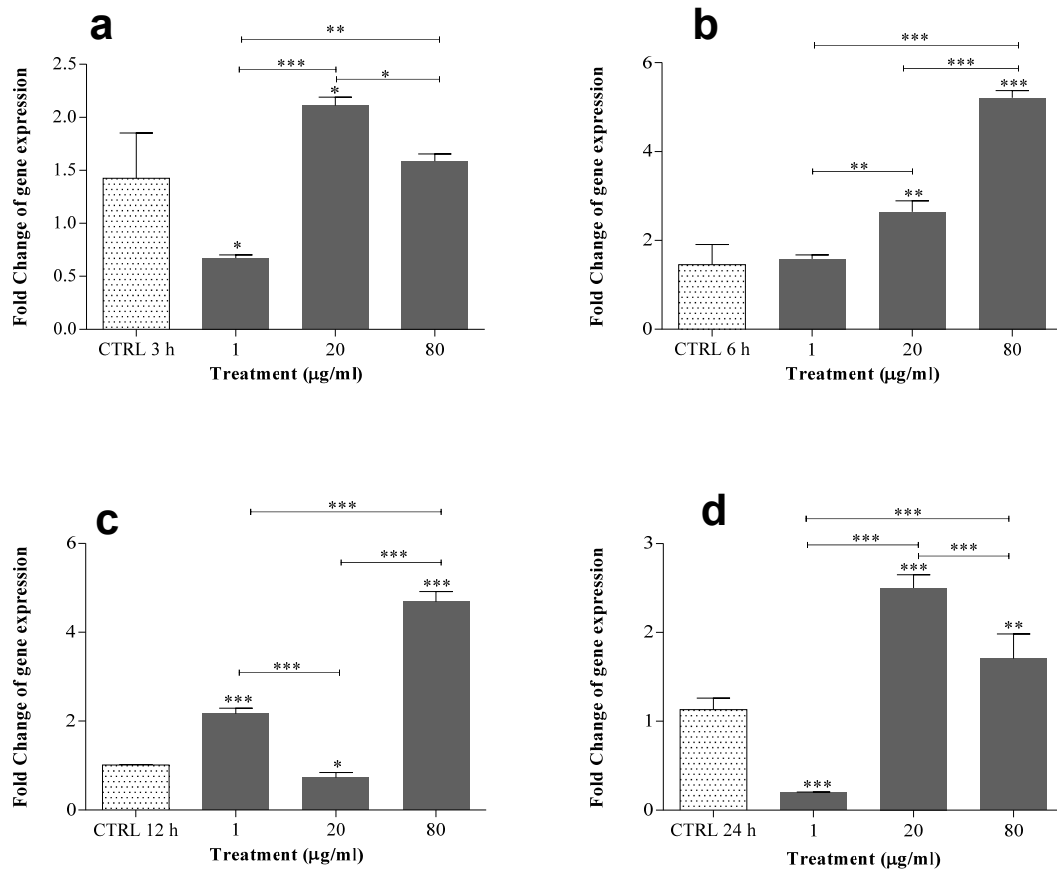


Figure 25: Fullerenol- $C_{60}(OH)_{24}$ dependent potentiation of *Dopamine-β-hydroxylase (DBH)* gene expression over 3, 6, 12, and 24 h; mRNA expression level are represented as fold change of gene expression. Bars and error bars represent the mean and standard error of the mean (SEM) of three independent experiments. Statistically significant differences (ordinary ANOVA followed by Holm-Sidak Multiple comparison test) with respect to the vehicle control are indicated as: * $p < 0.05$, ** $p < 0.01$, *** $p < 0.001$.

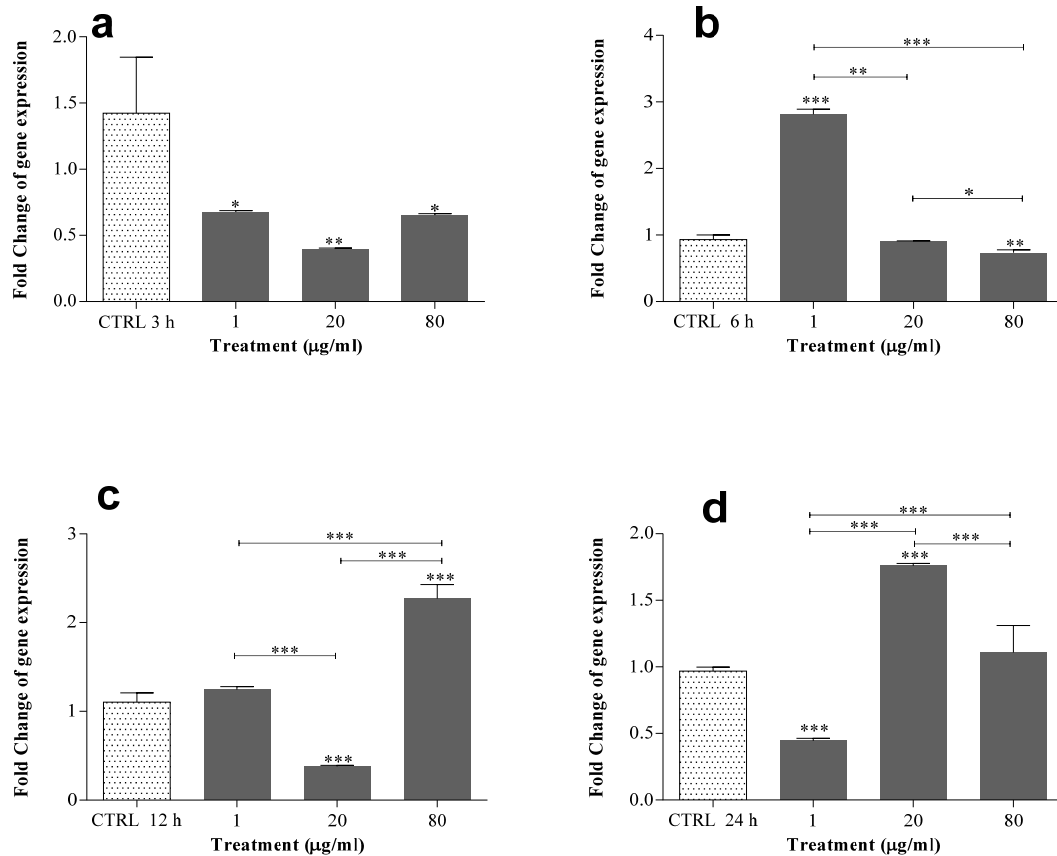


Figure 26: Fullerol - $C_{60}(OH)_{24}$ dependent potentiation of *Catalase* (CAT) gene expression over 3, 6, 12, and 24 h; mRNA expression level are represented as fold change of gene expression. Bars and error bars represent the mean and standard error of the mean (SEM) of three independent experiments. Statistically significant differences (ordinary ANOVA followed by Holm-Sidak Multiple comparison test) with respect to the vehicle control are indicated as: * $p < 0.05$, ** < 0.01 , *** < 0.001 .

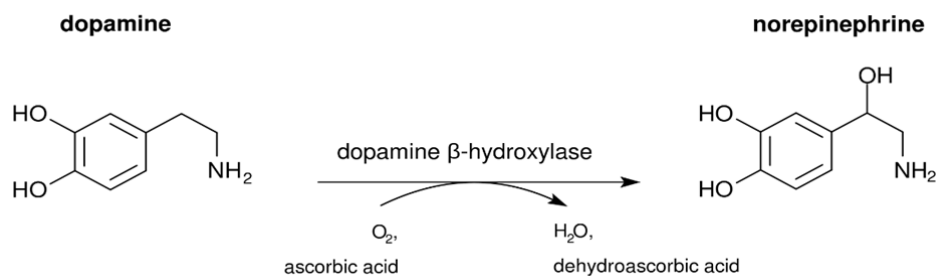
Discussion

Oxidative stress is a common pathway of toxicity and disease. An organism can undergo oxidative stress through several different mechanisms. First, it may be directly induced by an oxidizing agent such as H_2O_2 . Second, it may be produced through the induction of cytochrome P450, as is the case with many polycyclic aromatic hydrocarbons (PAHs). Third, a xenobiotic may inhibit the production of antioxidant molecules, such as glutathione (GSH), that function to maintain oxidative balance. *Glutathione-S-transferase* (GST) is a pivotal phase II detoxification enzyme in the biotransformation of xenobiotics like DDT,

and metabolites in rats and humans; forbidding cells or organisms from being damaged or even killed by exposure to toxicant.

Till the 3 h time point *Tetrahymena* does not induce GST gene at all the concentration, exposure medium is still in colloidal state. At 6 h, *Tetrahymena* increases the more and more amount of micronsize particles (see live imaging photographs of *T. thermophila*) that not only decrease the frequency of clearance but also cause hindrance in the movement of *Tetrahymena*. And thus the induction of GSTs by Fullerene (20 µg/ml) increases during 3 h to 6 h. Fullerenes also induces GSTs higher ($p < 0.01$) at 6 h time point. Finally, at 24 h, culture medium was full of micron fullerene aggregate and as aggregation formation increased further, *Tetrahymena* encounter less free-space for movement, difficulty in ingestion, and less food, thus elevates the *GST* gene to cope the resultant stress.

Dopamine β-hydroxylase (DBH) converts dopamine to norepinephrine. It is expressed in noradrenergic nerve terminals of the central and peripheral nervous systems, as well as in chromaffin cells of the adrenal medulla. Dopamine beta-hydroxylase catalyzes the hydroxylation of not only dopamine but also other phenylethylamine derivatives when available. The minimum requirement is presence of a benzene ring with a two-carbon side chain that terminates in an amino group. In 1967, Janakidevli et al. (Janakidevi et al., 1966) reported that *T. pyriformis* could synthesize epinephrine and norepinephrine from [¹⁴C]-L-tyrosine and [2-¹⁴C]-DL-dopa. In 1969 Pearse (Pearse, 1969) coined the term APUD (amine precursor uptake and decarboxylase) cells to describe the ability of certain non-neuronal cells of mammals to produce dopamine and norepinephrine upon the addition of L-DOPA. In the present study, we found that fullerene gives a mixed response on DBH expression while fullerenol significantly increases DBH transcription level over various time point and exposure concentrations.



Hydrogen peroxide is a harmful byproduct of many normal metabolic processes; to protect cells and tissues from this damage, it must be quickly converted into other, less dangerous substances. To this end, catalase is frequently used by cells to rapidly catalyze the decomposition of hydrogen peroxide into less-reactive gaseous oxygen and water molecules (Gaetani et al., 1996). The lower levels of catalase are associated with damages to lipids, proteins and DNA (Halliwell and Gutteridge, 2007). In our study, we found that from the 3 h exposure and going over time, we observed a change in the pattern, from a decrease in catalase with the increase in concentration at the earliest time point, to an intermediate situation where all the concentrations used are able to elicit an increase in the expression. Finally, after 12 h exposure to fullerene there is an extremely significant decrease than the control, but overall a general increase with the increase in concentration. The condition after 24 h remain the same, but less marked, with a significant difference between the groups and an increase at the highest concentration. From the data, it seems that in the short term (3 h) the biosynthesis of this enzyme is more prominent at the lowest concentration (1 $\mu\text{g/ml}$), while with the increase in time, it is the highest concentration (80 $\mu\text{g/ml}$) that induces an increase in the catalase gene transcription. Therefore, we hypothesized that an increase in the transcription, which is related to the stress of the newly formed radicals, indicates the ability of *Tetrahymena* to cope with the stress. After a period, however, this ability diminishes and we observe a less prominent expression for the enzyme, which is accordance with the idea that pollutants are able to decrease the antioxidant ability of the organisms.

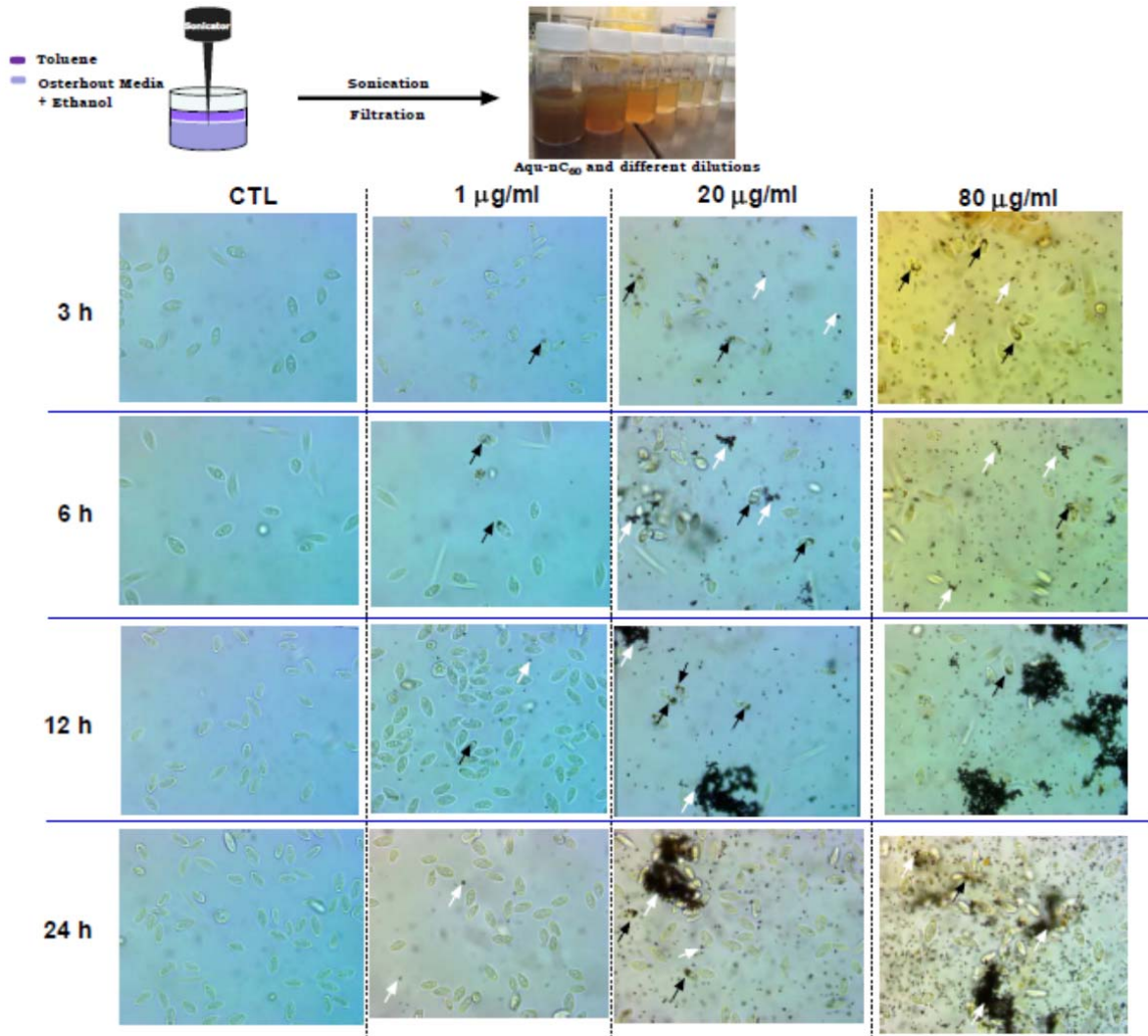
3.5 Microscopic behavior of *T. thermophila* in nanomaterial environment

Figure 27: Optical micrographs; the interaction of various concentration of fullerene and *T. thermophila* over 3, 6, 12 and 24 h with a video camera fitted in inverted microscope. Owing to the high mobility of the control cells, images were taken at a lower magnification. The black arrow indicates the formation of bigger visible particles inside the cells. The white arrow indicates the formation of bigger visible particle by the cells.

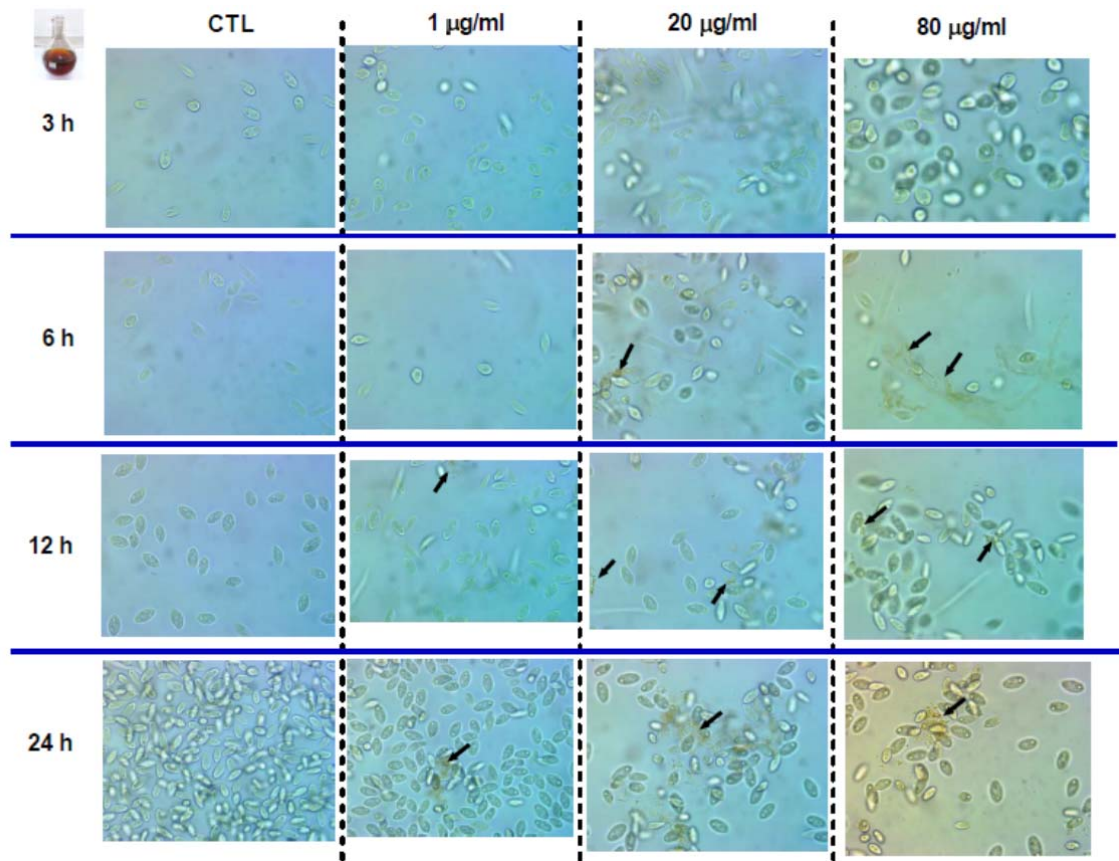


Figure 28: Optical micrographs; the interaction of various concentration of fullereneol and *T. thermophila* over 3, 6, 12 and 24 h with a video camera fitted in inverted microscope. Owing to the high mobility of the control cells, images were taken at a lower magnification. The black arrow indicates the formation of fibrous material by cells.

Discussion

Tetrahymena thermophila is unicellular eukaryote. While *T. thermophila* does not feel pain, they are capable of sensing chemoattractants and chemorepellents in their environment (Hennessey, 2005). This allows them to find food and possibly to escape predation (Lampert et al., 2013, Hennessey, 2005). A number of chemorepellents that have been characterized in *T. thermophila* are polycationic peptides, including lysozyme, the lysozyme fragment and nociceptive peptides including bradykinin (Kuruvilla et al., 1997). Lysozyme signaling involves a calcium-based depolarization (Kuruvilla and Hennessey, 1998). Interestingly, the microscopic studies of Aqu-nC₆₀ (Fig 27) and fullereneol (Fig 28) provided exciting

information about its fate inside protozoan cells. The protozoan cells are able to ingest these nanoparticles, but expel bigger particle as they cannot digest them completely. *Tetrahymen* is considered as efficient filter feeder on bacteria – by phagocytosis. *Tetrahymen* has oral apparatus – name *Tetrahymen* means four (tetra) membranes (hymena) at oral apparatus– that invaginate (by invagination) and form a food vacuoles in 20 s to 30 min. Digestion and subsequent removal of fecal pellet through cytoproact takes 30 min to several hours. Microscopic study over 3, 6, 12, and 24 h with different concentration – 1, 20 and 80 µg/ml – revealed that *Tetrahymena* immediately ingest the nanoparticles and form food vacuoles to store nanomaterial until removed as fecal pellet into the medium, Fig 27-28. In the food vacuoles, the both fullerene and fullerenol undergoes agglomeration and subsequently released as a bigger aggregate. *T. thermophila* aggregates nanoparticles to a larger one (finally, in micron size), over a period of 24 h. On the other hand, the nanoparticles can also self-aggregated by various environmental factors, thus, producing small aggregates. It seems that nanomaterials regardless of their chemical nature behave as chemorepellants, and thus their presence stress the *Tetrahymena*. Therefore, to overcome this stressful situation *Tetrahymena* acts by increasing the bio-aggregation of nanoparticles. These results provide the idea how the *Tetrahymena* influenced by presence of nanoparticles in its surroundings, and vice-versa.

Chapter 4: Conclusions

4.1 Fullerene and EROD induction

In this investigation, we provide documentation on EROD induction by PCDD/F, by simultaneous and sequential exposure to C₆₀ in the form of aqueous suspension of C₆₀, and by mixtures of C₆₀ and PCDD/F. The simultaneous and sequential exposure of nC₆₀ and PCB126, increase the overall EROD activity response of PCB 126. On the contrary, this study shows that there is equal response for simultaneous and sequential exposure of nC₆₀ and TCDD. Indeed, changes in toxicity and bioaccumulation due to the presence of C₆₀-aggregates may depend on several factors such as toxic mechanism and interaction of the compound with C₆₀-aggregates. When screening NPs; the present study instigates to consider the existing and emerging xenobiotic in both co-exposure and pre-exposure scenarios of engineered nanoparticles.

4.2 Interaction of organic nanomaterial with neural cell line

In this investigation, we observed dopamine depletion by fullerene, fullerenol and Printex[®]90 and the effects are varying in time of observation and concentration. We found decrease in catecholamine contents with increase in dose, which might be due to induction of gene involved in metabolism but could not rule out possible adsorptive or catalytic phenomena during the interaction with nanoparticle. For oxidative stress, at low exposure concentration, we found genes as preferred marker over the fluorescence-assay. Our data indicate possible Parkinson's disease induction by fullerene and fullerenol-*in vitro*-without showing significant sign of oxidative stress and decrease in viability. Based on results, it could be of significant importance to investigate neurodegenerative pathological marker *in vivo*.

4.3 Phenotypic behavior of *T. thermophila*

In this investigation, we observed the behavior of the protozoa toward the nanoparticles. *Tetrahymena* shows increased swim speed to eat the more food or perhaps to neutralize the negative effect of particles: this behavior changes with time. It would be of great interest to know about their chemorepellent or chemoattractant response and characterize them by behavioral assays.

4.4 Genotypic behavior of *T. thermophila*

The gene expressions identified by this work provide evidence that *Tetrahymena*'s response to fullerene and fullerenol involves biology shared with other eukaryotes. Our data showed that following the exposure of nanomaterial, variation in the gene expression –with the *GST* and *DBH* mRNA–can be detected.

Acknowledgements

References

Appendix

Acknowledgements

The research in the thesis was carried out from 2010 to 2013 at the Molecular EXposomics (MEX), Helmholtz Zentrum München, GmbH, Ingolstädter Landstraße 1, D-85764 Neuherberg, Germany. This project was sponsored by the Environmental ChemOinformatics Marie Curie Initial Training Network (ECO-ITN) within the seventh research framework programme of the European Union (238701).

Before beginning a new chapter of my life, I would like to extend a heartfelt thanks to the following people who supported, guided and inspired me throughout the journey of my PhD life.

First, I would like to express my best regards, profound gratitude, indebtedness and deep appreciation to my honorable supervisor **Prof. Dr. Dr. Karl-Werner Schramm**, Technical University Munich (TUM), Department für Biowissenschaftliche Grundlagen, Weihenstephaner Steig 23, D-85350 Freising, Germany for this intellectual suggestions and continuous support during Ph.D work. I would like to gratefully acknowledge Dr. Gerd Pfister, MEX, Helmholtz Zentrum München technical discussions and co-operation of HPLC work.

I would like to thanks to Frau Silke Bernhöft for helping in cell culture. I am very grateful to Dr Levy Lopez Walkiria, Molecular Exposomics, Helmholtz Zentrum München for technical discussions in EROD assay.

I wish to covey thanks and regards to Mr. Bernhard Henkelmann, Dr. Igor Tetko, , Dr Pandelova Marchella,Valentina Zingarelli, Magda Baba, Zhenlan Xu, John Mumbo and Dominik for their general advice.

Moreover, to Mr. Kocis Geza for support in lab as well as in keep-running my bicycle.

Many thanks to Dr. Johnston Blair and Mr. Andreas Blair for allowing me to use particle size analyzer, Mr. Ulrich Hafen and Frau Bianca Schmick for RT-PCR.

I would like to thank my friends—Sudeepta, Harsha, Ayush, Saray Ly-Verdu, and Raed—well I wishers for their cordial cooperation. Many thank to everybody who ever gave me help and support.

A big hand to ECO-itn and Project manager Dr. Eva Schlosser for providing joyful working condition, during the project.

My final, and most heartfelt, acknowledgment must go to my beloved parents, brothers, their in-laws, and other family members who paid all the support and encouragement during the period of PhD research. I also express appreciation to my wife for her patience during the preparation of this dissertation.

References:

- AITKEN, R., CHAUDHRY, M., BOXALL, A. & HULL, M. 2006. Manufacture and use of nanomaterials: current status in the UK and global trends. *Occupational medicine*, 56, 300-306.
- ANDRIEVSKY, G., KLOCHKOV, V., BORDYUH, A. & DOVBESHKO, G. 2002. Comparative analysis of two aqueous-colloidal solutions of C₆₀ fullerene with help of FTIR reflectance and UV-Vis spectroscopy. *Chemical Physics Letters*, 364, 8-17.
- ANDRIEVSKY, G., KOSEVICH, M. & VOVK..., M. 1995a. On the production of an aqueous colloidal solution of fullerenes. *J. Chem. Soc.*
- ANDRIEVSKY, G. V., KOSEVICH, M. V., VOVK, O. M., SHELKOVSKY, V. S. & VASHCHENKO, L. A. 1995b. On the production of an aqueous colloidal solution of fullerenes. *Journal of the Chemical Society, Chemical Communications*, 1281.
- ASAI, D. J. & FORNEY, J. D. 1999. *Tetrahymena thermophila*, Academic Press.
- BALASUBRAMANIAN, S. K., JITTIWAT, J., MANIKANDAN, J., ONG, C. N., YU, L. E. & ONG, W. Y. 2010. Biodistribution of gold nanoparticles and gene expression changes in the liver and spleen after intravenous administration in rats. *Biomaterials*, 31, 2034-2042.
- BALLESTEROS, E., GALLEGRO, M. & VALCARCEL, M. 2000. Analytical potential of fullerene as adsorbent for organic and organometallic compounds from aqueous solutions. *Journal of Chromatography A*.
- BANKER, G. & GOSLIN, K. 1998. *Culturing nerve cells*, The MIT press.
- BASMA, A. N., MORRIS, E. J., NICKLAS, W. J. & GELLER, H. M. 1995. L-DOPA Cytotoxicity to PC12 Cells in Culture Is via Its Autoxidation. *Journal of neurochemistry*, 64, 825-832.
- BASS, D., PARCE, J. W., DECHATELET, L. R., SZEJDA, P., SEEDS, M. & THOMAS, M. 1983. Flow cytometric studies of oxidative product formation by neutrophils: a graded response to membrane stimulation. *The Journal of Immunology*, 130, 1910-1917.
- BEDROV, D., SMITH, G., DAVANDE, H. & LI, L. 2008. Passive transport of C60 fullerenes through a lipid membrane: a molecular dynamics simulation study. *The journal of physical chemistry. B*, 112, 2078-2084.
- BENN, T. M., WESTERHOFF, P. & HERCKES, P. 2011. Detection of fullerenes (C(60) and C(70)) in commercial cosmetics. *Environmental Pollution*, 159, 1334-1342.
- BLACKBURN, E. H. & GALL, J. G. 1978. A tandemly repeated sequence at the termini of the extrachromosomal ribosomal RNA genes in *Tetrahymena*. *Journal of molecular biology*, 120, 33-53.
- BOGDANOVIĆ, G., KOJIĆ, V., DORDEVIĆ, A., CANADANOVIĆ-BRUNET, J., VOJINOVIĆ-MILORADOV, M. & BALTIC, V. 2004. Modulating activity of fullerol C60(OH)₂₂ on doxorubicin-induced cytotoxicity. *Toxicology in vitro : an international journal published in association with BIBRA*, 18, 629-637.
- CHANG, X. & VIKESLAND, P. J. 2009. Effects of carboxylic acids on nC(60) aggregate formation. *Environmental Pollution*, 157, 1072-1080.
- CHENG, X. K., KAN, A. T. & TOMSON, M. B. 2004. Naphthalene adsorption and desorption from Aqueous C-60 fullerene. *Journal of Chemical and Engineering Data*, 49, 675-683.
- CHRISTIE, M. S., JOHN, D. F., WENH, G., DELINA, L., ADINA, M. B., KEVIN, D. A., YIZHI, J. T., BALAJI, S., LON, J. W., JOSEPH, B. H., JENNIFER, L. W. & VICKI, L. C. 2004. The Differential Cytotoxicity of Water-Soluble Fullerenes. *Nano Letters*, 4.
- COLLECTION, A. T. C. 2011. *PC-12 (ATCC® CRL-1721™)* [Online]. Available: http://www.lgcstandards-atcc.org/products/all/CRL-1721.aspx?geo_country=de [Accessed 05/09/2013].

References:

- COLLINS, F., LANDER, E., ROGERS, J., WATERSTON, R. & CONSO, I. 2004. Finishing the euchromatic sequence of the human genome. *Nature*, 431, 931-945.
- COLVIN, V. L. 2003. The potential environmental impact of engineered nanomaterials. *Nature Biotechnology*, 21, 1166-1170.
- DAVIES, J. C. 2006. *Managing the effects of nanotechnology*, Woodrow Wilson International Center for Scholars, Project on Emerging Nanotechnologies.
- DEGUCHI, S., YAMAZAKI, T., MUKAI, S. A., USAMI, R. & HORIKOSHI, K. 2007. Stabilization of C60 nanoparticles by protein adsorption and its implications for toxicity studies. *Chem Res Toxicol*, 20, 854-8.
- DHAWAN, A., TAUROZZI, J. S., PANDEY, A. K., SHAN, W., MILLER, S. M., HASHSHAM, S. A. & TARABARA, V. V. 2006. Stable colloidal dispersions of C-60 fullerenes in water: Evidence for genotoxicity. *Environ Sci Technol*, 40, 7394-7401.
- DJORDJEVIĆ, A., BOGDANOVIĆ, G. & DOBRIĆ, S. 2006. Fullerenes in biomedicine. *Journal of B.U.ON. : official journal of the Balkan Union of Oncology*, 11, 391-404.
- DUGAN, L., GABRIELSEN, J., YU, S., LIN, T. & CHOI, D. 1996. Buckminsterfullerenol free radical scavengers reduce excitotoxic and apoptotic death of cultured cortical neurons. *Neurobiology of disease*, 3, 129-135.
- DURSTEWITZ, D., KELC, M. & GÜNTÜRKÜN, O. 1999. A neurocomputational theory of the dopaminergic modulation of working memory functions. *The Journal of neuroscience*, 19, 2807-2822.
- EISEN, J., COYNE, R., WU, M., WU, D., THIAGARAJAN, M., WORTMAN, J., BADGER, J., REN, Q., AMEDEO, P., JONES, K., TALLON, L., DELCHER, A., SALZBERG, S., SILVA, J., HAAS, B., MAJOROS, W., FARZAD, M., CARLTON, J., SMITH, R., GARG, J., PEARLMAN, R., KARRER, K., SUN, L., MANNING, G., ELDE, N., TURKEWITZ, A., ASAI, D., WILKES, D., WANG, Y., CAI, H., COLLINS, K., STEWART, B., LEE, S., WILAMOWSKA, K., WEINBERG, Z., RUZZO, W., WLOGA, D., GAERTIG, J., FRANKEL, J., TSAO, C.-C., GOROVSKY, M., KEELING, P., WALLER, R., PATRON, N., CHERRY, J., STOVER, N., KRIEGER, C., DEL TORO, C., RYDER, H., WILLIAMSON, S., BARBEAU, R., HAMILTON, E. & ORIAS, E. 2006. Macronuclear genome sequence of the ciliate *Tetrahymena thermophila*, a model eukaryote. *PLoS biology*, 4.
- ESPINASSE, B., HOTZE, E. M. & WIESNER, M. R. 2007. Transport and retention of colloidal aggregates of C60 in porous media: Effects of organic macromolecules, ionic composition, and preparation method. *Environmental science & technology*, 41, 7396-7402.
- FESCHET-CHASSOT, E., RASPAL, V., SIBAUD, Y., AWITOR, O. K., BONNEMOY, F., BONNET, J. L. & BOHATIER, J. 2011. Tunable functionality and toxicity studies of titanium dioxide nanotube layers. *Thin Solid Films*, 519.
- FINLAY, B. J., ESTEBAN, G. F. & FENCHEL, T. 1998. Protozoan diversity: converging estimates of the global number of free-living ciliate species. *Protist*, 149, 29-37.
- FOLEY, S., CROWLEY, C., SMAIHI, M., BONFILS, C., ERLANGER, B. F., SETA, P. & LARROQUE, C. 2002. Cellular localisation of a water-soluble fullerene derivative. *Biochemical and Biophysical Research Communications*, 294, 116-119.
- FORNAI, F., BATTAGLIA, G., GESI, M., GIORGI, F. S., ORZI, F., NICOLETTI, F. & RUGGIERI, S. 2000. Time-course and dose-response study on the effects of chronic L-DOPA administration on striatal dopamine levels and dopamine transporter following MPTP toxicity. *Brain research*, 887, 110-117.
- FORNAI, F., LENZI, P., LAZZERI, G., FERRUCCI, M., FULCERI, F., GIORGI, F., FALLENI, A., RUGGIERI, S. & PAPARELLI, A. 2007. Fine ultrastructure and biochemistry of PC12 cells: a comparative approach to understand neurotoxicity. *Brain research*, 1129, 174-190.

- FRANCO, A., HANSEN, S. F., OLSEN, S. I. & BUTTI, L. 2007. Limits and prospects of the “incremental approach” and the European legislation on the management of risks related to nanomaterials. *Regulatory Toxicology and Pharmacology*, 48, 171-183.
- FRATER, L., STOKES, E., LEE, R. & ORIOLA, T. 2006. An overview of the framework of current regulation affecting the development and marketing of nanomaterials. *ESRC Centre for Business Relationships Accountability Sustainability and Society (BRASS)-Cardiff University*.
- FROHLICH, E., KUEZNIK, T., SAMBERGER, C., ROBLEGG, E., WRIGHTON, C. & PIEBER, T. R. 2010. Size-dependent effects of nanoparticles on the activity of cytochrome P450 isoenzymes. *Toxicology and Applied Pharmacology*, 242, 326-332.
- FUJITA, K., MORIMOTO, Y., ENDOH, S., UCHIDA, K., FUKUI, H., OGAMI, A., TANAKA, I., HORIE, M., YOSHIDA, Y., IWAHASHI, H. & NAKANISHI, J. 2010. Identification of potential biomarkers from gene expression profiles in rat lungs intratracheally instilled with C(60) fullerenes. *Toxicology*, 274, 34-41.
- GAETANI, G. F., FERRARIS, A., ROLFO, M., MANGERINI, R., ARENA, S. & KIRKMAN, H. 1996. Predominant role of catalase in the disposal of hydrogen peroxide within human erythrocytes. *Blood*, 87, 1595-1599.
- GERHARDT, A., UD-DAULA, A. & SCHRAMM, K. 2010. Tetrahymena spp.(Protista, Ciliophora) as test species in rapid multilevel ecotoxicity tests. *Acta Protozoologica*.
- GHAFAARI, P., ST-DENIS, C., POWER, M., JIN, X., TSOU, V., MANDAL, H., BOLLS, N. & TANG, X. 2008. Impact of carbon nanotubes on the ingestion and digestion of bacteria by ciliated protozoa. *Nature nanotechnology*, 3, 347-351.
- GRAU, C. & GREENE, L. 2012. Use of PC12 cells and rat superior cervical ganglion sympathetic neurons as models for neuroprotective assays relevant to Parkinson's disease. *Methods in molecular biology (Clifton, N.J.)*, 846, 201-211.
- GREENE, L. A. & REIN, G. 1978. SHORT-TERM REGULATION OF CATECHOLAMINE BIOSYNTHESIS IN A NERVE GROWTH FACTOR RESPONSIVE CLONAL LINE OF RAT PHEOCHROMOCYTOMA CELLS. *Journal of neurochemistry*, 30, 549-555.
- GREENE, L. A. & TISCHLER, A. S. 1976. Establishment of a noradrenergic clonal line of rat adrenal pheochromocytoma cells which respond to nerve growth factor. *Proceedings of the National Academy of Sciences*, 73, 2424-2428.
- GREIDER, C. W. & BLACKBURN, E. H. 1985. Identification of a specific telomere terminal transferase activity in Tetrahymena extracts. *Cell*, 43, 405-413.
- GRIGORIY, V. A., MARINA, V. K., OLEH, M. V., VADIM, S. S. & LYUDMILA, A. V. 1995. On the production of an aqueous colloidal solution of fullerenes. *Journal of the Chemical Society, Chemical Communications*.
- GUO, J., ZHANG, X., ZHANG, S., ZHU, Y. & LI, W. 2008. The different bio-effects of functionalized multi-walled carbon nanotubes on Tetrahymena pyriformis. *Current Nanoscience*, 4, 240-245.
- GUSTAFSSON, C., GOVINDARAJAN, S. & MINSHULL, J. 2004. Codon bias and heterologous protein expression. *Trends in biotechnology*, 22, 346-353.
- HAITZER, M., HOSS, S., TRAUNSPURGER, W. & STEINBERG, C. 1998. Effects of dissolved organic matter (DOM) on the bioconcentration of organic chemicals in aquatic organisms - A review. *Chemosphere*, 37, 1335-1362.
- HALLIWELL, B. & GUTTERIDGE, J. 2007. Cellular responses to oxidative stress: adaptation, damage, repair, senescence and death. *Free radicals in biology and medicine*, 4.
- HENNESSEY, T. M. 2005. Responses of the ciliates Tetrahymena and Paramecium to external ATP and GTP. *Purinergic signalling*, 1, 101-110.

References:

- HEYMANN, D. 1996. Solubility of fullerenes C60 and C70 in seven normal alcohols and their deduced solubility in water. *FULLERENE SCIENCE & TECHNOLOGY*, 4, 509-515.
- HOFMAIER, A., SCHWIRZER, S., WIEBEL, F., SCHRAMM, K.-W., WEGENKE, M. & KETRUP, A. 1999. Bioassay zur Bestimmung von TCDD-Toxizitätsäquivalenten (TEQ) von Umweltproben und Reststoffen. 2-8.
- HUSSAIN, S., JAVORINA, A., SCHRAND, A., DUHART, H., ALI, S. & SCHLAGER, J. 2006. The interaction of manganese nanoparticles with PC-12 cells induces dopamine depletion. *Toxicological sciences : an official journal of the Society of Toxicology*, 92, 456-463.
- JACOBSEN, N. R., POJANA, G., WHITE, P., MØLLER, P., COHN, C. A., SMITH KORSHOLM, K., VOGEL, U., MARCOMINI, A., LOFT, S. & WALLIN, H. 2008. Genotoxicity, cytotoxicity, and reactive oxygen species induced by single-walled carbon nanotubes and C60 fullerenes in the FE1-Muta™ Mouse lung epithelial cells. *Environmental and molecular mutagenesis*, 49, 476-487.
- JANAKIDEVI, K., DEWEY, V. C. & KIDDER, G. 1966. The biosynthesis of catecholamines in two genera of protozoa. *Journal of Biological Chemistry*, 241, 2576-2578.
- JENSEN, A. W., WILSON, S. R. & SCHUSTER, D. I. 1996. Biological applications of fullerenes. *Bioorganic & medicinal chemistry*, 4, 767-779.
- KÄKINEN, A., BONDARENKO, O., IVASK, A. & KAHRU, A. 2011. The effect of composition of different ecotoxicological test media on free and bioavailable copper from CuSO4 and CuO nanoparticles: comparative evidence from a Cu-selective electrode and a Cu-biosensor. *Sensors (Basel, Switzerland)*, 11, 10502-10521.
- KAMAT, J., DEVASAGAYAM, T., PRIYADARSINI, K. & MOHAN, H. 2000. Reactive oxygen species mediated membrane damage induced by fullerene derivatives and its possible biological implications. *Toxicology*, 155, 55-61.
- KHATCHADOURIAN, A. & MAYSINGER, D. 2009. Lipid droplets: their role in nanoparticle-induced oxidative stress. *Molecular pharmaceuticals*, 6, 1125-1137.
- KIM, J., LEE, N., KIM, B., RHEE, W., YOON, S., HYEON, T. & PARK, T. 2011. Enhancement of neurite outgrowth in PC12 cells by iron oxide nanoparticles. *Biomaterials*, 32, 2871-2877.
- KITADA, T., ASAKAWA, S., HATTORI, N., MATSUMINE, H., YAMAMURA, Y., MINOSHIMA, S., YOKOCHI, M., MIZUNO, Y. & SHIMIZU, N. 1998. Mutations in the parkin gene cause autosomal recessive juvenile parkinsonism. *Nature*, 392, 605-608.
- KOCH, D. D. & POLZIN, G. L. 1987. Effect of sample preparation and liquid chromatography column choice on selectivity and precision of plasma catecholamine determination. *Journal of Chromatography A*, 386, 19-24.
- KORPANY, K. V., HABIB, F., MURUGESU, M. & BLUM, A. S. 2012. Stable water-soluble iron oxide nanoparticles using Tiron. *Materials Chemistry and Physics*.
- KROTO, H. W., ALLAF, A. W. & BALM, S. P. 1991. C60: Buckminsterfullerene. *Chemical Reviews*, 91.
- KROTO, H. W., HEATH, J. R., O'BRIEN, S. C., CURL, R. F. & SMALLEY, R. E. 1985. C 60: buckminsterfullerene. *Nature*, 318, 162-163.
- KRUSIC, P., WASSERMAN, E., KEIZER, P., MORTON, J. & PRESTON, K. 1991. Radical reactions of c60. *Science (New York, N.Y.)*, 254, 1183-1185.
- KULKARNI, P. & JAFVERT, C. 2008. Solubility of C60 in solvent mixtures. *Environmental science & technology*, 42, 845-851.
- KUMAR, A. M., KUMAR, M., FERNANDEZ, J. B., MELLMAN, T. A. & EISDORFER, C. 1991. A simplified HPLC-ECD technique for measurement of urinary free catecholamines. *Journal of liquid chromatography*, 14, 3547-3557.

References:

- KURUVILLA, H. G. & HENNESSEY, T. 1998. Purification and characterization of a novel chemorepellent receptor from *Tetrahymena thermophila*. *The Journal of membrane biology*, 162, 51-57.
- KURUVILLA, H. G., KIM, M. Y. & HENNESSEY, T. M. 1997. Chemosensory adaptation to lysozyme and GTP involves independently regulated receptors in *Tetrahymena thermophila*. *Journal of Eukaryotic Microbiology*, 44, 263-268.
- LAMPERT, T., NUGENT, C., WESTON, J., BRAUN, N. & KURUVILLA, H. 2013. Nociceptin Signaling Involves a Calcium-Based Depolarization in *Tetrahymena thermophila*. *International journal of peptides*, 2013, 573716-573716.
- LEE, V. S., NIMMANPIPUG, P., ARUKSAKUNWONG, O., PROMSRI, S., SOMPORNPISTUT, P. & HANNONGBUA, S. 2007. Structural analysis of lead fullerene-based inhibitor bound to human immunodeficiency virus type 1 protease in solution from molecular dynamics simulations. *Journal of Molecular Graphics and Modelling*, 26, 558-570.
- LENS, M. 2011. Recent progresses in application of fullerenes in cosmetics. *Recent patents on biotechnology*, 5, 67-73.
- LI, D., FORTNER, J. D., JOHNSON, D. R., CHEN, C., LI, Q. & ALVAREZ, P. J. 2010. Bioaccumulation of 14C60 by the earthworm *Eisenia fetida*. *Environ Sci Technol*, 44, 9170-5.
- LIMBACH, L. K., WICK, P., MANSER, P., GRASS, R. N., BRUININK, A. & STARK, W. J. 2007. Exposure of engineered nanoparticles to human lung epithelial cells: Influence of chemical composition and catalytic activity on oxidative stress. *Environ Sci Technol*, 41, 4158-4163.
- LIN, A. M. Y., CHYI, B. Y., WANG, S. D., YU, H. H., KANAKAMMA, P. P., LUH, T. Y., CHOU, C. K. & HO, L. T. 1999. Carboxyfullerene prevents iron-induced oxidative stress in rat brain. *Journal of neurochemistry*, 72, 1634-1640.
- LING, T.-R., SYU, Y., TASI, Y.-C., CHOU, T.-C. & LIU, C.-C. 2005. Size-selective recognition of catecholamines by molecular imprinting on silica-alumina gel. *Biosensors & bioelectronics*, 21, 901-907.
- LONG, R. Q. & YANG, R. T. 2001. Carbon nanotubes as superior sorbent for dioxin removal. *Journal of the American Chemical Society*, 123, 2058-2059.
- LONG, T. C., TAJUBA, J., SAMA, P., SALEH, N., SWARTZ, C., PARKER, J., HESTER, S., LOWRY, G. V. & VERONESI, B. 2007. Nanosize titanium dioxide stimulates reactive oxygen species in brain microglia and damages neurons in vitro. *Environmental health perspectives*, 115, 1631-1637.
- LOTHARIUS, J., DUGAN, L. L. & O'MALLEY, K. L. 1999. Distinct mechanisms underlie neurotoxin-mediated cell death in cultured dopaminergic neurons. *Journal of Neuroscience*, 19, 1284-1293.
- LUKACINOVA, A., MOJZIS, J., BENACKA, R., LOVASOVA, E., HIJOVÁ, E. & NISTIAR, F. 2007. TETRAHYMENA PYRIFORMIS AS A VALUABLE UNICELLULAR ANIMAL MODEL ORGANISM FOR DETERMINATION OF XENOBIOTICS.
- LYNCH, I., DAWSON, K. & LINSE, S. 2006. Detecting cryptic epitopes created by nanoparticles. *Science's STKE : signal transduction knowledge environment*, 2006.
- MAHER, P. 2006. Redox control of neural function: background, mechanisms, and significance. *Antioxidants & redox signaling*, 8, 1941-1970.
- MARKEY, K., KONDO, S., SHENKMAN, L. & GOLDSTEIN, M. 1980. Purification and characterization of tyrosine hydroxylase from a clonal pheochromocytoma cell line. *Molecular pharmacology*, 17, 79-85.
- MATESANZ, M.-C., VILA, M., FEITO, M.-J., LINARES, J., GONÇALVES, G., VALLET-REGI, M., MARQUES, P.-A. & PORTOLÉS, M.-T. 2013. The effects of graphene oxide

- nanosheets localized on F-actin filaments on cell-cycle alterations. *Biomaterials*, 34, 1562-1569.
- MAYER, P., FERNQVIST, M., CHRISTENSEN, P., KARLSON, U. & TRAPP, S. 2007. Enhanced diffusion of polycyclic aromatic hydrocarbons in artificial and natural aqueous solutions. *Environ Sci Technol*, 41, 6148-6155.
- MORTIMER, M., KASEMETS, K. & KAHRU, A. 2010. Toxicity of ZnO and CuO nanoparticles to ciliated protozoa *Tetrahymena thermophila*. *Toxicology*, 269, 182-189.
- MURDOCK, R., BRAYDICH-STOLLE, L., SCHRAND, A., SCHLAGER, J. & HUSSAIN, S. 2008. Characterization of nanomaterial dispersion in solution prior to in vitro exposure using dynamic light scattering technique. *Toxicological sciences : an official journal of the Society of Toxicology*, 101, 239-253.
- MURR, L., SOTO, K., GARZA, K., GUERRERO, P., MARTINEZ, F., ESQUIVEL, E., RAMIREZ, D., SHI, Y., BANG, J. & VENZOR, J. 2006. Combustion-generated nanoparticulates in the El Paso, TX, USA / Juarez, Mexico Metroplex: their comparative characterization and potential for adverse health effects. *International journal of environmental research and public health*, 3, 48-66.
- NEL, A., XIA, T., MÄDLER, L. & LI, N. 2006. Toxic potential of materials at the nanolevel. *Science (New York, N.Y.)*, 311, 622-627.
- NEL, A., XIA, T., MENG, H., WANG, X., LIN, S., JI, Z. & ZHANG, H. 2012. Nanomaterial Toxicity Testing in the 21st Century: Use of a Predictive Toxicological Approach and High-Throughput Screening. *Accounts of chemical research*.
- NIELSEN, G., ROURSGAARD, M., JENSEN, K., POULSEN, S. & LARSEN, S. 2008. In vivo biology and toxicology of fullerenes and their derivatives. *Basic & clinical pharmacology & toxicology*, 103, 197-208.
- OBERDÖRSTER, E. 2004a. Manufactured Nanomaterials (Fullerenes, C60) Induce Oxidative Stress in the Brain of Juvenile Largemouth Bass. *Environ Health Perspect*, 112, 1058-1062.
- OBERDÖRSTER, E. 2004b. Manufactured nanomaterials (fullerenes, C60) induce oxidative stress in the brain of juvenile largemouth bass. *Environmental health perspectives*, 112, 1058-1062.
- OBERDORSTER, E., ZHU, S., BLICKLEY, T., MCCLELLANGREEN, P. & HAASCH, M. 2006. Ecotoxicology of carbon-based engineered nanoparticles: Effects of fullerene (C60) on aquatic organisms. *Carbon*, 44, 1112-1120.
- OBERDÖRSTER, G., OBERDÖRSTER, E. & OBERDÖRSTER, J. 2005. Nanotoxicology: an emerging discipline evolving from studies of ultrafine particles. *Environmental health perspectives*, 113, 823-839.
- PAN, B., LIN, D., MASHAYEKHI, H. & XING, B. 2008. Adsorption and Hysteresis of Bisphenol A and 17 α -Ethinyl Estradiol on Carbon Nanomaterials.
- PARK, J.-W., HENRY, T. B., MENN, F.-M., COMPTON, R. N. & SAYLER, G. 2010. No bioavailability of 17 α -ethinylestradiol when associated with nC(60) aggregates during dietary exposure in adult male zebrafish (*Danio rerio*). *Chemosphere*, 81, 1227-1232.
- PATENAUDE, A., MURTHY, M. & MIRAULT, M. E. 2005. Emerging roles of thioredoxin cycle enzymes in the central nervous system. *Cellular and molecular life sciences : CMLS*, 62, 1063-1080.
- PEARSE, A. 1969. The cytochemistry and ultrastructure of polypeptide hormone-producing cells of the APUD series and the embryologic, physiologic and pathologic implications of the concept. *Journal of Histochemistry & Cytochemistry*, 17, 303-313.
- PICKERING, K. & WIESNER, M. 2005. Fullerol-sensitized production of reactive oxygen species in aqueous solution. *Environmental science & technology*, 39, 1359-1365.

References:

- PISANIC, T., BLACKWELL, J., SHUBAYEV, V., FIÑONES, R. & JIN, S. 2007. Nanotoxicity of iron oxide nanoparticle internalization in growing neurons. *Biomaterials*, 28, 2572-2581.
- PITOT, H., PERAINO, C., MORSE JR, P. & POTTER, V. R. 1964. Hepatomas in tissue culture compared with adapting liver in vivo. *National Cancer Institute Monograph*, 13, 229.
- PLESNER, P., RASMUSSEN, L. & ZEUTHEN, E. 1964. Techniques used in the study of synchronous Tetrahymena. *Synchrony in cell division and growth*, 544-563.
- POORKAJ, P., NUTT, J. G., JAMES, D., GANCHER, S., BIRD, T. D., STEINBART, E., SCHELLENBERG, G. D. & PAYAMI, H. 2004. parkin mutation analysis in clinic patients with early-onset Parkinson's disease. *American Journal of Medical Genetics Part A*, 129A, 44-50.
- PRZEDBORSKI, S., CHEN, Q. P., VILA, M., GIASSON, B. I., DJALDATTI, R., VUKOSAVIC, S., SOUZA, J. M., JACKSON-LEWIS, V., LEE, V. M. Y. & ISCHIROPOULOS, H. 2001. Oxidative post-translational modifications of alpha-synuclein in the 1-methyl-4-phenyl-1,2,3,6-tetrahydropyridine (MPTP) mouse model of Parkinson's disease. *Journal of neurochemistry*, 76, 637-640.
- PRZYBYTKOWSKI, E., BEHRENDT, M., DUBOIS, D. & MAYSINGER, D. 2009. Nanoparticles can induce changes in the intracellular metabolism of lipids without compromising cellular viability. *The FEBS journal*, 276, 6204-6217.
- REINHARD, J. F., JR., SMITH, G. K. & NICHOL, C. A. 1986. A rapid and sensitive assay for tyrosine-3-monooxygenase based upon the release of $3H_2O$ and adsorption of $3H$ -tyrosine by charcoal. *Life sciences*, 39, 2185-9.
- RODA, L., NOLAN, J., KIM, S. & HOGUE-ANGELETTI, R. 1980. Isolation and characterization of chromaffin granules from a pheochromocytoma (PC 12) cell line. *Experimental cell research*, 128, 103-109.
- ROGER, T. & DAVID, R. M. W. 1993. The chemistry of fullerenes. *Nature*, 363.
- ROTHEN-RUTISHAUSER, B., SCHÜRCH, S., HAENNI, B., KAPP, N. & GEHR, P. 2006. Interaction of fine particles and nanoparticles with red blood cells visualized with advanced microscopic techniques. *Environmental Science & Technology*, 40, 4353-4359.
- ROUSE, J. G., YANG, J., RYMAN-RASMUSSEN, J. P., BARRON, A. R. & MONTEIRO-RIVIERE, N. A. 2007. Effects of mechanical flexion on the penetration of fullerene amino acid-derivatized peptide nanoparticles through skin. *Nano Letters*, 7, 155-160.
- SAHU, S. C. & CASCACIANO, D. 2009. *Nanotoxicity*, Wiley Online Library.
- SAMPATH, D., JACKSON, G. R., WERRBACH-PEREZ, K. & PEREZ-POLO, J. R. 1994. Effects of nerve growth factor on glutathione peroxidase and catalase in PC 12 cells. *Journal of neurochemistry*, 62, 2476-2479.
- SAYES, C., GOBIN, A., AUSMAN, K., MENDEZ, J., WEST, J. & COLVIN, V. 2005. Nano-C60 cytotoxicity is due to lipid peroxidation. *Biomaterials*, 26, 7587-7595.
- SCHMITTGEN, T. & LIVAK, K. 2008. Analyzing real-time PCR data by the comparative C(T) method. *Nature protocols*, 3, 1101-1108.
- SCHWIRZER, S. M. G., HOFMAIER, A. M., KETTRUP, A., NERDINGER, P. E., SCHRAMM, K. W., THOMA, H., WEGENKE, M. & WIEBEL, F. J. 1998. Establishment of a simple cleanup procedure and bioassay for determining 2,3,7,8-tetrachlorodibenzo-p-dioxin toxicity equivalents of environmental samples. *Ecotoxicol Environ Saf*, 41, 77-82.
- SCOWN, T., VAN AERLE, R. & TYLER, C. 2010a. Review: Do engineered nanoparticles pose a significant threat to the aquatic environment? *Critical reviews in toxicology*, 40, 653-670.
- SCOWN, T. M., VAN AERLE, R. & TYLER, C. R. 2010b. Review: Do engineered nanoparticles pose a significant threat to the aquatic environment? *Crit Rev Toxicol*, 40, 653-70.

References:

- SCRIVENS, W. A., TOUR, J. M., CREEK, K. E. & PIRISI, L. 1994. Synthesis of ¹⁴C-labeled C₆₀, its suspension in water, and its uptake by human keratinocytes. *Journal of the American Chemical Society*, 116, 4517-4518.
- SEREEMASPUN, A., ROJANATHANES, R. & WIWANITKIT, V. 2008. Effect of gold nanoparticle on renal cell: an implication for exposure risk. *Renal failure*, 30, 323-325.
- SIJM, D. & VAN DER LINDE, A. 1995. Size-dependent bioconcentration kinetics of hydrophobic organic chemicals in fish based on diffusive mass transfer and allometric relationships. *Environmental science & technology*, 29, 2769-2777.
- SMALLEY, R. E. & YAKOBSON, B. I. 1998. The future of the fullerenes. *Solid State Communications*, 107, 597-606.
- SOENEN, S., MANSHIAN, B., MONTENEGRO, J., AMIN, F., MEERMANN, B., THIRON, T., CORNELISSEN, M., VANHAECKE, F., DOAK, S., PARAK, W., DE SMEDT, S. & BRAECKMANS, K. 2012. Cytotoxic effects of gold nanoparticles: a multiparametric study. *ACS nano*, 6, 5767-5783.
- STONE, V., NOWACK, B., BAUN, A., VAN DEN BRINK, N., KAMMER, F. V. D., DUSINSKA, M., HANDY, R., HANKIN, S., HASSELLÖV, M., JONER, E. & FERNANDES, T. 2010. Nanomaterials for environmental studies: classification, reference material issues, and strategies for physico-chemical characterisation. *The Science of the total environment*, 408, 1745-1754.
- STOVER, N., KRIEGER, C., BINKLEY, G., DONG, Q., FISK, D., NASH, R., SETHURAMAN, A., WENG, S. & CHERRY, J. 2006. Tetrahymena Genome Database (TGD): a new genomic resource for Tetrahymena thermophila research. *Nucleic acids research*, 34, 3.
- TAO, X., FORTNER, J. D., ZHANG, B., HE, Y., CHEN, Y. & HUGHES, J. B. 2009. Effects of aqueous stable fullerene nanocrystals (nC(60)) on *Daphnia magna*: Evaluation of sub-lethal reproductive responses and accumulation. *Chemosphere*, 77, 1482-1487.
- TENG, K., ANGELASTRO, J., CUNNINGHAM, M. & GREENE, L. 2006. PC12 Cells: A Model Function, Differentiation, and Survival.
- TERASHIMA, M. & NAGAO, S. 2007. Solubilization of C₆₀ fullerene in water by aquatic humic substances. *Chemistry Letters*, 36, 302-303.
- THOMAS, L. 1998. Albumin. *Thomas L (Hg.) Labor und Diagnose. Indikation und Bewertung von Laborbefunden für die medizinische Diagnostik*, 5, 668-669.
- TILLITT, D. E., GIESY, J. P. & ANKLEY, G. T. 1991. Characterization of the H4IIE rat hepatoma cell bioassay as a tool for assessing toxic potency of planar halogenated hydrocarbons in environmental samples. *Environmental science & technology*, 25, 87-92.
- TISCHLER, A. S. 2002. Chromaffin cells as models of endocrine cells and neurons. *Annals of the New York Academy of Sciences*, 971, 366-370.
- TORMEY, W., CARNEY, M. & FITZGERALD, R. 1999. Catecholamines in urine after death. *Forensic science international*, 103, 67-71.
- UENG, T., KANG, J., WANG, H., CHENG, Y. & CHIANG, L. 1997. Suppression of microsomal cytochrome P450-dependent monooxygenases and mitochondrial oxidative phosphorylation by fullereneol, a polyhydroxylated fullerene C₆₀. *Toxicology letters*, 93, 29-37.
- USENKO, C., HARPER, S. & TANGUAY, R. 2008. Fullerene C₆₀ exposure elicits an oxidative stress response in embryonic zebrafish. *Toxicology and applied pharmacology*, 229, 44-55.
- VACCARO, K. K., LIANG, B., PERELLE, B. & PERLMAN, R. L. 1980. Tyrosine 3-monooxygenase regulates catecholamine synthesis in pheochromocytoma cells. *Journal of Biological Chemistry*, 255, 6539-6541.
- VALET, P. & SAULNIER-BLACHE, J. [Metabolic and trophic role of catecholamines in the development of white adipose tissue]. *Annales d'endocrinologie*, 1999, 167-174.

References:

- VAN DE PEER, Y. 2004. Computational approaches to unveiling ancient genome duplications. *Nature Reviews Genetics*, 5, 752-763.
- VENTER, J. C., ADAMS, M. D., MYERS, E. W., LI, P. W., MURAL, R. J., SUTTON, G. G., SMITH, H. O., YANDELL, M., EVANS, C. A. & HOLT, R. A. 2001. The sequence of the human genome. *science*, 291, 1304-1351.
- VERTEGEL, A. A., SIEGEL, R. W. & DORDICK, J. S. 2004. Silica nanoparticle size influences the structure and enzymatic activity of adsorbed lysozyme. *Langmuir*, 20, 6800-6807.
- VILA, M., VUKOSAVIC, S., JACKSON-LEWIS, V., NEYSTAT, M., JAKOWEC, M. & PRZEDBORSKI, S. 2000. alpha-synuclein up-regulation in substantia nigra dopaminergic neurons following administration of the Parkinsonian toxin MPTP. *Journal of neurochemistry*, 74, 721-729.
- WALKINSHAW, G. & WATERS, C. M. 1995. Induction of apoptosis in catecholaminergic PC12 cells by L-DOPA. Implications for the treatment of Parkinson's disease. *Journal of Clinical Investigation*, 95, 2458.
- WANG, C. C., GUO, Z. X., FU, S. K., WU, W. & ZHU, D. B. 2004. Polymers containing fullerene or carbon nanotube structures. *Progress in Polymer Science*, 29, 1079-1141.
- WANG, J., CHEN, C., LI, B., YU, H., ZHAO, Y., SUN, J., LI, Y., XING, G., YUAN, H., TANG, J., CHEN, Z., MENG, H., GAO, Y., YE, C., CHAI, Z., ZHU, C., MA, B., FANG, X. & WAN, L. 2006. Antioxidative function and biodistribution of [Gd@C82(OH)22]n nanoparticles in tumor-bearing mice. *Biochemical pharmacology*, 71, 872-881.
- WANG, J., RAHMAN, M., DUHART, H., NEWPORT, G., PATTERSON, T., MURDOCK, R., HUSSAIN, S., SCHLAGER, J. & ALI, S. 2009. Expression changes of dopaminergic system-related genes in PC12 cells induced by manganese, silver, or copper nanoparticles. *Neurotoxicology*, 30, 926-933.
- WANG, S. & BUSECK, P. R. 1991. Packing of C60 molecules and related fullerenes in crystals: a direct view. *Chemical Physics Letters*, 182, 1-4.
- WANG, Z., UD-DAULA, A., FIEDLER, S. & SCHRAMM, K.-W. 2010. Impact of fluorotelomer alcohols (FTOH) on the molecular and macroscopic phenotype of *Tetrahymena thermophila*. *Environmental Science and Pollution Research*, 17, 154-164.
- WERLIN, R., PRIESTER, J., MIELKE, R., KRÄMER, S., JACKSON, S., STOIMENOV, P., STUCKY, G., CHERR, G., ORIAS, E. & HOLDEN, P. 2011. Biomagnification of cadmium selenide quantum dots in a simple experimental microbial food chain. *Nature nanotechnology*, 6, 65-71.
- WESTERINK, R. H. S. & EWING, A. G. 2008. The PC12 cell as model for neurosecretion. *Acta Physiologica*, 192, 273-285.
- WONG-EKKABUT, J., BAOUKINA, S., TRIAMPO, W., TANG, I. M., TIELEMAN, D. P. & MONTICELLI, L. 2008. Computer simulation study of fullerene translocation through lipid membranes. *Nat Nanotechnol*, 3, 363-8.
- XUE, Y., WU, J. & SUN, J. 2012. Four Types of Inorganic Nanoparticles Stimulate the Inflammatory Reaction in Brain Microglia and Damage Neurons in Vitro. *Toxicology letters*.
- YANG, K., ZHU, L. Z. & XING, B. S. 2006. Adsorption of polycyclic aromatic hydrocarbons by carbon nanomaterials. *Environmental Science & Technology*, 40, 1855-1861.
- YOO, M., CHUN, H., SON, J., DEGIORGIO, L., KIM, D., PENG, C. & SON, J. 2003. Oxidative stress regulated genes in nigral dopaminergic neuronal cells: correlation with the known pathology in Parkinson's disease. *Brain research. Molecular brain research*, 110, 76-84.
- YUAN, H., GAO, F., ZHANG, Z., MIAO, L., YU, R., ZHAO, H. & LAN, M. 2010. Study on controllable preparation of silica nanoparticles with multi-sizes and their size-dependent

References:

- cytotoxicity in pheochromocytoma cells and human embryonic kidney cells. *Journal of Health Science*, 56, 632-640.
- ZHANG, X., SUN, H., ZHANG, Z., NIU, Q., CHEN, Y. & CRITTENDEN, J. C. 2007. Enhanced bioaccumulation of cadmium in carp in the presence of titanium dioxide nanoparticles. *Chemosphere*, 67, 160-6.
- ZHAO, J., YAO, Y., LIU, S., ZHANG, T., REN, G. & YANG, Z. 2012. Involvement of reactive oxygen species and high-voltage-activated calcium currents in nanoparticle zinc oxide-induced cytotoxicity in vitro. *Journal of Nanoparticle Research*, 14, 1-14.

Appendix:

Content Type	Description	Page Nr.
Figure 1	Fullerene (C ₆₀) dependent potentiation of Ca ²⁺ -transporting P-type ATPase (ATPase) over 3, 6, 12, 24 h; mRNA expression level are represented as fold change of gene expression	114
Figure 2	Fullerenol - C ₆₀ (OH) ₂₄ dependent potentiation of Ca ²⁺ -transporting P-type ATPase (ATPase) over 3, 6, 12, 24 h; mRNA expression level are represented as fold change of gene expression	115
Figure 3	Real time PCR plot for the GST gene of <i>Tetrahymena thermophila</i> (n=3) exposed to 0, 1, 20 and 80 ppm C ₆₀ nanoparticles (fullerene) for 0, 3, 6, 12 and 24 hours	116
Figure 4	Real time PCR plot for the β-actin gene of <i>Tetrahymena thermophila</i> (n=3) exposed to 0, 1, 20 and 80 ppm C ₆₀ nanoparticles (fullerene) for 0, 3, 6, 12 and 24 hours.	117
Figure 5	Fullerenol - C ₆₀ (OH) ₂₄ (colour background) and fullerene (white background) dependent potentiation of <i>ACTH</i> and <i>calcium-ATPase</i> (ATPase) at 3 h; mRNA expression level are represented as fold change of gene expression.	118

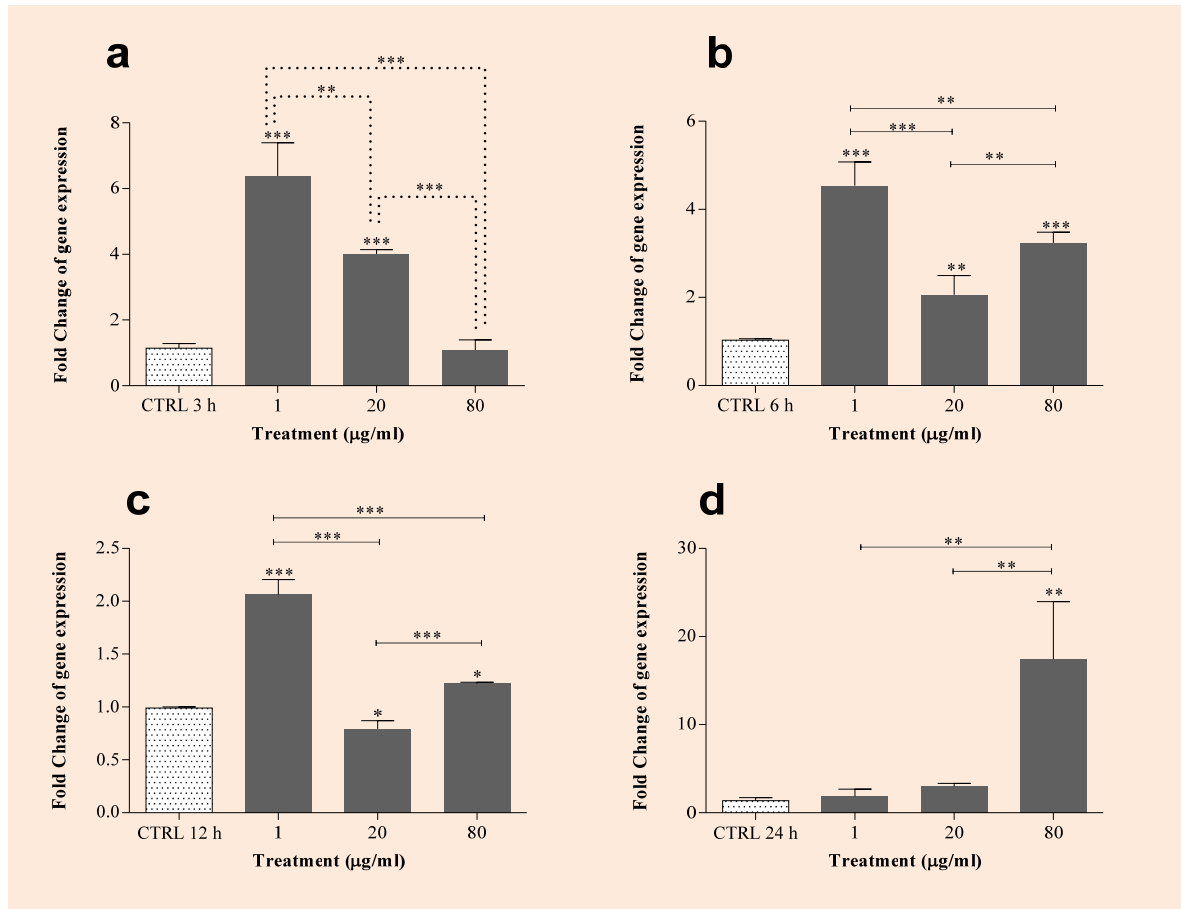


Figure 1: Fullerene (C_{60}) dependent potentiation of Ca^{2+} -transporting P-type ATPase (ATPase) over 3, 6, 12, 24 h; mRNA expression level are represented as fold change of gene expression. Bars and error bars represent the mean and standard error of the mean (SEM) of three independent experiments. Statistically significant differences (ordinary ANOVA followed by Holm-Sidak Multiple comparison test) with respect to the vehicle control are indicated as: * $p < 0.05$, ** < 0.01 , *** < 0.001 .

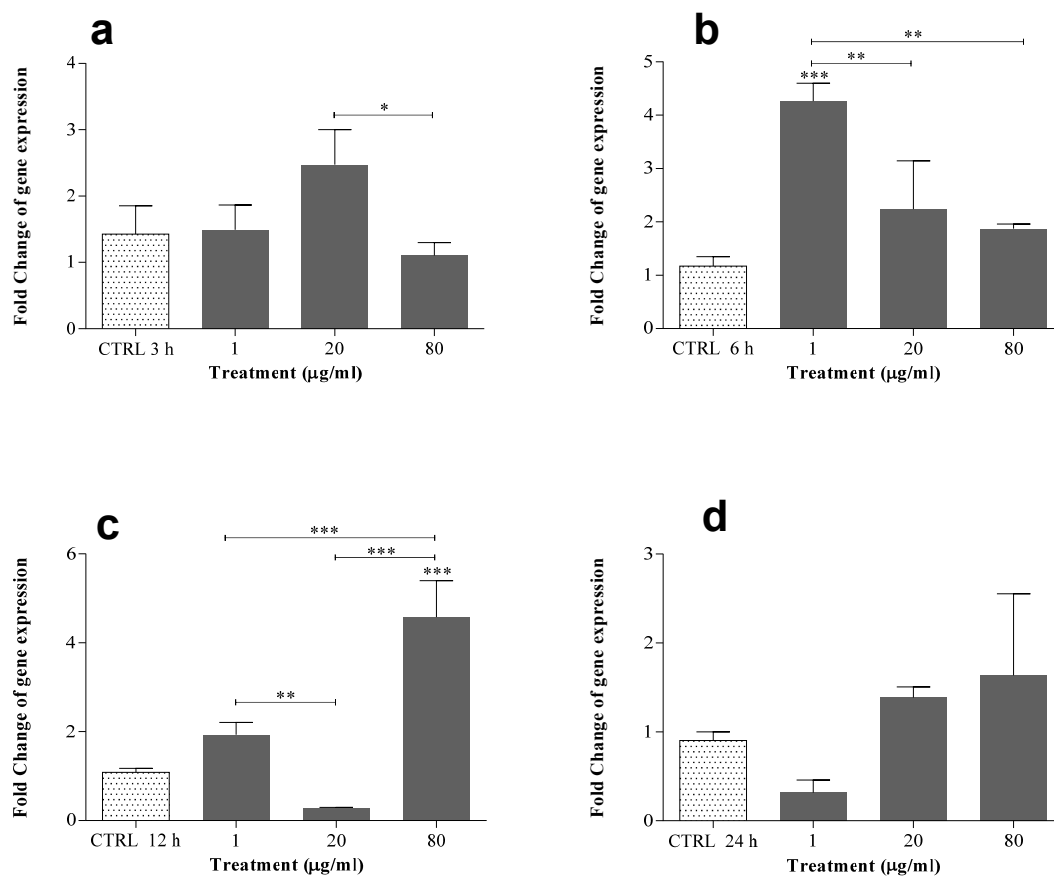


Figure 2: Fulleranol - $C_{60}(\text{OH})_{24}$ dependent potentiation of Ca^{2+} -transporting P-type ATPase (ATPase) over 3, 6, 12, 24 h; mRNA expression level are represented as fold change of gene expression. Bars and error bars represent the mean and standard error of the mean (SEM) of three independent experiments. Statistically significant differences (ordinary ANOVA followed by Holm-Sidak Multiple comparison test) with respect to the vehicle control are indicated as: * $p < 0.05$, ** < 0.01 , *** < 0.001 .

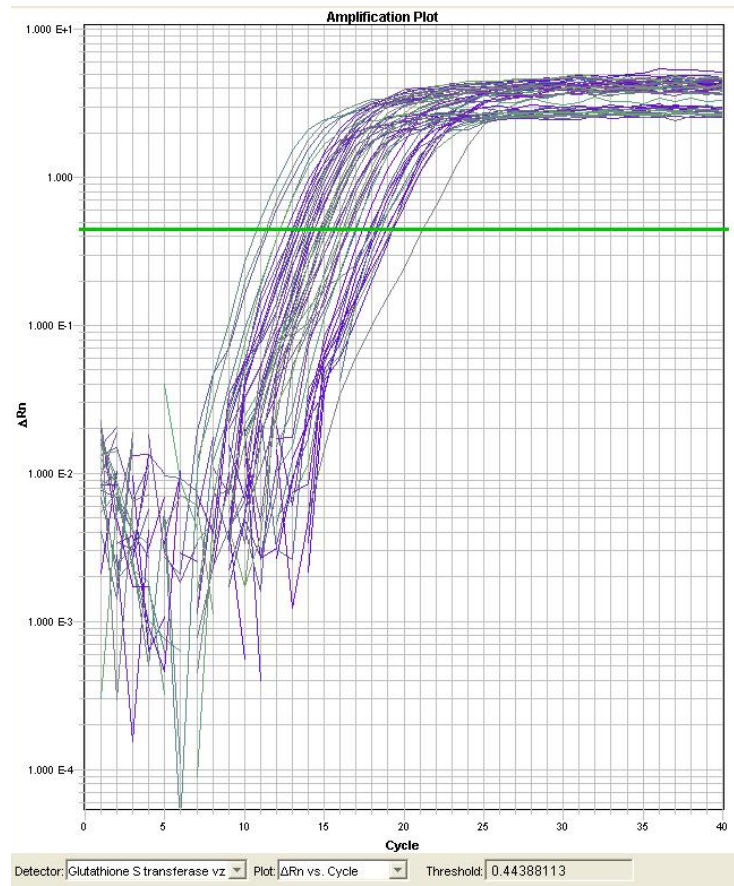


Figure 3. Real time PCR plot for the GST gene of *Tetrahymena thermophila* ($n=3$) exposed to 0, 1, 20 and 80 ppm C_{60} nanoparticles (fullerene) for 0, 3, 6, 12 and 24 hours

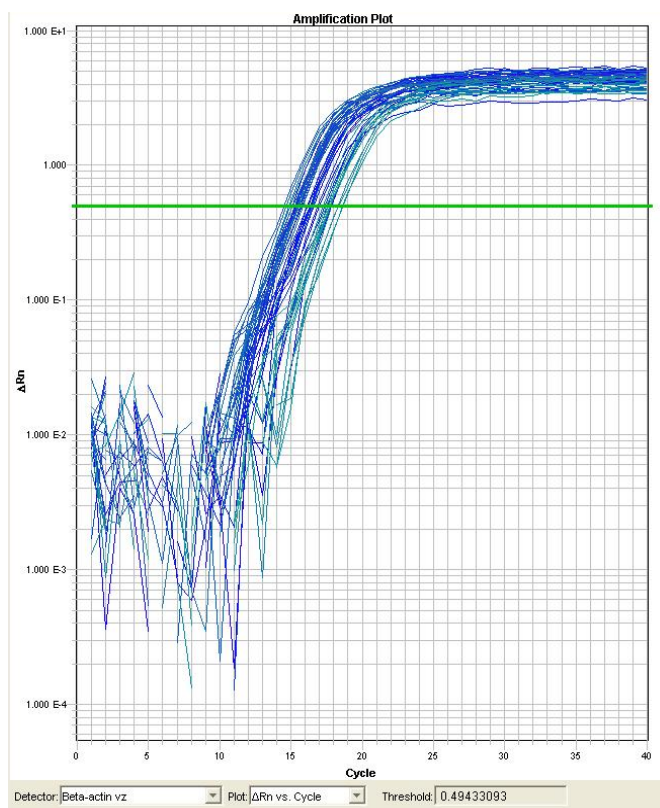


Figure 4. Real time PCR plot for the β -actin gene of *Tetrahymena thermophila* ($n=3$) exposed to 0, 1, 20 and 80 ppm C_{60} nanoparticles (fullerene) for 0, 3, 6, 12 and 24 hours.

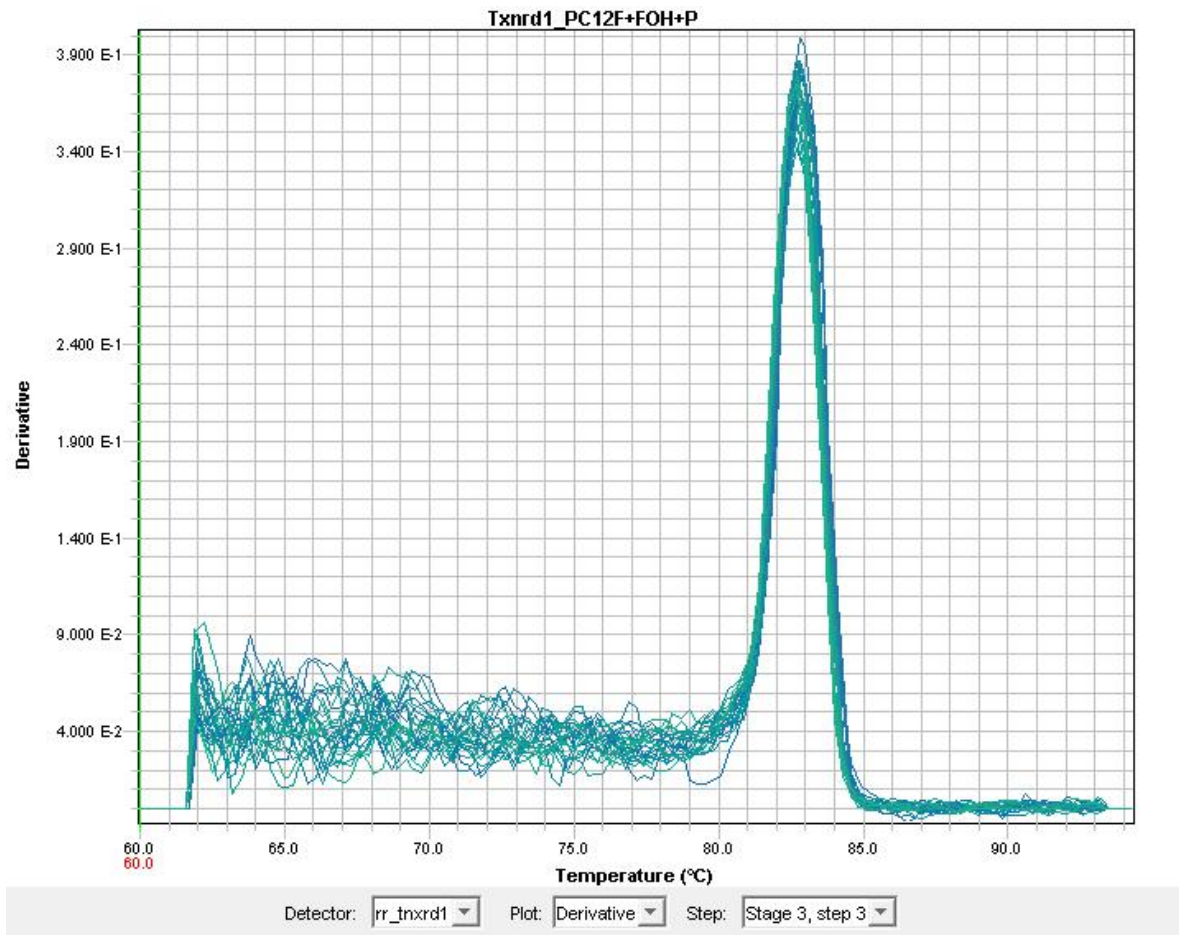


Figure 5. Real time PCR dissociation curve of *Thioredoxin reductase 1* (*Txnrd1*) of PC12 exposed to 0, 1, 20 and 50 ppm Fullerene, fullerenol and Printex®90 for 6 and 24 h.

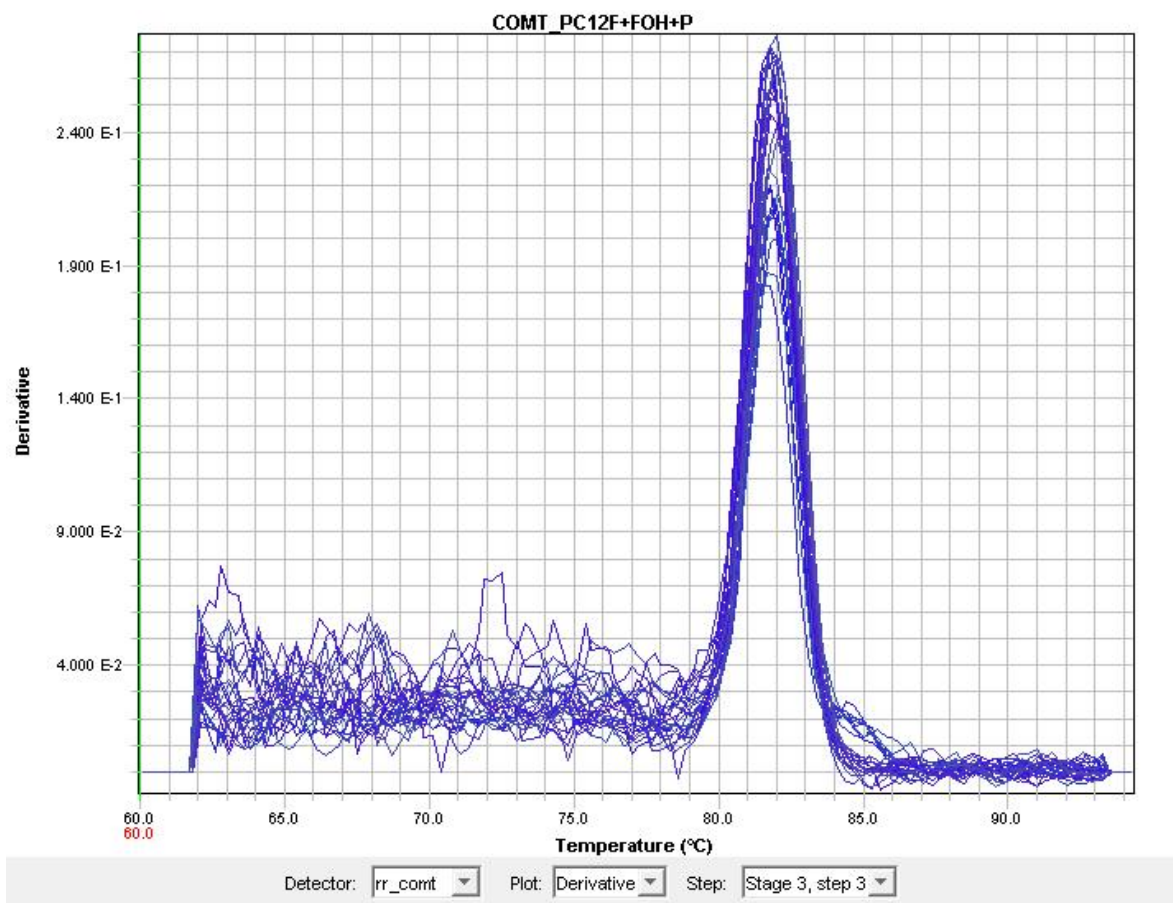


Figure 6. Real time PCR dissociation curve of *Carboxy-O-methyltransferase* (*Comt*) of PC12 exposed to 0, 1, 20 and 50 ppm Fullerene, fulleranol and Printex®90 for 6 and 24 h.

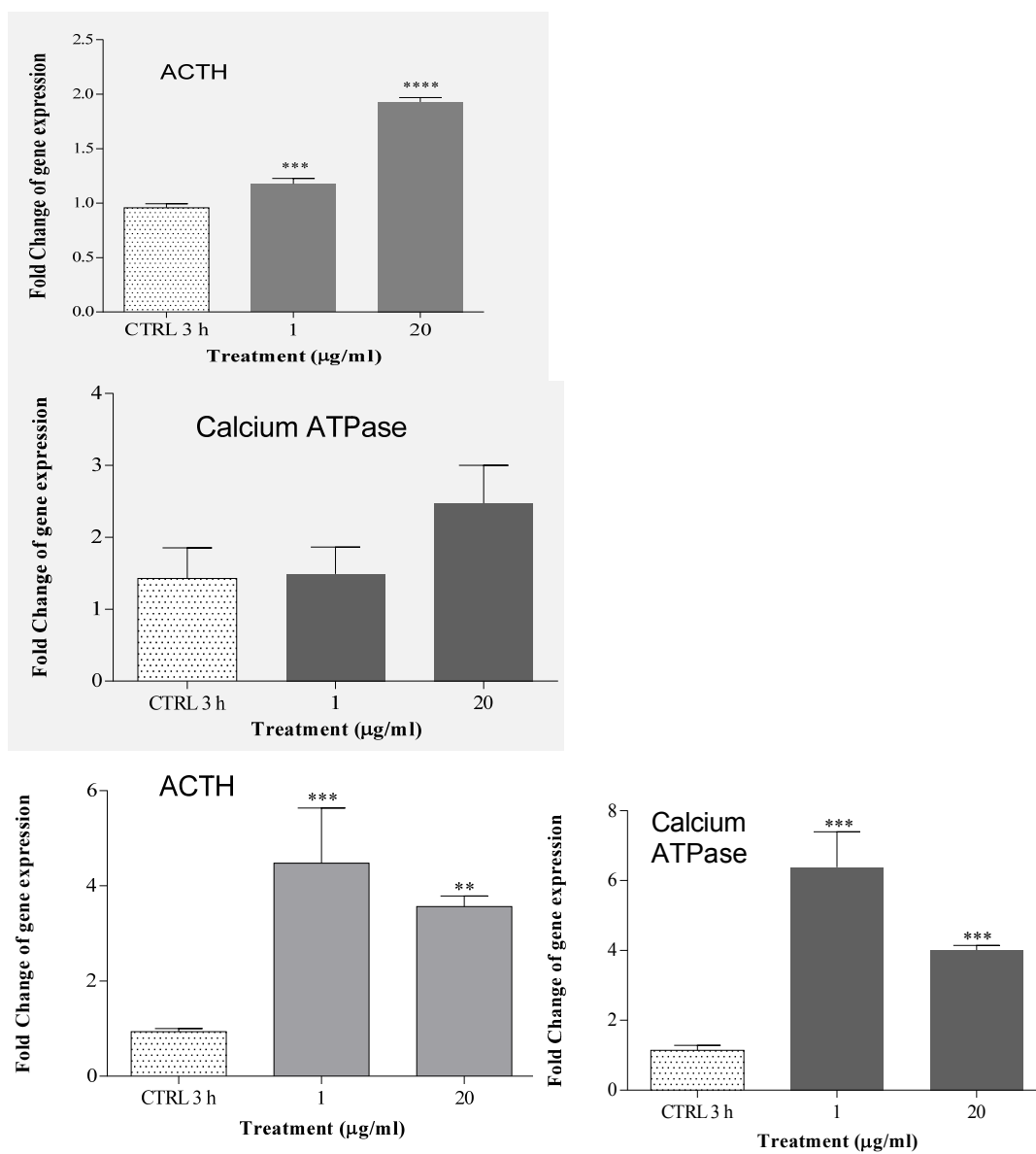


Figure 7: Fullerenol - $C_{60}(OH)_{24}$ (colour background) and fullerene (white background) dependent potentiation of *ACTH* and *calcium-ATPase* (*ATPase*) at 3 h; mRNA expression level are represented as fold change of gene expression. Bars and error bars represent the mean and standard error of the mean (SEM) of three independent experiments. Statistically significant differences (ordinary ANOVA followed by Holm-Sidak Multiple comparison test) with respect to the vehicle control are indicated as: * p < 0.05, ** < 0.01, *** < 0.001.

RAJESH RATHORE

Felsennelkenanger 19/130, 80937 München

rathorerjs@gmail.com

LEBENS LAUF

PERSÖNLICHE DATEN

Geburtsdatum: 20th April 1981

Geburtsort: Indore

Staatangehörigkeit: Indien

Familienstand: verheiratet

ARBEITSERFAHRUNG

06/2010 – 2013 Gastwissenschaftlicher, Helmholtz Zentrum München GmbH, München, Deutschland

10/2009 - 04/2010 Wissenschaftlicher Mitarbeiter im „Center for Life Science Automation“ Rostock, Deutschland

11/2007 – 09/2009 Dozent im „ Dept. Of Pharmacy, SGS Inst. Of Technology and Science“, Indore, Indien

07/2006 – 09/2007 Wissenschaftlicher Mitarbeiter im „ Pharmaceutical R&D, Piramal Research Centre“, Mumbai, Indien

AUSBILDUNG

06/2004 – 06/2006 Studium der Dept. Of Pharmaceutics National Institute of Pharmaceutical Education and Research (NIPER), Mohali, Indien
Abschluss: MS (Pharm) Pharmaceutics (cGPA 8.10 von 10)

06/2000 – 06/2004 Studium der Dept. Of Pharmacy, SGS Inst. Of Technology and Science, Indore, Indien
Abschluss: B. Pharmacy (64.50 %), 96.54 percentile in GATE 2004(Graduate Aptitude Test in Engineering, by IIT Delhi)

PUBLIKATION

Rathorea R., Jain JP, Srivastav A., Jachak SM, Kumara N; Simultaneous determination of ahydrazinocurcumin and phenol red in samples from rat intestinal permeability studies: HPLC method development and validation
Journal of Pharmaceutical and Biomedical Analysis 46 (2008) 374–380

München, 26.03.2014